



**UNIVERSITY OF
KWAZULU-NATAL**

**INYUVESI
YAKWAZULU-NATALI**

**Fumonisin B₁-induced oxidative stress in
human liver (HepG2) cells – an alternate
mechanism of carcinogenesis**

BY

Thilona Arumugam

B. Med. Sc. (Hons) (UKZN)

Submitted in fulfilment of the requirements for the degree of

Master of Medical Science

in the Discipline of Medical Biochemistry

School of Laboratory Medicine and Medical Sciences

College of Health Sciences

University of Kwa-Zulu Natal

Durban

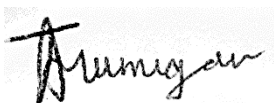
2017

DECLARATION

I, Thilona Arumugam declare that:

- (i) The research reported in this dissertation, except where otherwise indicated, is my original work.
- (ii) This dissertation has not been submitted for any degree or examination at any other university.
- (iii) This dissertation does not contain other persons' data, pictures, graphs or other information, unless specifically acknowledged as being sourced from other persons.
- (iv) This dissertation does not contain other persons' writing, unless specifically acknowledged as being sourced from other researchers. Where other written sources have been quoted, then:
 - a) their words have been re-written but the general information attributed to them has been referenced;
 - b) where their exact words have been used, their writing has been placed inside quotation marks, and referenced.
- (v) This dissertation does not contain text, graphics or tables copied and pasted from the Internet, unless specifically acknowledged, and the source being detailed in the dissertation and in the References sections

The research described in this study was carried out in the Discipline of Medical Biochemistry, School of Laboratory Medicine and Medical Science, College of Health Sciences, University of Kwa-Zulu Natal, under the supervision of Professor A.A. Chuturgoon, Dr S. Nagiah and Ms. Y. Pillay.



Ms Thilona Arumugam

28 November 2017

Date

ACKNOWLEDGEMENTS

My family

Thank you for your guidance, support and allowing me every opportunity to further my education and knowledge. I appreciate everything that you have done for me, your continuous encouragement, support and patience is deeply appreciated.

Prof Anil Chuturgoon

Thank you for the opportunity to not only grow as a scientist but to be inspired and motivated. I will always be grateful to you for your guidance, encouragement during difficult times and never allowing me to lose sight of my own worth. It is an honour to learn from a great and dedicated scientist such as yourself.

Dr Savania Nagiah

I cannot thank you enough for all your patience, advice, corrections, suggestions and contributions that enabled me to complete this dissertation and become a better scientist. You are an amazing mentor.

Ms Yashodani Pillay

Thank you for all your guidance.

Miss Terisha Ghazi and Mr. Naeem Sheik-Abdul

Thank you for all your assistance in and out of laboratory.

Fellow Master Students (2017)

To the extraordinary women that I was lucky to spend this year with; thank you for your friendship and encouragement.

National Research Foundation (NRF) and College of Health Sciences (CHS-UKZN)

I would like to thank NRF and CHS (UKZN) for scholarships and funding.

PRESENTATIONS

Fumonisin B₁ induced oxidative stress in human liver (HepG2) cells- an alternate mechanism of carcinogenesis.

Arumugam, T., Nagiah, S., Pillay, Y., Chuturgoon, A.A.

College of Health Sciences Research Symposium (5th – 6th October 2017), University of Kwa-Zulu Natal, Durban, South Africa – 2nd Prize Oral Presentation

Table of Contents

DECLARATION	ii
ACKNOWLEDGEMENTS	iii
PRESENTATIONS	iv
ABBREVIATIONS.....	ix
LIST OF FIGURES.....	xiii
LIST OF EQUATIONS	xvii
LIST OF TABLES	xviii
ABSTRACT.....	xix
CHAPTER 1 – INTRODUCTION	1
CHAPTER 2 – LITERATURE REVIEW	4
2.1. The Fumonisin	4
2.1.1 Fumonisin B ₁	4
2.1.1.1. Chemical Structure	5
2.1.1.2. Mechanism of action.....	5
2.1.1.3. Toxicity	7
A) Toxicity in animals.....	7
B) Toxicity in humans	8
2.2 Oxidative stress	8
2.2.1 Reactive oxygen species: The good, the bad and the ugly.....	9
2.2.1.1. Sources of reactive oxygen species.....	10
2.2.1.2. Molecular targets of reactive oxygen species.....	12
A) Lipid peroxidation	12
B) Protein oxidation	13
C) Deoxyribonucleic acid oxidation	14
2.2.2. Anti-oxidant response	15
2.2.2.1. Types of Anti-oxidants:.....	15
A) Enzymatic anti-oxidants:.....	15
B) Non-enzymatic anti-oxidants:.....	17
2.2.2.2. Nuclear-factor-erythroid 2 p45-related factor 2: Master regulator of the anti-oxidant response	18
2.2.3. Mitochondrial response	20

2.3. The role of oxidative stress in cancer.....	21
CHAPTER 3 – MATERIALS AND METHOD	23
3.1. Materials	23
3.2. Cell Culture	23
3.2.1. Cell culture conditions.....	23
3.2.2. Preparation of Fumonisin B ₁	23
3.2.3. Cell preparation for assays.....	23
3.3. 2',7'-dichlorodihydrofluorescein-diacetate assay	24
3.3.1. Principle.....	24
3.3.2. Protocol	24
3.4. Thiobarbituric acid reactive substances assay	24
3.4.1. Principle.....	24
3.4.2. Protocol	25
3.5. Protein Isolation, quantification and standardization	26
3.5.1. Principle.....	26
3.5.2. Protocol	27
3.6. Protein Carbonyl Assay	28
3.6.1. Principle.....	28
3.6.2. Protocol	28
3.7. Reduced glutathione assay	29
3.7.1. Principle.....	29
3.7.2. Protocol	30
3.8. Catalase activity assay.....	31
3.8.1. Principle.....	31
3.8.2. Protocol	31
3.9. Sodium dodecyl sulphate–polyacrylamide gel electrophoresis and Western Blotting ...	31
3.9.1. Principle.....	31
A) Sample preparation	31
B) Sodium Dodecyl Sulphate – Polyacrylamide Gel Electrophoresis	32
C) Western blotting.....	33
3.9.2. Protocol	34
A) Sample preparation	34
B) Sodium Dodecyl Sulphate – Polyacrylamide Gel Electrophoresis	34
C) Western blotting.....	35

3.10.1. Principle.....	37
3.10.2. Protocol.....	39
A) Ribonucleic acid isolation	39
B) Complementary deoxyribonucleic acid synthesis.....	39
C) Quantitative Polymerase Chain Reaction	39
3.11. JC-1 - Mitochondrial Membrane Potential Assay.....	40
3.11.1 Principle.....	40
3.11.2. Protocol.....	41
3.12. Statistical analysis.....	41
CHAPTER 4 – RESULTS	42
4.1. Assessment of oxidative stress	42
4.1.1. Analysis of intracellular reactive oxygen species	42
4.1.2. Lipid peroxidation.....	43
4.1.3. Protein carbonylation.....	44
4.1.4. DNA oxidation	45
4.2. The anti-oxidant response	46
4.2.1. Anti-oxidant regulation	46
4.2.2. Superoxide detoxification	47
4.2.3. Detoxification of peroxides	48
A) Catalase.....	48
B) Glutathione peroxidase and glutathione	49
4.3. Mitochondrial stress response.....	50
4.4. Expression of cancer-related genes	53
4.4.1. c-Myc expression.....	53
4.4.2. p53 expression	54
Chapter 5 – Discussion.....	55
5.1. Limitations and future studies	60
CHAPTER 6 – CONCLUSION.....	62
REFERENCES.....	63
APPENDIX A	74
APPENDIX B	75
APPENDIX C	76
APPENDIX D	77

APPENDIX E.....	78
APPENDIX F.....	79

ABBREVIATIONS

$\Delta\psi_m$	Mitochondrial Membrane Potential
8-oxoG	8-oxo-Guanine
A	Adenine
AO	Anti-oxidants
APS	Ammonium persulphate
ARE	Anti-oxidant Response Element
ATP	Adenosine-triphosphate
BCA	Bicinchoninic acid
BHT	Butylated hydroxytoluene
BSA	Bovine serum albumin
C	Cytosine
CAT	Catalase
CCM	Complete culture media
cdNA	Complementary deoxyribonucleic acid
Cu	Copper
Cu¹⁺	Cuprous ions
Cu²⁺	Cupric ions
Cul3	Cullin 3
CYP450 3A4	Cytochrome P450 3A4
DCFH	2,7-dichlorfluorescein
DEX	Dexamethasone
DNA	Deoxyribonucleic acid
DNP	2,4-dinitrophenylhydrazones
DNPH	2,4-dinitrophenylhydrazine
dNTPs	Deoxynucleoside triphosphates
e⁻	Electrons
ELEM	Equine leukoencephalomalacia
EMEM	Eagle's Essential Minimal Media
ERK	Extracellular signal-regulated kinases
ERK1/2	Extracellular signal-regulated kinases 1/2
ES	Electrophilic species
ETC	Electron transport chain
FB₁	Fumonisin B ₁

FB₂	Fumonisin B ₂
FB₃	Fumonisin B ₃
Fe	Iron
G	Guanine
GPx	Glutathione peroxidase
GR	Glutathione reductase
GSH	Glutathione (Reduced)
GSSG	Glutathione (Oxidised)
GST	Glutathione-s-transferase
h	Hours
H	Hydrogen
H₂DCF	2,7-dichlorodihydrofluorescein
H₂DCF-DA	2,7-dichlorodihydrofluorescein-diacetate
H₂O	Water
HO₂[·]	Hydroperoxyl
H₂O₂	Hydrogen peroxide
H₃PO₄	Phosphoric acid
HCl	Hydrogen chloride
HepG2	Heptatocellular carcinoma
HOCl	Hypochlorous acid
HMG	High mobility group
HNE	4-hydroxynonenal
HRP	Horse radish peroxidase
IARC	International Agency for Research on Cancer
IC₅₀	Inhibitory concentration of 50%
IDH2	Isocitrate dehydrogenase 2
Keap-1	Kelch-like ECH associated protein 1
L[·]	Lipid radical
LDH	Lactate dehydrogenase
Lon-P1	Lon-protease 1
LOO[·]	Lipid peroxy radical
MAPK	Mitogen-activated protein kinase
min	Minute
MDA	Malondialdehyde
MMP	Matrix metalloproteinase

Mn	Manganese
mRNA	Messenger ribonucleic acid
mtDNA	Mitochondrial deoxyribonucleic acid
NAD⁺	Nicotinamide adenine dinucleotide
NADPH	Nicotinamide adenine dinucleotide phosphate
Neh2	Nrf2-ECH homolog h2
Nrf2	Nuclear-factor-erythroid 2 p45-related factor 2
NTD	Neuronal tube defects
O₂	Oxygen
O₂^{•-}	Superoxide radicals
O₃	Ozone
OGG1	8-oxoG DNA glycosylase
OH	Hydroxyl
OH[•]	Hydroxyl radical
Palmitoyl CoA	Palmitoyl Coenzyme A
PBMC	Peripheral blood mononuclear cells
PBS	Phosphate buffered saline
PCA	Protein carbonyl assay
PCR	Polymerase chain reaction
PKC	Protein kinase C
pNrf2	Phosphorylated nuclear-factor-erythroid 2 p45-related factor 2
PPO	Porcine pulmonary oedema
p-ser20-p53	Phosphorylated serine 20 p53
pSirt 1	Phosphorylated sirtuin 1
PUFA	Polyunsaturated fatty acids
Q	Coenzyme Q
QH₂O	Reduced Coenzyme Q
qPCR	Quantitative polymerase chain reaction
RBD	Relative band density
RLU	Relative light units
RO[•]	Alkoxy
RO₂[•]	Peroxy/ Alkperoxy
ROOH	Alkyl hydroperoxide
ROS	Reactive oxygen species
RT	Room temperature

SDS	Sodium dodecyl sulphate
SDS-PAGE	Sodium dodecyl sulphate–polyacrylamide gel electrophoresis
SIR2	Silent information regulator 2
Sirt 1	Sirtuin 1
Sirt 3	Sirtuin 3
SOD	Superoxide dismutase
SOD2	Superoxide dismutase 2
T	Thymine
TBA	Thiobarbituric acid
TBA/BHT	Thiobarbituric acid/butylated hydroxytoluene
TBARS	Thiobarbituric acid reactive substances
TCA	Tricarboxylic acid
Tfam	Mitochondrial transcription factor A
TMED	Tetramethylethylenediamine
TTBS	Tween 20-Tris buffered saline
Zn	Zinc

LIST OF FIGURES

CHAPTER 2: LITERATURE REVIEW

Figure 2.1.	Structure of FB ₁ (Stockmann-Juvala and Savolainen 2008 – modified by author).	5
Figure 2.2.	The disruption of sphingolipid metabolism by FB ₁ (prepared by author).	6
Figure 2.3.	The most physiologically abundant ROS (prepared by author).	9
Figure 2.4.	Formation of prevalent ROS from O ₂ (prepared by author).	10
Figure 2.5.	Production of O ₂ ^{•-} via the ETC in the inner mitochondrial membrane of the mitochondria (Prepared by author).	11
Figure 2.6.	ROS reacts with lipid membranes and generates reactive aldehydes including MDA and HNE, in three phase reactions (Shah, Mahajan et al. 2014).	13
Figure 2.7.	Modification of guanine to 8-oxoG. The deoxyribose sugar of DNA is represented by dR (prepared by author).	15
Figure 2.8.	The catalytic (A) and peroxidatic (B) manner of CAT action (prepared by author).	16
Figure 2.9.	The detoxification of O ₂ ^{•-} and H ₂ O ₂ by major enzymatic A.O (prepared by author).	17
Figure 2.10.	The GSH redox cycle (prepared by author).	18
Figure 2.11.	The repression and activation of Nrf2 by Keap-1 (prepared by author).	20

CHAPTER 3: METHOD AND MATERIALS

Figure 3.1.	The reaction between 2-TBA and MDA during the TBARS assay (prepared by author).	25
Figure 3.2.	The principle of the BCA assay used to quantify proteins. Reaction A represents the reduction of Cu ²⁺ and reaction B represents the chelation of BCA to Cu ¹⁺ (prepared by author).	26

Figure 3.3.	The formation of DNP-derived protein used the detection of protein carbonyl groups (prepared by author).	28
Figure 3.4.	The glutathione cycle (prepared by author).	29
Figure 3.5.	The light producing reaction between GSH and luciferin (prepared by author).	30
Figure 3.6.	Migration of proteins through gel layers based on size (prepared by author).	33
Figure 3.7.	Signal emission after immunoblotting (prepared by author).	34
Figure 3.8.	The steps of one PCR cycle leading up to DNA amplification (prepared by author).	38

CHAPTER 4: RESULTS

Figure 4.1.	FB ₁ exposure heightened the production of intracellular ROS (**p=0.0002)	42
Figure 4.2.	Extracellular MDA concentration was significantly higher in FB ₁ treated cells (*p=0.0205).	43
Figure 4.3.	FB ₁ induced oxidative stress in HepG2 cells as evidenced by the significant increase in the concentration of protein carbonyls (**p<0.0001).	44
Figure 4.4.	The expression of <i>OGG1</i> was negatively regulated by FB ₁ (**p=0.0004).	45
Figure 4.5.	There was a decrease in total Nrf2 expression (A: p=0.1111) after FB ₁ exposure, however pNrf2 expression was significantly increased (B: *p=0.0311).	46
Figure 4.6.	SOD2 protein expression was positively regulated (A: **p= 0.0043) with an accompanying increase in <i>SOD2</i> gene expression (B: *p= 0.0172) after FB ₁ exposure.	47
Figure 4.7.	FB ₁ enhanced the protein (A: p= 0.0725) and mRNA levels (B:**p= 0.0093) of CAT however, CAT activity was significantly reduced (C:**p= 0.0032).	48
Figure 4.8.	The transcript levels of the enzymatic AO <i>GPx</i> (A: **p= 0.0001) and the associated AO, GSH (B:*p= 0.0124) was significantly higher after FB ₁ exposure.	49

Figure 4.9.	After a 24h exposure to FB ₁ , there was a minor reduction in the $\Delta m\psi$ of HepG2 cells (p= 0.2049).	50
Figure 4.10.	FB ₁ stimulated cells exhibited a significant increase in <i>TFAM</i> gene expression (*p= 0.0117).	51
Figure 4.11.	Mitochondrial stress response was heightened after FB ₁ exposure; Sirt 3 (A: ***p= 0.0003) and Lon-P1 (B: ***p= 0.0004) were both significantly upregulated.	52
Figure 4.12.	Analysis of c-Myc protein expression revealed that there was a decrease (A:p= 0.4594) however <i>c-Myc</i> transcript levels were significantly increased (B:***p= 0.0004) after exposure to FB ₁ .	53
Figure 4.13.	The protein expression of p-ser20-p53 was significantly increased post FB ₁ exposure (A: ***p<0.0001), however total p53 expression was lower (B: p= 0.0558).	54

CHAPTER 5: DISCUSSION

Figure 5.1.	Summarised account of events. FB ₁ inhibits the ETC, accelerating ROS production. Excessive ROS results in the formation of lipid peroxides and protein carbonyls. ROS also results in the phosphorylation and translocation of Nrf2 and hence the increased expression of SOD2, CAT and GPx. Tfam, Sirt 3 and Lon-P1 expression were also increased. Along with SOD2, these proteins reduce mitochondrial stress. With excessive ROS, improved functioning of the mitochondria and prolonged activation of Nrf2, FB ₁ is able to mediate cancer progression (prepared by author).	60
--------------------	--	-----------

APPENDIX A

- Figure 6** There was a 1.3 fold increase in the activity of CYP450 3A4 in FB₁ treated cells (*p<0.05). **74**

APPENDIX B

- Figure 7** FB1 significantly downregulated the expression of pSirt 1 (**p<0.0001). **75**

APPENDIX C

- Figure 8** FB₁ disrupted membrane integrity evidenced by significant LDH leakage (*p< 0.0177). There was a 1.1 fold increase in LDH leakage in FB₁ treatments. **76**

APPENDIX D

- Figure 9** Standard curve obtained from GSH standards and the equation obtained from it. **78**

APPENDIX F

- Figure 10** Amplification curve (A) and melt peak (B) analysis for *OGG1*. **79**
- Figure 11** Amplification curve (A) and melt peak (B) analysis for *SOD2* **79**
- Figure 12** Amplification curve (A) and melt peak (B) analysis for *CAT* **80**
- Figure 13** Amplification curve (A) and melt peak (B) analysis for *GPx* **80**
- Figure 14** Amplification curve (A) and melt peak (B) analysis for *Tfam* **81**
- Figure 15** Amplification curve (A) and melt peak (B) analysis for *c-Myc* **81**

LIST OF EQUATIONS

CHAPTER 3: METHOD AND MATERIALS

Equation 3.1.	Calculation used to determine the MDA concentration (in mM), where 156mM^{-1} is the extinction co-efficient of the MDA-TBA adduct.	26
Equation 3.2.	Calculation used to determine the protein carbonyl concentration of cells (in μM), where 1cm is the path length and $22\ 000\text{M}^{-1}\text{cm}^{-1}$ is the extinction co-efficient of DNP.	29
Equation 3.3.	Equation 3.3: Equation used to calculated CAT activity. Results were expressed in percentage (%).	31
Equation 3.4.	Calculation used to determine mitochondrial membrane potential.	41

LIST OF TABLES

CHAPTER 3: METHOD AND MATERIALS

Table 3.1.	Components of Laemmli buffer with their respective functions.	32
Table 3.2.	Antibodies and antibody dilutions used in western blotting.	36
Table 3.3.	The annealing temperatures and primers sequences for the genes of interest.	40

ABSTRACT

Fusarium fungal species are major contaminants of maize and produce a highly toxic mycotoxin – Fumonisin B₁ (FB₁). Fumonisin B₁ is the causative agent for many incidents of animal-related mycotoxicoses and has been implicated in human and animal cancer. Oxidative stress and mitochondrial integrity is of current research interest with regards to tumorigenesis. The aim of this study was to investigate the effect of FB₁ on oxidative stress-related survival responses in HepG2 cells.

Intracellular ROS levels (H₂DCF-DA assay), and markers of oxidative stress: lipid peroxidation (TBARS) and protein oxidation (protein carbonyl assay) were quantified using spectrophotometry. Luminometric quantification of GSH and CAT activity was determined as a measure of intracellular antioxidant potential. The relative expression of oxidative stress and mitochondrial stress response proteins (Nrf2, pNrf2, SOD2, CAT, Sirt 3 and Lon-P1) were quantified by western blotting, while gene expression levels of *SOD2*, *CAT*, *GPx*, *Tfam* and *OGG1* were assessed using qPCR. The fluorometric, JC-1 assay was used to determine mitochondrial polarisation ($\Delta\psi_m$). Lastly, the expression of cancer related proteins (c-Myc, p53 and p-ser20-p53) were also determined using qPCR and western blotting.

FB₁ significantly elevated intracellular ROS ($p \leq 0.001$), and induced lipid peroxidation ($p < 0.05$) and protein carbonylation ($p \leq 0.0001$), with a corresponding increase in GSH levels ($p < 0.05$). A significant increase in pNrf2, SOD2, *SOD2*, CAT ($p < 0.05$), *CAT* ($p \leq 0.01$), *GPx* ($p \leq 0.001$) expression was observed, however total Nrf2 ($p > 0.05$), *OGG1* expression and CAT activity ($p \leq 0.01$) was reduced. There was also a minor reduction in the $\Delta\psi_m$ of HepG2 cells ($p < 0.05$), however the expression of *Tfam* ($p < 0.05$), Sirt 3 and Lon-P1 ($p \leq 0.001$) were upregulated. Although, transcript levels of the *c-Myc* were increased ($p \leq 0.001$); protein expression was reduced ($p > 0.05$). The protein expression of p-ser20-p53 ($p < 0.0001$) was elevated, however expression of total p53 was decreased ($p > 0.05$).

Fumonisin B₁ induced oxidative stress in HepG2 cells. Although cell survival responses were initiated, the anti-oxidant capacity was not enough to deal with the excessive ROS. Furthermore, mitochondrial survival responses initiated by the cell may possibly contribute to pro-survival phenotypes, promoting tumorigenesis. This pathway may be implicated in FB₁-mediated cancer progression.

CHAPTER 1 – INTRODUCTION

Maize is a staple component in the diet of millions worldwide (Ranum, Peña-Rosas et al. 2014). This cereal crop, however, is under constant threat from pests, parasites and fungi. Fungal contamination is especially dangerous as secondary metabolites (mycotoxins) have demonstrated toxic effects in humans and animals. The *Fusarium* fungal genus is a major mycotoxin producer and maize contaminant (Fandohan, Hell et al. 2003). *Fusarium verticillioides* and *F. proliferatum* are commonly associated with maize contamination and are the most abundant producers of the Fumonisin family of mycotoxins (Rheeder, Marasas et al. 2002).

The most toxicologically significant member of the Fumonisin family is Fumonisin B₁ (FB₁). The structure of FB₁ bears close resemblance to sphingolipid precursors and therefore exerts its toxicity by inhibiting the *de novo* synthesis of sphingolipids. This inhibitory action interferes with signal transduction, cell cycle regulation and the functioning of lipid containing molecules such as cell membranes (Desai, Sullards et al. 2002, Voss, Howard et al. 2002).

Owing to FB₁'s resistance to food processing and storage conditions, it poses a significant hazard to both animal and human health. It has been linked to equine leukoencephalomalacia (ELEM); porcine pulmonary oedema (PPO) and the development of carcinomas and hepatotoxicity in rodents (Šegvić and Pepeljnjak 2001). Humans are constantly exposed to low doses of FB₁. Despite the tolerable daily intake of FB₁ being 2µg; daily intake can range from 12 to 140µg/person, peaking at 2 500µg/person in regions where maize is a staple dietary component (WHO 2012). Epidemiological studies have shown a correlation between regions with a high maize consumption and a high occurrence of oesophageal and hepatocellular carcinomas (Stockmann-Juvala and Savolainen 2008, Persson, Sewram et al. 2012). Therefore FB₁ has been classified as a class 2B carcinogen by the International Agency for Research on Cancer (IARC) (Stockmann-Juvala and Savolainen 2008).

Although a major portion of FB₁ is distributed to the liver, few studies have investigated the effects of FB₁ on the development of hepatotoxicity and liver cancer. While it is known that FB₁ is involved in tumorigenesis, the underlying mechanism of its cancer promoting properties are not well established. Recently, chromatin instability through FB₁ induced hypomethylation of global DNA has been implicated as an alternative mechanism of FB₁-mediated tumorigenesis (Chuturgoon, Phulukdaree et al. 2014).

Fumonisin B₁-induced oxidative stress has received close review in recent years, however it has not been investigated as a factor that could contribute to FB₁-mediated tumorigenesis. Oxidative

stress occurs when there is a rise in the production of reactive oxygen species (ROS) and/or reduction in the anti-oxidant (AO) capacity of cells (Birben, Sahiner et al. 2012). Mitochondria house the electron transport chain (ETC), which leaks unpaired electrons (e^-) into the mitochondrial matrix. These e^- react with molecular oxygen (O_2) to form ROS (Bratic, Larsson et al.). FB_1 is able to disrupt mitochondrial respiration by inhibiting complex I of the ETC, accelerating the generation of ROS by the mitochondria (Domijan and Abramov 2011).

The first line of defence against oxidative stress in cells is the induction of endogenous AO proteins, which scavenge ROS and dampen oxidative damage to macromolecules. Nuclear-factor-erythroid 2 p45-related factor 2 (Nrf2) is a transcription factor that regulates the Antioxidant Response Element (ARE), responsible for the expression of AO genes such as glutathione peroxidase (GPx), superoxide dismutase (SOD) and catalase (CAT) (Nguyen, Nioi et al. 2009).

Considering that dysregulation of the ETC by FB_1 is involved in the generation of excess ROS, mitochondrial health may be affected (Chen, Vazquez et al. 2003). Mitochondrial transcription factor A (Tfam), silent information regulator 3 (Sirt 3) and Lon-protease 1 (Lon-P1) contribute to mitochondrial well-being under oxidative stress conditions. Sirtuin 3 activates mitochondrial AO such as Super oxide dismutase 2 (SOD2), increasing the detoxification capacity of the mitochondria (Ansari, Rahman et al. 2017). Lon-protease 1 and Tfam do not have any direct AO capabilities; Tfam protects mitochondrial DNA (mtDNA) against oxidative damage, whereas Lon-P1 is involved in degrading oxidised proteins within the mitochondria (Bezawork-Geleta, Brodie et al. 2015, Oka, Leon et al. 2016).

Functional mitochondria are essential for the survival of cancer cells. Although high levels of ROS within the mitochondrial matrix cause mutations to mtDNA, these mutation do not usually disrupt the functioning of mitochondria but rather alter the bio-energetic and bio-synthetic states to ensure that the energy and growth requirements of cancer cells are met (Wallace 2012). While high ROS levels are beneficial to cancer cells they must be maintained at certain levels to ensure that cell death pathways are not initiated (Liou and Storz 2010). Furthermore a close relationship exists between ROS, and tumour suppressor genes (p53) and oncogenes (c-Myc and KRAS). Similarly, Nrf2 also has tumour suppressing and oncogenic properties. Nrf2 inhibits the early stages of carcinogenesis, however prolonged activation of Nrf2 promotes the survival of cancer cells (Sporn and Liby 2012).

The role of oxidative stress and the activation of Nrf2 in relation to tumorigenesis is of current research interest. While it is known that FB_1 is linked to tumorigenesis, the underlying mechanism of its cancer promoting properties are not well established. Therefore this study focused on the

effect of FB₁ on oxidative stress-related survival responses in HepG2 cells following 24 hours exposure – as an alternative mechanism of FB₁ mediated cancer progression.

1.1. Aim:

To investigate the effect of FB₁ on oxidative stress-related survival responses in HepG2 cells.

1.2. Hypothesis:

Excess ROS generated by FB₁ exposure would trigger oxidative stress-related responses and alter the expression of cancer-related proteins.

1.3. Objectives:

- ❖ To determine the extent of ROS generation and oxidative damage by FB₁ in HepG2 cells.
- ❖ To determine the Nrf2-mediated AO response and AO capacity of HepG2 cells when exposed to FB₁.
- ❖ To determine the effects of FB₁ on mitochondrial stress responses.
- ❖ To determine the effects of ROS on the expression of cancer related proteins.

CHAPTER 2 – LITERATURE REVIEW

2.1. The Fumonisin

Fungal secondary metabolism produces an assortment of diverse molecules which exhibit potent; sometimes toxic, biological activities. The adverse health outcomes in animals and humans associated with these secondary metabolites, known as mycotoxins, are often overlooked (Bennett and Klich 2003).

Humans and animals are frequently exposed to mycotoxins through the consumption of mouldy agricultural commodities such as wheat, rice, tea, sorghum, fruit, vegetables and most importantly, maize (Yazar and Omurtag 2008). Maize forms a vital part of the African staple diet due to its high yields, adaptability to different climates and versatile uses and storage capabilities (Fandohan, Hell et al. 2003).

Unfortunately, more than 60% of all maize and maize based products are contaminated by the family of mycotoxins known as Fumonisin. In addition to maize, the occurrence of Fumonisin have been reported in rice, sorghum, beans and wheat (Yazar and Omurtag 2008). Fumonisin were first isolated in 1988 during an Equine leukoencephalomalacia (ELEM) outbreak in South Africa (Marasas 2001). They are produced by the fungal genus *Fusarium* and the highest producers of fumonisin include *F. verticillioides*, *F. proliferatum* and *F. anthophilum*. Presently, there are 28 fumonisin analogues that are classified into 4 groups: A, B, C and P. Fumonisin B₁ (FB₁), Fumonisin B₂ (FB₂) and Fumonisin B₃ (FB₃) are the principal fumonisin found in maize, with FB₁ being the most predominant and toxic (Yazar and Omurtag 2008).

2.1.1 Fumonisin B₁

The first fumonisin discovered was FB₁ and it remains the most toxicologically significant. It has been reported as the causative agent for many incidents of animal related mycotoxicoses and has been implicated in both human and animal cancer (EC 2002).

Maize contaminated with FB₁ is usually symptomless; thus infected maize easily enters the food chain. It is a relatively stable compound that is temperature resistant, and can therefore persist during food processing. It is poorly absorbed when consumed and is rapidly eliminated from the body. A pool of FB₁, however, does persist in the liver and kidney, where it exerts most of its toxicity (WHO 2001).

2.1.1.1. Chemical Structure

The structure of FB₁ is represented as a diester of propane-1,2,3-tricarboxylic acid and 2-amino-12,16-dimethyl-14,15-dihydroxyecosane in which the hydroxyl (OH) groups of carbon 14 and 15 are esterified to tricarboxylic acid (TCA). Unlike most mycotoxins which consist of cyclic structures, FB₁ has a long polyketide-derived backbone to which TCA, methyl, OH and amino groups are attached (Figure 2.1) (Stockmann-Juvala and Savolainen 2008). It is a polar molecule and is therefore soluble in water and other aqueous solvents (WHO 2001).

The primary amino group in FB₁ closely resembles the sphingolipid precursors, sphinganine and sphingosine. This characteristic allows FB₁ to disrupt sphingolipid metabolism. Studies have also shown that the acetylation of the amino group in FB₁ inhibits its toxicity and ability to disrupt sphingolipid metabolism (Stockmann-Juvala and Savolainen 2008).

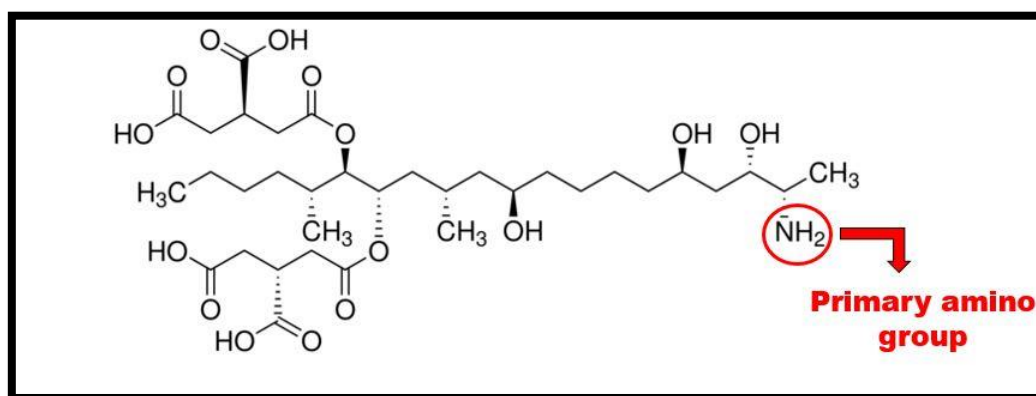


Figure 2.1: Structure of FB₁ (Stockmann-Juvala and Savolainen 2008 – modified by author).

2.1.1.2. Mechanism of action

The remarkable structural similarity between FB₁ and sphingoid bases suggests FB₁ exerts its toxicity through the disruption of sphingolipid metabolism (Heidtmann-Bemvenuti, Mendes et al. 2011). Sphingolipids are abundant in all eukaryotic cells as they form major components of membranes, lipoproteins and other lipid rich structures. They are critical in maintaining the structure of membranes and modulating the activity of receptors (Merrill, Schmelz et al. 1997). Sphingolipids and its metabolites also mediate vital signalling pathways such as differentiation, cell cycle progression, proliferation, and apoptosis (Merrill, Sullards et al. 2001).

Synthesis of sphingolipids occurs *de novo* in the endoplasmic reticulum. Serine palmitoyltransferase initiates sphingolipid synthesis by catalysing the condensation of serine and

palmitoyl Coenzyme A (palmitoyl CoA) to form 3-ketosphinganine. 3-ketosphinganine is reduced to sphinganine in a nicotinamide adenine dinucleotide phosphate (NADPH)-dependant manner (Futerman and Riezman 2005). Sphinganine can either undergo phosphorylation to form sphinganine-1-phosphate or acylation to form dihydroceramide by ceramide synthase. Dihydroceramide is desaturated to ceramide, which can then be converted to complex sphingolipids such as glycosphingolipids and sphingomyelin. As seen in figure 2.2, ceramide synthase is also responsible for reacylation of sphingosine to ceramide via the sphingolipid degradation pathway (Šegvić and Pepeljnjak 2001).

Both FB₁ and sphingoid bases contain an aminopentol backbone. Due to this similarity, ceramide synthase recognizes FB₁ as a substrate and allows it to compete with sphingoid bases for the same binding site in ceramide synthase. The tricarboxylic group of FB₁ also obstructs the fatty acyl-CoA binding site of ceramide synthase, thus inhibiting ceramide synthase (Wang, Norred et al. 1991). The inhibition of ceramide synthase impedes ceramide biosynthesis; thus obstructing the formation of complex sphingolipids; increasing sphingosine and sphinganine accumulation, and reducing reacylation of sphingosine (Figure 2.2). At high concentrations sphingoid bases become cytotoxic and can trigger cell injury and membrane degradation (Merrill, Sullards et al. 2001).

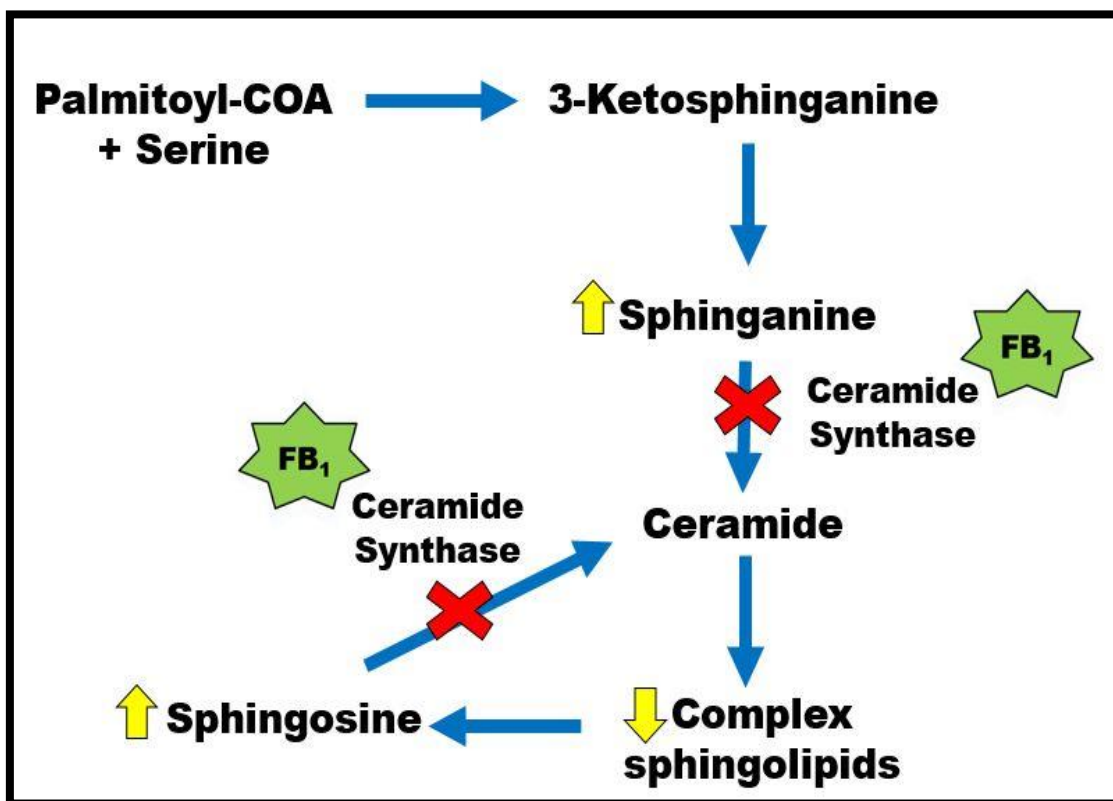


Figure 2.2: The disruption of sphingolipid metabolism by FB₁ (prepared by author).

2.1.1.3. Toxicity

A) Toxicity in animals

The pathogenic effects of FB₁ has been well established in many farm and laboratory animals. Livestock are most risk as their feed are generally contaminated by FB₁ and other mycotoxins. The liver and kidney are major targets of FB₁ in almost all animal species and, depending on the animal, may exhibit additional effects (WHO 2001).

During the twentieth century, there were several outbreaks of the fatal ELEM across a number of countries such as the Unites States and South Africa (Stockmann-Juvala and Savolainen 2008). This neurotoxic disease was associated with the consumption of mouldy corn contaminated with FB₁. It occurs only in equids and is characterised by the presence of liquefactive necrotic lesions in the subcortical white matter of the cerebrum. Necrotic lesions may also develop in the brain stem, cerebellum and spinal cord (Šegvić and Pepeljnjak 2001). Affected equids present with depression, ataxia and convulsions; and death can occur within several hours after the first symptoms occur (EC 2002). Other organs that are affected include: the liver, which shows signs of swelling and irregular white nodules; and the kidney, where nephrosis and nephropathy occur (Šegvić and Pepeljnjak 2001).

In swine, the most relevant toxicosis of FB₁ is PPO and hydrothorax (Šegvić and Pepeljnjak 2001). Swine develop PPO within a week of consuming FB₁ contaminated feed. Common symptoms include dyspnoea, cyanosis, respiratory distress, decreased heart rate and inactivity just before death (Haschek, Gumprecht et al. 2001, EC 2002). Alongside PPO, swine experience lesions and necrosis in the liver and kidney and the concentration of sphingoid bases are elevated in the lung, liver and kidney (Šegvić and Pepeljnjak 2001).

Several subacute and chronic studies with FB₁ have been performed in rat and mouse models. Nephrotoxicity and hepatotoxicity were observed in rats but only hepatotoxicity was observed in mice. FB₁-induced hepatotoxicity consisted of necrosis accompanied by changes in the lipid ratios, distortion of liver lobules, and the development of hyperplastic nodules. Nephrotoxicity was characterised by hyperplasia, necrosis of tubules, fatty changes and pyknosis (EC 2002).

The potential of carcinogenicity of FB₁ has been studied in primates, rats and mice. In some species of male rats, cholangiocarcinomas, hepatocellular carcinomas and renal tubular tumours have been observed, while female rats did not show any signs of carcinogenicity. Fumonisin B₁ also induced hepatocellular carcinomas and adenomas in male mice; while female mice were not affected (Stockmann-Juvala and Savolainen 2008). There is presently no evidence that suggests FB₁ induces carcinogenicity in primates (Šegvić and Pepeljnjak 2001).

B) Toxicity in humans

Humans are constantly exposed to low doses of FB₁. Despite the tolerable daily intake of FB₁ being 2µg (WHO 2002), consumption per day can range from 12 to 140µg/person, and peaks at 2 500µg/person in regions where maize is a staple (WHO 2012). Epidemiological studies have shown a correlation between regions with a high maize consumption and a high occurrence of oesophageal and hepatocellular carcinomas in parts of South Africa, China, Iran, Italy, United States, Zimbabwe, Kenya and Brazil (Sun, Wang et al. 2007, Stockmann-Juvala and Savolainen 2008, Ncube, Bradley C. Flett et al. 2011, Alizadeh, Rohandel et al. 2012, Persson, Sewram et al. 2012). The International Agency for Research on Cancer (IARC) has therefore classified FB₁ as a class 2B carcinogen; a class of molecules that are carcinogenic to animals and possibly humans (Stockmann-Juvala and Savolainen 2008).

Consumption of FB₁ contaminated maize by pregnant woman, is involved in development of neuronal tube defects (NTD) in their offspring. This embryonic defect results from malformation of neuronal tubes in the brain and spinal cord (WHO 2001). Folate deficiency is a major cause of NTD. Alterations in sphingolipid content of cell membranes, distorts receptors such as the folate receptor and prevents the uptake of folate which increases the risk of NTD (Sadler, Merrill et al. 2002).

Consumption of FB₁ can also lead to acute mycotoxicosis. This was evidenced by an outbreak of diarrhoea and abdominal pain in 27 villages in India after residents consumed rain damaged mouldy maize and sorghum that contained high levels of FB₁ when analysed (Stockmann-Juvala and Savolainen 2008).

2.2 Oxidative stress

Oxygen, the most essential element for living organisms, is required for the generation of adenosine triphosphate (ATP). This process results in the production ROS, which can be both beneficial and harmful to cells. Excess ROS leads to the disruption of redox signalling and damage to cellular structures. In order to neutralize the effects of excess ROS, cells employ AO to scavenge ROS and prevent/repair ROS induced damage (Kabel 2014). Oxidative stress is a condition whereby the balance between ROS and AO is shifted towards ROS. Oxidative damage has been implicated with a myriad of pathological conditions such as cancer, neurodegenerative disorders, cardiovascular diseases, auto-immune disorders and contributes to biological aging (Rahal, Kumar et al. 2014).

2.2.1 Reactive oxygen species: The good, the bad and the ugly

In vertebrates, the evolution of aerobic metabolic processes such as respiration have unavoidably led to the production of ROS. Molecular oxygen (O_2) has two unpaired e^- , which makes it prone to e^- transfer reactions. When O_2 gains an e^- it forms the reactive anion, superoxide ($O_2^{\cdot-}$) (Figure 2.4); which can be sequentially reduced to hydrogen peroxide (H_2O_2) and hydroxyl radicals (OH^{\cdot}) (Apel and Hirt 2004). Thus, ROS is the collective term used to describe unstable molecules that are primarily derived from O_2 (Gorrini, Harris et al. 2013). The most abundant ROS – which includes the radicals: $O_2^{\cdot-}$, OH^{\cdot} , peroxy (RO_2^{\cdot}), hydroperoxyl (HO_2^{\cdot}) and non-radical oxidizing agents such as H_2O_2 and ozone (O_3) – are listed in figure 2.3 (Bayir 2005).

Radicals		Non-radicals	
Superoxide	$O_2^{\cdot-}$	Hydrogen peroxide	H_2O_2
Hydroxyl	OH^{\cdot}	Hypochlorous acid	$HOCl$
Hydroperoxyl	HO_2^{\cdot}	Ozone	O_3
Alkoxy	RO^{\cdot}	Singlet oxygen	O_2
Alkperoxyl	RO_2^{\cdot}	Alkyl hydroperoxide	$ROOH$

Figure 2.3: The most physiologically abundant ROS (prepared by author).

Reactive oxygen species are double edged swords. At low concentrations ROS play an important part in mediating many metabolic and cellular processes such as gene expression, phagocytosis, immunity, proliferation, cell growth, cell death and is involved in maintaining cellular homeostasis in the body (Noori 2012). Conversely, any alterations in homeostasis that results in enhanced ROS production, can damage cell membranes via lipid peroxidation, form lethal DNA lesions and enhances protein modifications and degradation. Many more radicals are produced during this process, sparking off a chain of destruction (Jimenez-Del-Rio and Velez-Pardo 2012).

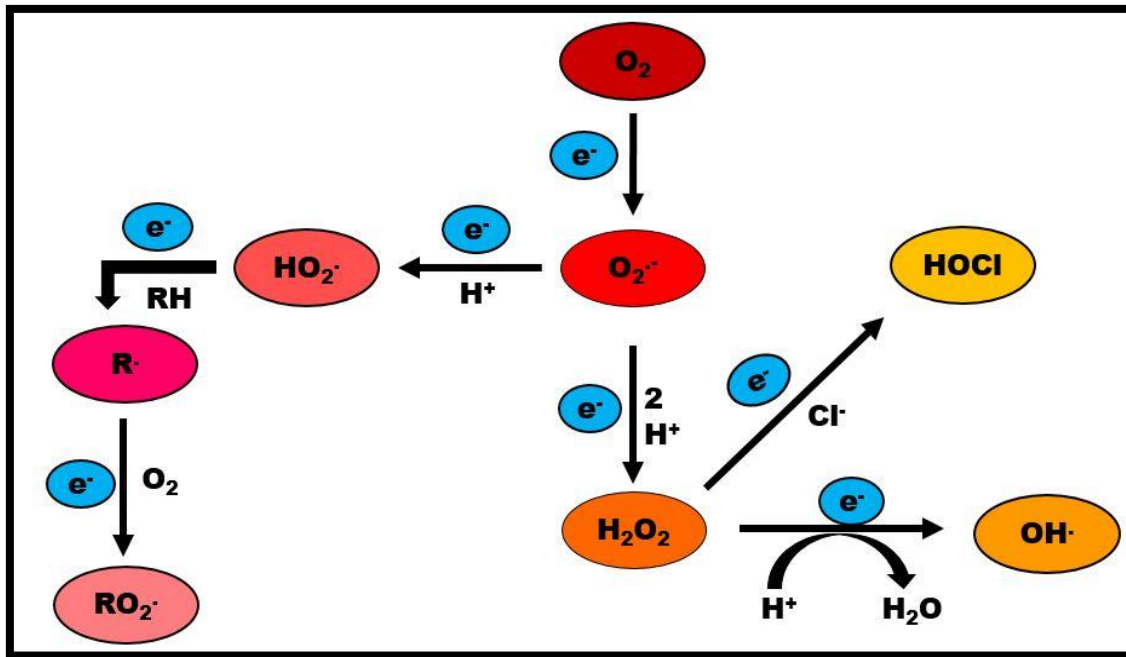


Figure 2.4: Formation of prevalent ROS from O_2 (prepared by author).

2.2.1.1. Sources of reactive oxygen species

Reactive oxygen species are produced by endogenous and exogenous sources. The major intracellular producer of ROS is the ETC in the mitochondria. Complex I and III of the ETC produces $O_2^{\cdot-}$ anions. The Q cycle in the ETC also produces $O_2^{\cdot-}$ anions. The transfer of e^- s from complex I or II to coenzyme Q (Q) results in the formation of reduced coenzyme Q (QH_2). Coenzyme Q is regenerated via a reaction between QH_2 and an unstable semiquinone anion ($Q^{\cdot-}$), which immediately transfers e^- s to O_2 , forming $O_2^{\cdot-}$ (Figure 2.5). The Q cycle is non-enzymatic, therefore increased respiration will lead to increased ROS production. Other mitochondrial components such as monoamine oxidase, p66sch and α -ketoglutarate dehydrogenase are also involved in the mitochondrial production of ROS (Phaniendra, Jestadi et al. 2015).

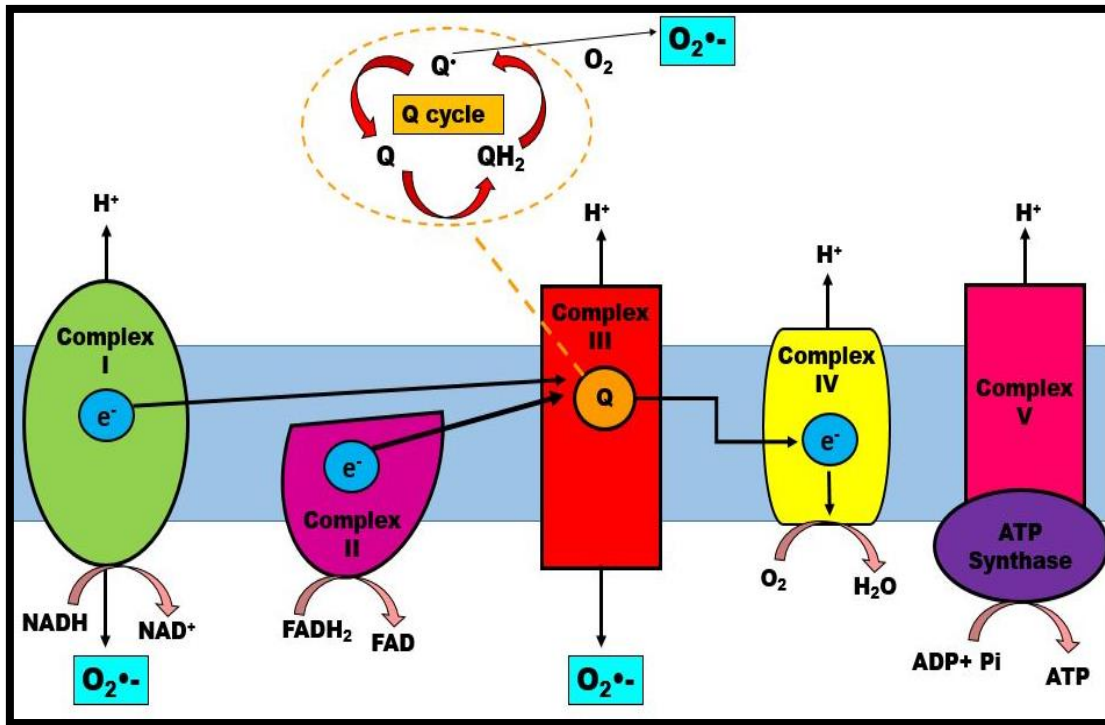


Figure 2.5: Production of O₂^{•-} via the ETC in the inner mitochondrial membrane of the mitochondria (prepared by author).

The respiratory burst produced by NADPH oxidase during the phagocytosis of microbes is the second major source of ROS in the body (Claudia Borza, Danina Muntean et al. 2013). Peroxisomes contain an array of enzymes that have been shown to produce various ROS. The respiratory pathway in peroxisomes are also involved in the transfer of e⁻ to various metabolites and leads to the formation of O₂^{•-}, OH[•], and H₂O₂. β-oxidation of fatty acids within peroxisomes generate H₂O₂ as well (Noori 2012). The endoplasmic reticulum, lysosomes and various cytochromes also contribute to endogenous ROS (Claudia Borza, Danina Muntean et al. 2013).

The body is subjected to assault from several agents that are capable of producing ROS. Cigarette smoke contains many free radicals such as O₂^{•-} and nitric oxide. Inhalation of smoke activates endogenous ROS producing mechanisms which further increase oxidative injury (Birben, Sahiner et al. 2012). Ultra violet and ionizing radiation induces the synthesis of ROS via photosensitizing agents. In the presence of O₂, these photosensitizing agents convert O₂^{•-} and organic radicals to H₂O₂ and organic hydroperoxides. Hydroperoxides can react with active redox metals to induce oxidative stress (Claudia Borza, Danina Muntean et al. 2013).

Detoxification of consumed drugs by cytochrome P450-dependant enzymes lead to the activation of O_2 and formation of ROS, which enhances lipid peroxidation (Claudia Borza, Danina Muntean et al. 2013). Exposure to O_3 and enhanced atmospheric O_2 levels also lead to lipid peroxidation and ROS formation (Birben, Sahiner et al. 2012).

Lastly, the consumption of alcohol can initiate ROS synthesis by the activation of xanthine oxidase and aldehyde oxidase. The oxidation of acetaldehyde, the primary metabolite of ethanol, results in the formation of $O_2^{\cdot-}$ (Claudia Borza, Danina Muntean et al. 2013).

2.2.1.2. Molecular targets of reactive oxygen species

Reactive oxygen species readily reacts with biological macromolecules, resulting in oxidative modifications which promote the unfolding of proteins, shortening of telomeres, and destruction of lipids, nucleic acids, small organic molecules and much more (Phaniendra, Jestadi et al. 2015).

A) Lipid peroxidation

Lipids are a diverse group of organic compounds that form major building blocks of cell membranes, and are important in maintaining the structure and function of cells (Pamplona 2008). Lipids, especially those high in polyunsaturated fatty acids (PUFA) and cholesterol, are the most vulnerable to attacks by ROS, as free radicals can easily “steal” electrons from them. Oxidative degradation of lipids is known as lipid peroxidation and has been implicated with various pathological states (Yin, Xu et al. 2011).

Lipid peroxidation is a complex process that is accomplished in 3 phases: initiation, propagation and decomposition (Figure 2.6) (Claudia Borza, Danina Muntean et al. 2013). It begins with the removal of allylic H atom from the PUFA moiety of lipids by ROO^{\cdot} or RO^{\cdot} . The carbon-centred lipid radical (L^{\cdot}) that is formed reacts with O_2 to form lipid peroxy radical (LOO^{\cdot}). LOO^{\cdot} can further propagate the peroxidation process by removing hydrogen (H) atoms from adjacent PUFA moieties. Propagation occurs until O_2 or un-oxidised PUFA moieties run out. Thereafter, LOO^{\cdot} undergo decomposition to form ROO^{\cdot} and RO^{\cdot} (Rice-Evans 1994). The accumulation of LOO^{\cdot} , ROO^{\cdot} and RO^{\cdot} accelerate the peroxidation of PUFA moieties and leads to the structural disorganization of cell membranes that may inhibit membrane bound receptors and enzymes, decrease lipid fluidity, alter membrane permeability and ion transport (Birben, Sahiner et al. 2012). Cleavage of carbon double bonds during peroxidation results in the formation of reactive aldehydes such as malondialdehyde (MDA) and 4-hydroxynonenal (HNE). Malondialdehyde and HNE are the most commonly studied products of lipid peroxidation and are measured as markers of oxidative stress (Rice-Evans 1994).

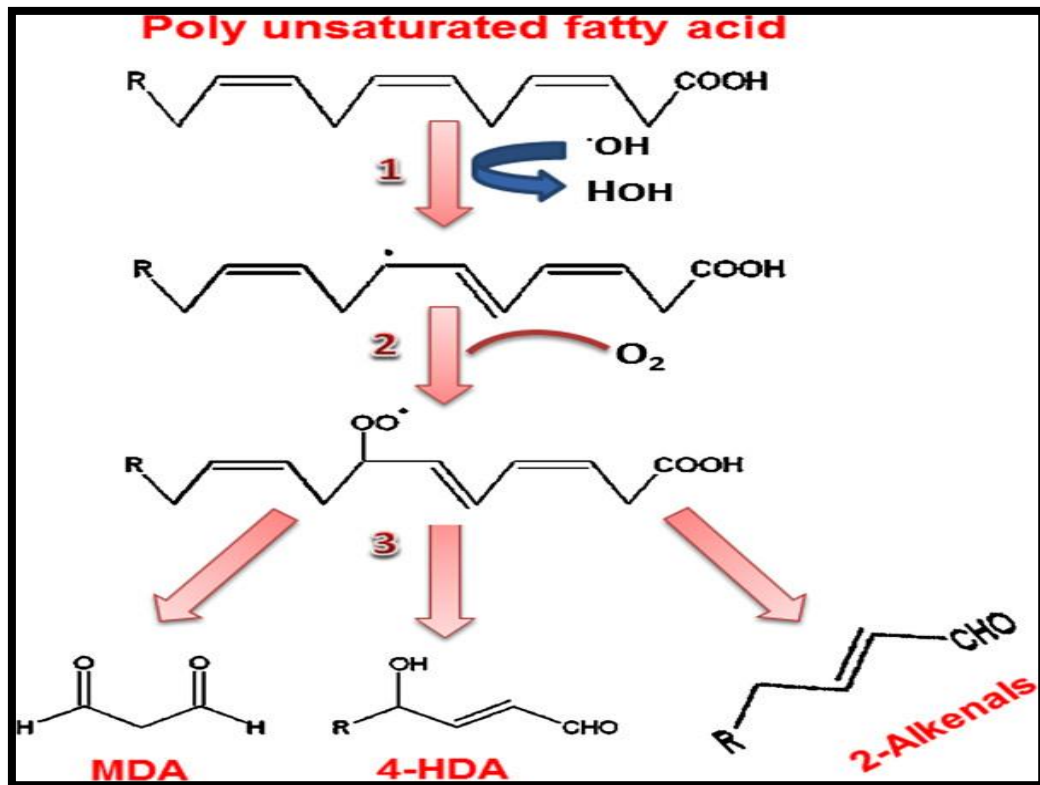


Figure 2.6: ROS reacts with lipid membranes and generates reactive aldehydes including MDA and HNE, in three phase reactions (Shah, Mahajan et al. 2014).

B) Protein oxidation

Various ROS including the by-products of lipid peroxidation interact with proteins. This often leads to oxidative modifications to amino acid residues and cofactors. These modifications result in fragmentation of polypeptide chains, alteration in electrical charges, increased proteolysis and loss of protein function (Noori 2012).

Sulphur-containing amino acids such as cysteine and methionine form key components of AO; regrettably these amino acids are the most susceptible to oxidation (Costa, Quintanilha et al. 2007). Oxidation of cysteine and methionine form thiyl radicals and methionine sulphoxide respectively. Oxidation of sulphur containing amino acid residues cause conformational changes to protein structure, unfolding and degradation (Birben, Sahiner et al. 2012).

Oxidation of basic amino acid and proline residues, as well as cleavage at acidic amino acid residues, lead to carbonylation of proteins (Birben, Sahiner et al. 2012). Carbonyl groups may also be incorporated into proteins via reactions with aldehydes produced during lipid

peroxidation. The formation of protein carbonyls is irreversible and is therefore used as a marker for protein oxidation (Berlett and Stadtman 1997, Costa, Quintanilha et al. 2007).

Hydroxyl radicals are also involved in the cleavage of the polypeptide backbone by abstracting the α -H atom of amino acid residues. This results in the formation of carbon centred radicals, which react rapidly with O_2 forming RO_2^{\cdot} , ROOH and ultimately RO^{\cdot} . Alkoxy and its intermediates can react with other amino acid residues forming new carbon centred radicals. The formation of RO^{\cdot} sets the stage for the cleavage of peptide bonds by either the diamide or α -amide pathways (Berlett and Stadtman 1997).

Proteins, especially enzymes that undergo irreversible oxidation and fragmentation can no longer function effectively and must undergo proteolytic degradation. Failure to remove this ineffective proteins allow for oxidized proteins to become severely oxidized or cross-linked (Costa, Quintanilha et al. 2007).

C) Deoxyribonucleic acid oxidation

Deoxyribonucleic acid (DNA) consists of a double helix formed from two complementary strands of nucleotides held together by H bonds between pyrimidine [thymine (T) and cytosine (C)] and purine [guanine (G) and adenine (A)] pairs (Alberts B, Johnson A et al. 2002). However ROS can disrupt this double helix via base damage, base removal, DNA strand breaks, protein-DNA cross linkage, modifications to the sugar moiety, mutations, deletions and translocations (Bayir 2005). Most of these modifications have been linked with aging, cancer, autoimmune and neurodegenerative disorders (Birben, Sahiner et al. 2012) .

Due to its low redox potential, G is the most vulnerable nucleobase to oxidation. The dominant product of G oxidation is 8-oxo-guanine (8-oxoG) (Figure 2.7) and is therefore used as a cellular biomarker of oxidative stress (Aguiar, Furtado et al. 2013). During DNA replication, DNA polymerase incorporates 8-oxoG into the nascent DNA strand. This modified nucleotide mimics T and thus produces the following transverse mutations: A:T to C:C or G:C to T:A. These mutations are possible due to the ability of 8-oxoG to pair with both cytosine and adenine (Barzilai and Yamamoto 2004). Transcription factor binding sites in the promoter regions of genes are especially prone to these mutations as they contain high GC rich sequences. Incorporation of 8-oxoG or its mutations in the transcription factor binding sites can modify the binding of transcription factors and alter the expression of genes (Birben, Sahiner et al. 2012). These mutations also promote the formation of DNA double strand breaks, which inactivate key genes, and initiates apoptosis. Removal of 8-oxoG is achieved by the base excision repair enzyme, 8-oxoG DNA glycosylase (OGG1) (Barzilai and Yamamoto 2004).

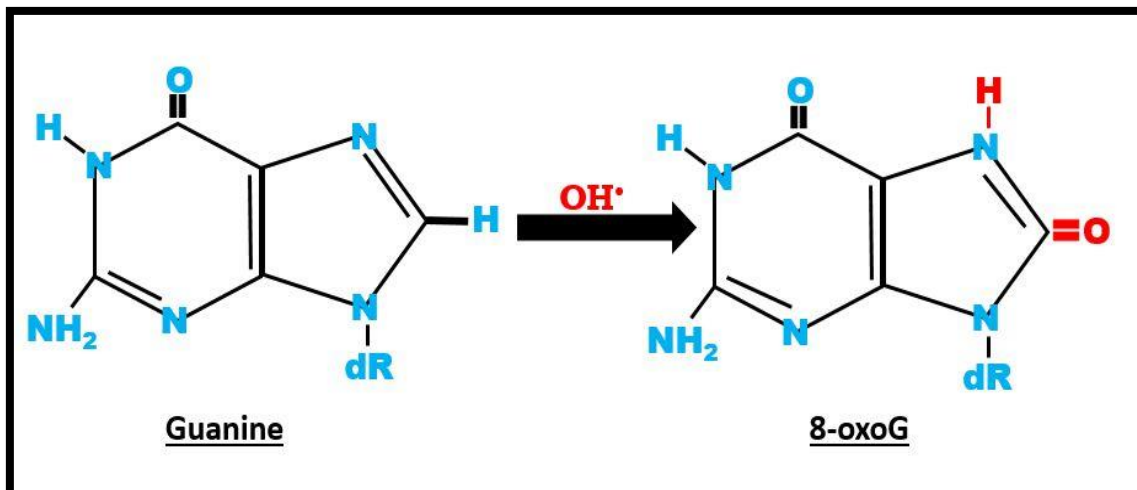


Figure 2.7: Modification of guanine to 8-oxoG. The deoxy ribose sugar of DNA is represented by dR (prepared by author).

2.2.2. Anti-oxidant response

In order to combat excess ROS, cells are equipped with a well-balanced defence mechanism mediated by an endogenous AO system. Anti-oxidants are phenol containing compounds that inhibit the oxidation of substrates and/or neutralize the possible adverse-effects of ROS. Oxidation reactions can produce free radicals, which often initiate chain reactions that lead to cell injury (Noori 2012). Anti-oxidants are often termed reducing agents because they terminate these chain reactions by removing radical intermediates and inhibiting other oxidation reactions by being oxidized themselves (Lü, Lin et al. 2010).

These free radical scavengers are present at low levels in plasma (e.g. β -carotene and ascorbic acid), cell membranes (e.g. α -tocopherol) and intracellularly [e.g. SOD and CAT] (Rahal, Kumar et al. 2014).

2.2.2.1. Types of Anti-oxidants:

Anti-oxidants can be classified into enzymatic AO and non-enzymatic AO.

A) Enzymatic anti-oxidants:

All cells in the body contain powerful AO enzymes. The 3 major classes of enzymatic AO are: SOD, CAT, and GPx (Noori 2012). Superoxide dismutase acts as the first line of defence, catalysing the conversion of $O_2^{\cdot-}$ to H_2O_2 , while CAT and GPx further detoxify H_2O_2 (Krinsky 1992).

Superoxide dismutase is of primary importance in most cells as it catalyses the dismutation and removal of $O_2^{\cdot-}$ (Kabel 2014). It also repairs damage and reduces the harmful effects of the $O_2^{\cdot-}$ by converting it to the less damaging H_2O_2 (Figure 2.9). Metals such as copper (Cu), zinc (Zn), manganese (Mn) or iron (Fe) are incorporated into SOD. Super oxide dismutase incorporated with Cu or Zn are located in the cytosol, while Mn-SOD is abundant in the mitochondria and is also known as SOD2 (Birben, Sahiner et al. 2012). Iron incorporated SOD is localized in the extra-cellular matrix. In the absence of SOD, non-enzymatic AO reduce $O_2^{\cdot-}$ but at a much slower rate (Kabel 2014) .

Although less harmful than $O_2^{\cdot-}$, H_2O_2 damages enzymes by oxidizing thiol groups and iron-sulphur centres. If not detoxified, H_2O_2 can also be further converted to OH^{\cdot} that often causes mutagenic and lethal lesions. Therefore CAT and GPx are important in catalysing the degradation of H_2O_2 to H_2O and O_2 (Sharma, Jha et al. 2012).

Catalase has one of the highest turnover rates of all enzymes; one molecule of catalase can detoxify millions of H_2O_2 molecules. Catalase consists of four 500 amino acid long polypeptide chains and four porphyrin heme containing rings that are able to react with H_2O_2 . It is highly expressed in peroxisomes of all cells with the exception of erythrocytes and can detoxify H_2O_2 in two manners i.e. catalytic manner and peroxidatic manner (Figure 2.8) (Kabel 2014). The catalytic manner catalyses the conversion of H_2O_2 into H_2O and O_2 , while the peroxidatic manner involves CAT reacting with H-donors such as methanol and ethanol. By doing so, CAT oxidizes these substrates by using an O_2 molecule from one molecule of H_2O_2 and in the process H_2O_2 is converted to water (Sichak and Dounce 1986).

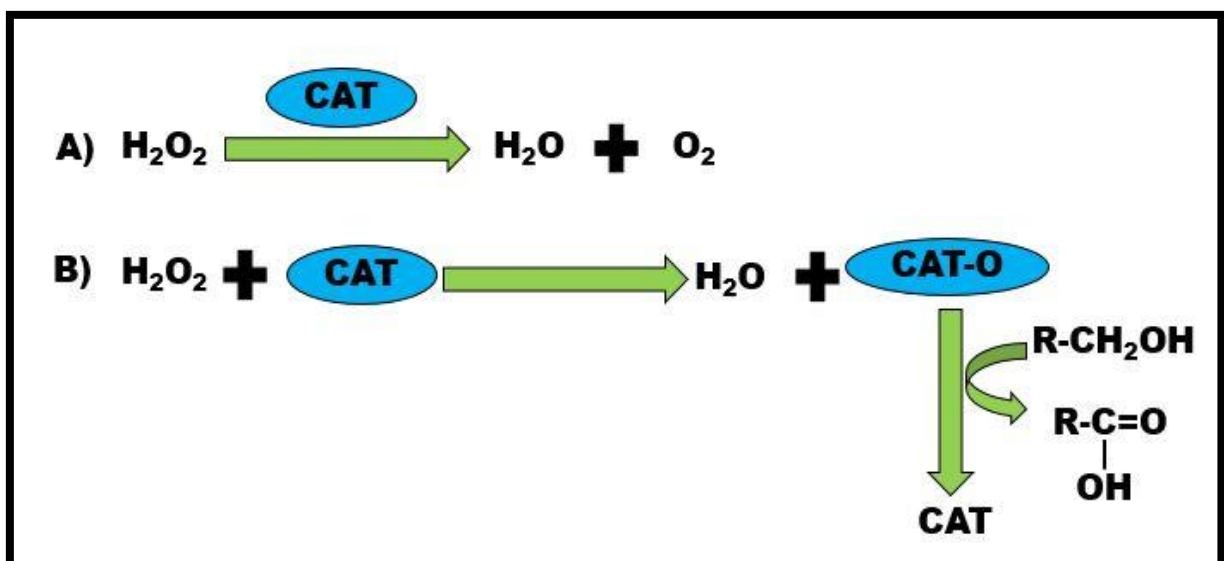


Figure 2.8: The catalytic (A) and peroxidatic (B) manner of CAT action (prepared by author).

The second H_2O_2 detoxifying enzyme is GPx. It contains the unique amino acid selenocysteine in its active sites and uses low molecular weight thiols such as glutathione as cofactors to convert H_2O_2 (Figure 2.9) and lipid peroxides to H_2O and its corresponding alcohols. Four GPx isoforms have been identified, cellular GPx (GPx-1), gastrointestinal GPx (GPx-2), extracellular GPx (GPx-3) and membrane-bound GPx (GPx-4) (Birben, Sahiner et al. 2012).

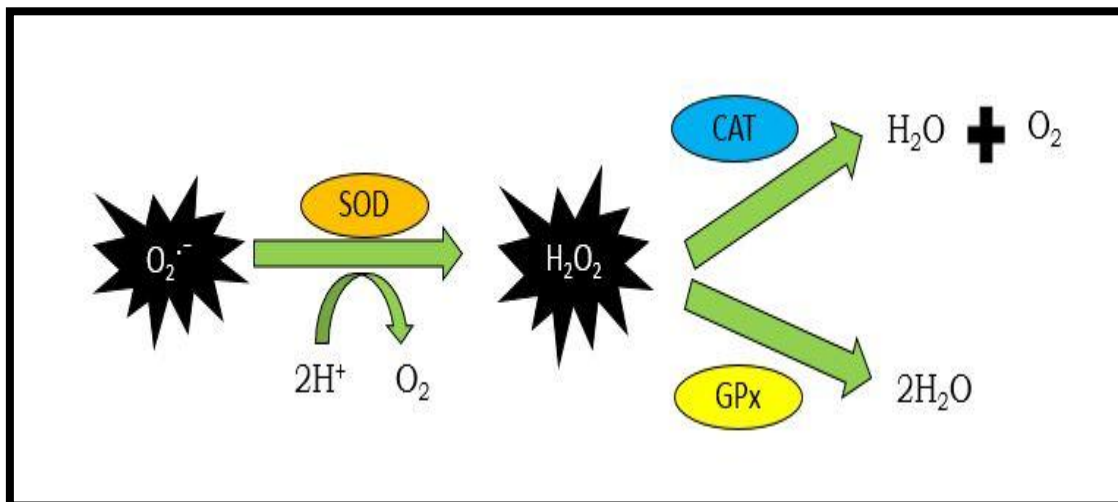


Figure 2.9: The detoxification of $\text{O}_2^{\bullet -}$ and H_2O_2 by major enzymatic AO (prepared by author).

B) Non-enzymatic anti-oxidants:

A large number of lipid/water soluble compounds have shown some measure of AO activity. Most non-enzymatic AO cannot be synthesized by the human body and are thus obtained from the diet. Major non-enzymatic AO include reduced glutathione (GSH), vitamin A, vitamin C, and vitamin D (Noori 2012).

Vitamin C (ascorbate) acts as a pro-oxidant and AO. In the presence of transition metals, vitamin C can generate oxygen free radicals. As an AO vitamin C work synergistically with vitamin E to reduce oxidised vitamin E and restore its AO properties (Patekar, Kheur et al. 2013).

Vitamin E (tocopherols and tocotrienols) is an important lipophilic AO which is localized in cell membranes. It defends membranes and lipids against peroxides by donating an e^- to peroxy radicals that are produced during lipid peroxidation chain reactions. In the process, vitamin E is oxidised to quinone; however, vitamin C is able to reverse the oxidation of vitamin E (Birben, Sahiner et al. 2012).

β -Carotene, a vitamin A precursor, also has both pro-oxidant and AO effects. At high O_2 concentration it functions as a pro-oxidant but at low O_2 concentrations it protects membranes against lipid peroxidation by scavenging peroxy, OH^\bullet and O_2^\bullet radicals (Patekar, Kheur et al. 2013).

The tripeptide, glutathione is often referred to as the body's master AO. It can be present in its reduced state – GSH; or oxidised state (GSSG). The GSH/GSSG ratio is often used as an indicator of oxidative stress (Filomeni, Rotilio et al. 2002). Reduced glutathione directly quenches OH^\bullet , and other oxygen-centred free radicals. It also acts a cofactor for thiol containing AO enzymes such as GPx and is involved in converting vitamin C and vitamin E back to their active, reduced states (Birben, Sahiner et al. 2012).

The GSH/GSSG ratio is often maintained by the recycling of GSSG back to GSH. The enzymatic AO, GPx often uses GSH as a substrate in the detoxification of peroxides such as H_2O_2 and lipid peroxides (Figure 2.10). This results in the generation of GSSG, which is subsequently reduced by glutathione reductase (GR) in a reaction that requires NADPH (Lushchak 2012).

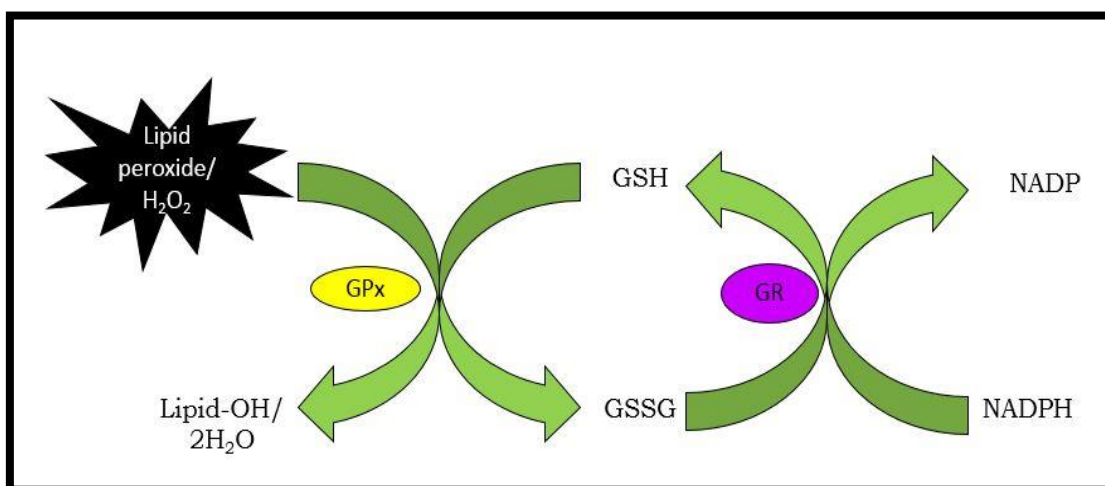


Figure 2.10: The GSH redox cycle (prepared by author).

2.2.2.2. Nuclear-factor-erythroid 2 p45-related factor 2: Master regulator of the anti-oxidant response

Numerous regulators of the AO exist but none are as important as the Nrf2-ARE signalling pathway (Itoh, Tong et al. 2004). As a basic leucine zipper transcription factor, Nrf2 integrates cellular stressors and responds by promoting the transcription of phase II and III detoxifying

enzymes, cellular regenerating enzymes, xenobiotic metabolising enzymes and AO (Jaramillo and Zhang 2013).

Under basal physiological conditions, Nrf2 is sequestered in the cytoplasm, and undergoes constant degradation through Kelch-like ECH associated protein 1 (Keap-1) ubiquitination. It was initially thought that the binding and tethering of Keap-1 to Nrf2 was involved in Nrf2 repression (Zhang 2006); however, recent studies have demonstrated that Keap-1 does not only passively sequester Nrf2 to the cytoplasm but interacts with the Nrf2-ECH homolog h2 (Neh2) domain of Nrf2. The Neh2 domain contains several lysine residues that are targets for ubiquitination by Keap-1 via cullin 3 (CUL3) ubiquitin ligase (Rojo de la Vega, Dodson et al. 2016).

Electrophilic species (ES) and ROS disrupts the Keap-1 dependant repression of Nrf2, allowing cytoplasmic accumulation and subsequent nuclear translocation of Nrf2 (Figure 2.11). The twenty-seven cysteine residues of Keap-1 are attractive targets for ROS and ES. Oxidative modification of these cysteine residues, results in structural modifications to Keap-1, weakening its activity as a ligase adaptor (Sporn and Liby 2012). This leads to the dissociation of Keap-1 from the Neh domain, allowing the accumulation of Nrf2 in the cytosol. Modifications to Nrf2 indirectly by ROS such as the phosphorylation of Nrf2's serine 40 also induces the dissociation of Nrf2 from Keap-1 (Huang, Nguyen et al. 2002). The now stabilized Nrf2 translocates to the nucleus where it binds to the ARE of its target gene. It cannot bind directly to the ARE as a monomer or homodimer; Nrf2 must first dimerize with small Maf proteins. The Nrf2-Maf dimers bind to the ARE, inducing the transcription of its target AO genes (Figure 2.11) (Nguyen, Nioi et al. 2009).

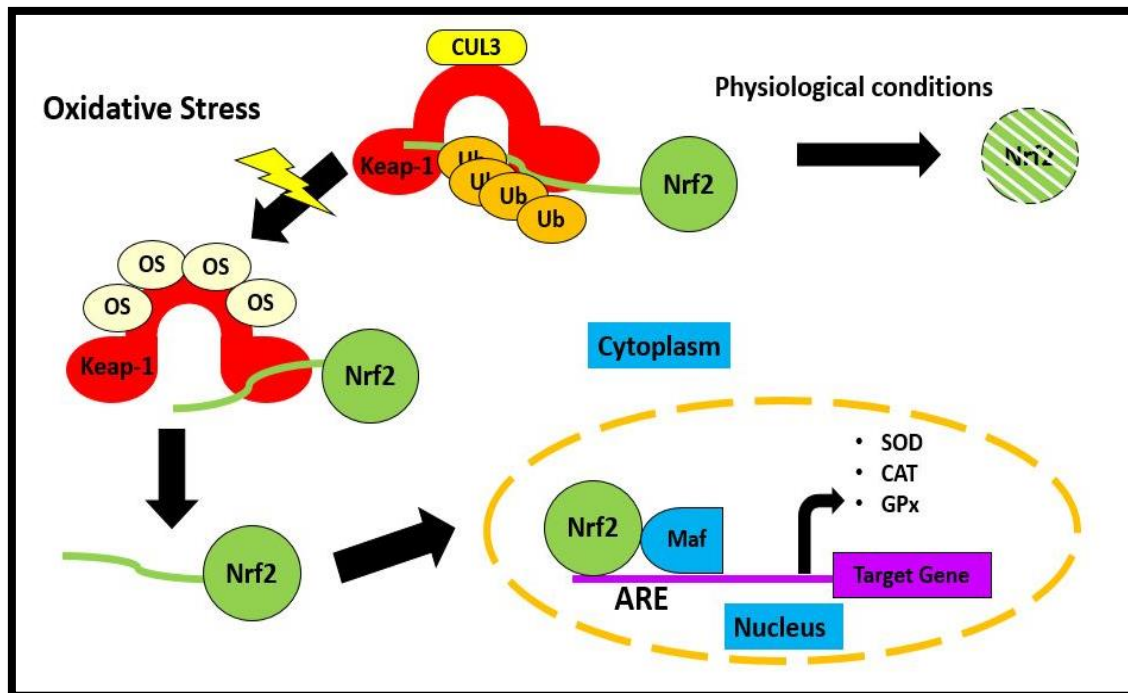


Figure 2.11: The repression and activation of Nrf2 by Keap-1 (prepared by author).

2.2.3. Mitochondrial response

Dysregulation of the ETC in the mitochondria enhances the generation of ROS within the mitochondrial matrix. In order to defend itself against oxidative damage, the expression of certain proteins are upregulated. The proteins include: Tfam, Sirt 3 and Lon-P1 and contribute to mitochondrial well-being under oxidative stress.

Sirtuin 3 is a nicotinamide adenine dinucleotide (NAD⁺)-dependant proteins that belongs to the silent information regulator 2 (SIR2) family. As it found exclusively in the mitochondria, Sirt 3 can regulate many central aspects of mitochondrial function including metabolism, ATP generation and oxidative stress responses (Ansari, Rahman et al. 2017). Oxidative stress stimulates Sirt 3 transcription which leads to the deacetylation of the mitochondrial AO, SOD2. The deacetylation of SOD2 significantly enhances its ability to scavenge ROS. Deacetylation and activation of isocitrate dehydrogenase 2 (IDH2) by Sirt 3 is also able to alleviate oxidative stress. Although IDH2 does not have any direct AO capabilities, it catalyzes the conversion of isocitrate to α -ketoglutarate; which produces nicotinamide adenine dinucleotide phosphate (NADPH). This molecule is necessary for the regeneration of GSH from GSSG (Kincaid and Bossy-Wetzel 2013).

Lon-protease 1 is also post-transcriptionally regulated by Sirt 3 (Gibellini, Pinti et al. 2014). Proteins within the mitochondrial are continuously exposed to ROS. Oxidative damage to proteins can lead to aggregation of proteins, formation of adducts, and ultimately lead to cellular dysfunction (Pinti, Gibellini et al. 2015). Damaged proteins are selectively degraded by the ATP-dependant Lon-P1; which is post-transcriptionally regulated by Sirt 3 (Gibellini, Pinti et al. 2014). The regulation of Lon-P1 is bi-phasic as it is highly inducible under transient stress, however Lon-P1 levels decline under chronic stress conditions (Ngo, Pomatto et al. 2013). Furthermore, Lon-P1 is involved in the regulation of mitochondrial gene expression and controls mtDNA copy number by degrading Tfam (Lu, Lee et al. 2013).

The mitochondrial transcription factor, Tfam is a member of the high mobility group (HMG) proteins. It is capable of binding, wrapping, bending and unwinding DNA regardless of sequence specificity (Istiaq Alam, Kanki et al. 2003). The close proximity of mtDNA to the ETC, makes it prone to attacks by ROS. Therefore mtDNA is localized in a nucleoid structure to prevent DNA oxidation. The transcription of components that form the nucleoid is activated by Tfam. Furthermore, Tfam binds directing to DNA giving it additional protection from oxidative damage (Kanki, Ohgaki et al. 2004).

2.3. The role of oxidative stress in cancer

Cancer is a complex disease in which cells undergo profound metabolic and behavioural alterations that allow for uncontrolled cell growth and ability to escape immune surveillance. (Gorrini, Harris et al. 2013). It is a multi-step process that consists of 3 stages: initiation, promotion and progression. Oxidative stress is involved in all 3 stages of cancer development. At low concentrations ROS can initiate carcinogenesis by modifying DNA which leads to gene mutations; or they can act as a signalling molecule that activate molecules linked with cancer cell growth and survival such as mitogen-activated protein kinase (MAPK) and Cyclin D1 (Reuter, Gupta et al. 2010, Sosa, Moliné et al. 2013). The promotion stage is characterised by increased cell proliferation and decreased apoptosis. Reactive oxygen species contributes to this through the disruption of cell to cell communication, induction of abnormal gene expression, modification of second messenger systems and activation of extracellular-regulated kinase 1/2 (ERK1/2) (Reuter, Gupta et al. 2010). Further DNA alterations by ROS in the rest of cell population leads to the final stage – progression (Reuter, Gupta et al. 2010). High levels of ROS also contributes to tumour invasion and metastasis through the overexpression of matrix metalloproteinase (MMP) and its secretion into the extracellular matrix (Sosa, Moliné et al. 2013).

At very high concentrations, however, ROS causes cells to detach from the cell matrix, induces severe cell damage and promotes cell death. Cancer cells have a high AO capacity that regulates ROS to levels that are beneficial to the cancer cell but at the same time higher than normal cells (Sosa, Moliné et al. 2013).

Like ROS, Nrf2 has both oncogenic and tumour suppressing properties. Nrf2 is important in suppressing carcinogenesis during its early stages (Sporn and Liby 2012). Knock out studies involving Nrf2 in mice have shown that Nrf2 protects against tumorigenesis in the stomach, bladder and skin. Further evidence supporting the protective role of Nrf2 comes from studies with mice that contain polymorphisms in the promoter regions of the Nrf2 gene. These mice had reduced Nrf2 expression and increased susceptibility to non-small cell lung cancer (Jaramillo and Zhang 2013).

In addition to promoting the survival of healthy cells, prolonged activation of Nrf2 promotes the survival of cancer cells as well. Prolonged Nrf2 activation favours the proliferation of lung, breast, ovarian and endometrial cancer cells by promoting the transcription of genes that support glucose flux and generate the building blocks of macromolecules (Gorrini, Harris et al. 2013, Jaramillo and Zhang 2013). The ability of Nrf2 to induce AO-responses that maintain balance between redox levels that initiate cell death and promote cancer cell survival is also important (Gorrini, Harris et al. 2013).

The role of oxidative stress and the activation of Nrf2 in relation to tumorigenesis is of current interest amongst researchers. While it is known that FB₁ is linked to tumorigenesis, the underlying mechanism of its cancer promoting properties are not well established. Therefore the focus of this study was to investigate the effect of FB₁ on oxidative stress-related survival responses in HepG2 cells following 24 hours exposure – as an alternative mechanism of FB₁ mediated cancer progression.

CHAPTER 3 – MATERIALS AND METHOD

3.1. Materials

Fumonisin B₁ (FB₁), isolated from *Fusarium moniliforme*, was obtained from Sigma-Aldrich (St Louis, MO, USA). The human hepatocellular carcinoma (HepG2) cell line was acquired from Highveld Biologicals (Johannesburg, South Africa). Cell culture reagents and supplements were purchased from Lonza BioWhittaker (Basel, Switzerland). Western blot reagents were procured from Bio-Rad (Hercules, CA, USA) and anti-bodies were purchased from Abcam (Cambridge, UK), Sigma-Aldrich (St Louis, MO, USA), Cell Signalling Technologies (Danvers, MA, USA) and Santa Cruz (Dallas, TX, USA). All other reagents were purchased from Merck (Darmstadt, Germany) unless otherwise stated.

3.2. Cell Culture

The liver is the first site of detoxification of harmful substances including FB₁. Exposure to the highly hepatotoxic FB₁ has been a reported cause of hepatocarcinogenicity. The liver also has a high density of mitochondria which regulates a variety of functions including cell survival and detoxification. It is for these reasons that the HepG2 cell line was used in this study.

3.2.1. Cell culture conditions

The HepG2 cells were cultured in monolayer (10⁶ cells per 25cm³ culture flask) using complete culture media [CCM: Eagle's Essential Minimal Media (EMEM) supplemented with: 10% foetal calf serum, 1% penstrepfungizone, and 1% L-glutamine] at 37°C in a humidified incubator. Every second day, cells were rinsed with 0.1M phosphate buffered saline (PBS) and reconstituted with CCM (5ml).

3.2.2. Preparation of Fumonisin B₁

A 5mM stock of FB₁ was prepared by dissolving 2mg FB₁ in 0.1M PBS (554.2µl).

3.2.3. Cell preparation for assays

Cells were allowed to reach 80% confluence in 25cm³ flasks before treatment. An inhibitory concentration of 50% (IC₅₀: 200µM) at 24 hours (h) was obtained from literature (Chuturgoon, Phulukdaree et al. 2014) and used in all subsequent assays. An untreated control, containing only CCM, was also prepared.

After the 24h incubation, cells were detached by trypsinisation and agitation; the Trypan Blue exclusion method of cell counting was employed to determine cell viability and cell number as

required per assay performed (Strober 2001). The control was used for statistical comparison against FB₁ treatment and all experiments were done in triplicate, independently from each other.

3.3. 2',7'-dichlorodihydrofluorescein-diacetate assay

3.3.1. Principle

Intracellular ROS was quantified by the simple, yet sensitive fluorometric 2',7'-dichlorodihydrofluorescein-diacetate (H₂DCF-DA) assay. Cells are treated with the membrane permeable, non-fluorescent H₂DCF-DA probe (Wan, Zhou et al. 2005). Once H₂DCF-DA is inside the cell; it is deacetylated to 2',7'-dichlorofluorescein (DCFH), which is also non-fluorescent. Within the cell, DCFH undergoes two e⁻ oxidation by ROS to form the fluorescent, 2',7'-dichlorodihydrofluorescein (H₂DCF). The fluorescence produced by H₂DCF can be measured using flow cytometry, luminometry or microscopy. (Kalyanaraman, Darley-Usmar et al. 2012).

3.3.2. Protocol

Control and treated cells (50 000 cells per treatment) were incubated in 500µl of 5µM H₂DCF-DA stain (30 minutes [min], 37°C). The stain was removed via centrifugation (400xg, 10min, 24°C) and washed twice with 0.1M PBS. Cells were resuspended in 400µl of 0.1M PBS and seeded in triplicate (100µl/well) in a 96-well opaque microtiter-plate. A blank consisting of only PBS was plated in triplicate as well. The fluorescence produced by cells were read on a Modulus™ microplate luminometer (Turner Biosystems, Sunnyvale, CA) using a blue filter with an excitation wavelength of 503nm and emission wavelength of 529nm. The fluorescence of each sample was calculated by subtracting the average fluorescence of the blank from the fluorescence of each sample.

3.4. Thiobarbituric acid reactive substances assay

3.4.1. Principle

A well-used method for assessing oxidative damage in cells is the thiobarbituric acid reactive substances (TBARS) assay, which quantifies a by-product of lipid peroxidation – malondialdehyde (MDA). This assay is based on the formation of a chromogenic adduct of thiobarbituric acid (TBA) with MDA. One molecule of MDA undergoes nucleophilic attack by two molecules of TBA to yield a pink chromogen with an absorbance maximum of 532nm (Figure 3.1). The reaction takes place optimally under high temperatures (90-100°C) and acidic conditions (Grotto, Maria et al. 2009).

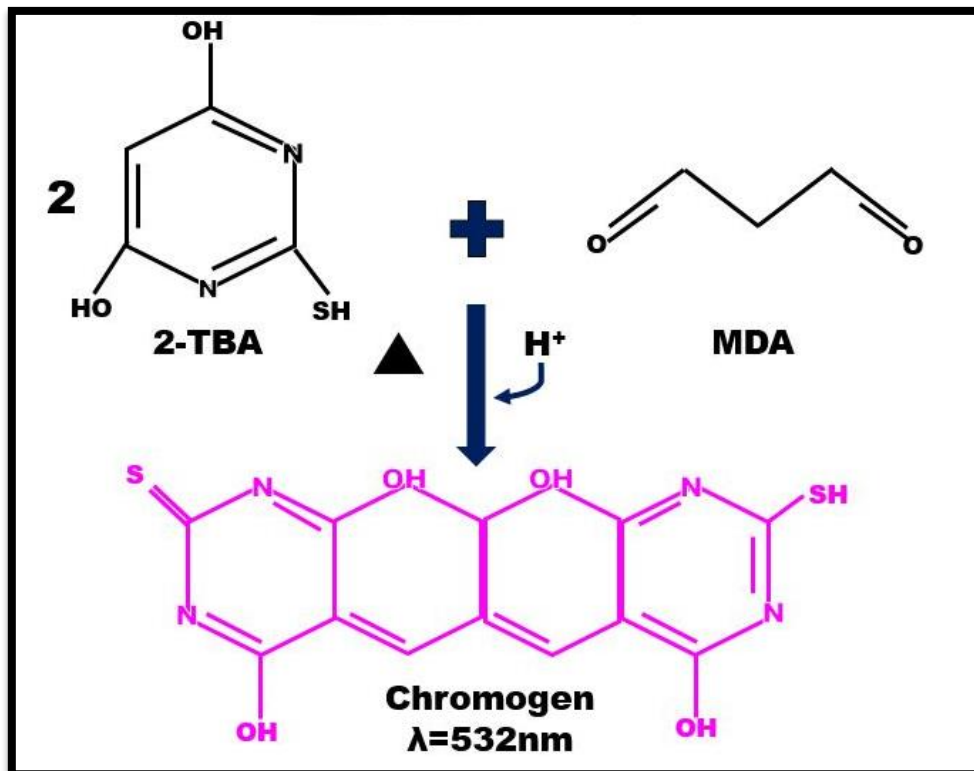


Figure 3.1: The reaction between 2-TBA and MDA during the TBARS assay (prepared by author).

Phosphoric acid (H_3PO_4) provides the acidic environment, while TBA from thiobarbituric acid/butylated hydroxytoluene (TBA/BHT) reagent detects MDA found in the sample. Formation of non-specific chromophores are inhibited by BHT and butanol is used to extract the MDA-TBA adduct from the sample (Grotto, Maria et al. 2009) .

A positive control and blank are usually prepared along with the samples. The blank does not contain any MDA and assesses contamination of reagents that would otherwise give false positives. The positive control, which contains MDA, evaluates whether the experimental procedure was done correctly.

3.4.2. Protocol

Four glass test tubes were prepared: positive control, negative control (blank), untreated control and treatment. Supernatant (400 μl) from control and FB_1 -treated cells were dispensed into the respective test tubes. Phosphoric acid (H_3PO_4) (7%, 200 μl) was dispensed into each test tube,

followed by TBA/BHT (200 μ l). Instead of TBA/BHT, hydrogen chloride (HCl) (3mM, 400 μ l) was added to the negative control and MDA (1 μ l) to the positive control. The pH of all samples were adjusted to pH 1.5 using 1M HCl and samples were boiled for 15min. Once cooled to room temperature (RT), the MDA-TBA adducts were extracted using butanol (1.5ml) and samples were allowed to settle until two distinct phases were visible. The butanol phase (500 μ l) from each sample was dispensed in triplicate into a 96-well microtiter plate. The optical density was measured using a spectrophotometer (Bio-Tek μ Quant, Winooski, VT, USA) at 532nm and a reference wavelength of 600nm. The concentration of MDA in samples were calculated using equation 3.1 (Devasagayam, Bolloor et al. 2003).

$$\text{MDA Concentration} = \frac{\text{Average Absorbance Sample} - \text{Average Absorbance Blank}}{156\text{mM}^{-1}}$$

Equation 3.1: Calculation used to determine the MDA concentration (in mM), where 156mM⁻¹ is the extinction co-efficient of the MDA-TBA adduct (Devasagayam, Bolloor et al. 2003).

3.5. Protein Isolation, quantification and standardization

3.5.1. Principle

Protein was isolated for both the protein carbonyl assay (PCA) and western blotting. The isolation process was carried out on ice to prevent proteins from degrading. Crude protein was quantified and standardized to ensure that the protein concentration was sufficient to carry out the assays and to ensure that comparisons between samples could be made (Huang, Long et al. 2010).

Protein concentration was determined using the highly sensitive, bicinchoninic acid (BCA) assay. This assay relies on two chemical reactions that take place under alkaline conditions. The first reaction is known as the biuret reaction and involves the reduction of cupric ions (Cu²⁺) to cuprous ions (Cu¹⁺) by peptide bonds (Figure 3.2). This is followed by the chelation of Cu¹⁺ with two molecules of BCA resulting in the formation of an intense purple chromophore, which has an absorbance maximum of 562nm. The protein present in the sample is directly proportional to the reduction of Cu²⁺. Furthermore, the protein concentration of samples can be determined by comparing their absorbance values with the absorbance values obtained from the bovine serum standards (BSA) (Huang, Long et al. 2010).

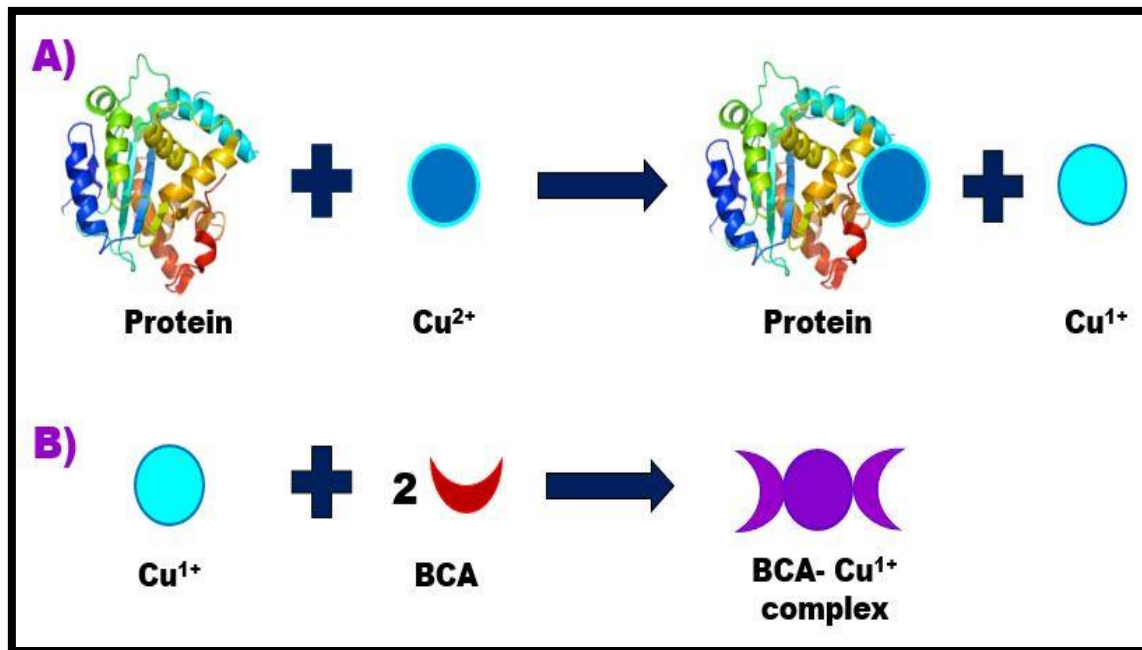


Figure 3.2: The principle of the BCA assay used to quantify proteins. Reaction A represents the reduction of Cu^{2+} and reaction B represents the chelation of BCA to Cu^{1+} (prepared by author).

3.5.2. Protocol

Protein was isolated using cell lysis buffer (200 μl) for the PCA assay and 200 μl of Cytobuster™ (Novagen, USA) supplemented with protease and phosphatase inhibitors (Roche, 05892791001 and 04906837001, respectively) for western blotting.

Cells were incubated in lysis solutions on ice for 10min, then mechanically lysed and decanted into micro-centrifuge tubes. The cell lysate was centrifuged (13 000xg, 10 min, 4°C) to obtain crude protein; which was quantified using the BCA assay.

Bovine serum albumin (BSA) standards (0–1 mg/ml) were prepared and 25 μl of sample (duplicate) and standards (triplicate) were dispensed into a 96-well microtiter plate. BCA working solution (196 μl BCA: 4 μl CuSO_4 per well) was dispensed into each well, followed by a 30min incubation at 37°C. The optical density of the samples were measured at 562nm using a spectrophotometer (Bio-Tek μQuant). The mean absorbance values of the standards were used to construct a standard curve, which determined the protein concentration of the samples. Quantified proteins were standardised to 1mg/ml using cell lysis buffer for PCA, whereas protein required for western blotting was standardised with Cytobuster.

3.6. Protein Carbonyl Assay

3.6.1. Principle

Protein oxidation was measured by quantifying intracellular protein carbonyl groups. The carbonylation of protein represents the introduction of carbonyl groups (aldehyde or ketone) into the protein structure, through several mechanisms: 1) direct oxidation of specific amino acid residues from the protein chain, 2) interaction of lipid peroxidation products and aldehyde groups (such as 4-hydroxy-2-nonenal, MDA, 2-propenal), 3) the interaction of carbonyl groups, formed from the degradation of lipids or glycooxidation. The aforementioned molecular changes occur during oxidative stress. In comparison to other oxidative changes, the carbonylation process is irreversible, therefore the final compounds are stable and can be quantified (Purdel, Margina et al. 2014).

The standard method for assessing protein carbonyls involves the derivatisation of the carbonyl groups with 2,4-dinitrophenylhydrazine (DNPH) in order to obtain 2,4-dinitrophenylhydrazones (DNP). This stable product (yellow) has an absorption maximum at 370 nm and can be quantified spectrophotometrically (Figure 3.3) (Purdel, Margina et al. 2014).

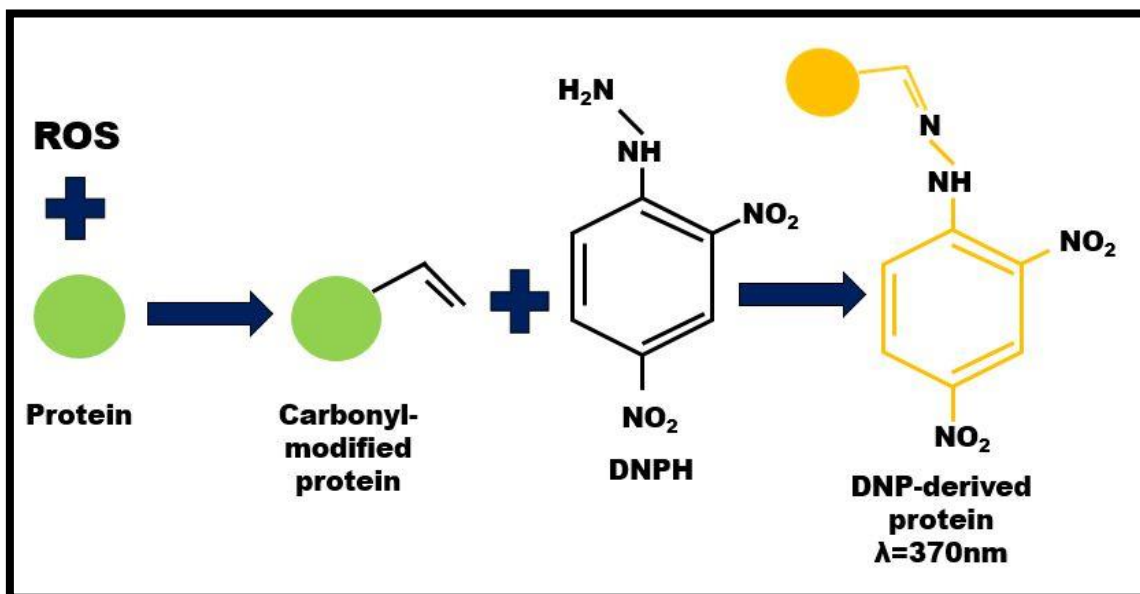


Figure 3.3: The formation of DNP-derived protein used the detection of protein carbonyl groups (prepared by author).

3.6.2. Protocol

Standardised protein was incubated at RT for 1h with DNPH (800 μL). A blank, containing standardized protein from control cells and 2.5M HCl (800 μl) was also prepared. Proteins were

precipitated with 20% Trichloroacetic acid (1ml), vortexed and centrifuged (2 000xg, 10min, 24°C). The pellet was washed twice with 1ml ethanol-ethyl acetate (1:1), this eliminated traces of DNPH and solubilized residual lipids. Lastly, proteins were dissolved in 6M guanidine HCl (1ml). Samples were incubated (10min, 37°C) before any insoluble material was removed with centrifugation (2 000g, 10min, 24°C). The supernatant was collected and dispensed in triplicate in 96-well plate (100µl/well). Absorbance was measured at 370nm using a spectrophotometer and carbonyl content was calculated using equation 3.2 (Mercier, Gatellier et al. 2004).

$$\text{Carbonyl Concentration } (\mu\text{M}) = \frac{1\text{cm} (\text{Absorbance}_{\text{sample}} - \text{Absorbance}_{\text{blank}})}{22\,000\text{M}^{-1}\text{cm}^{-1}}$$

Equation 3.2: Calculation used to determine the protein carbonyl concentration of cells (in µM), where 1cm is the path length and 22 000M⁻¹cm⁻¹ is the extinction co-efficient of DNP (Mercier, Gatellier et al. 2004).

3.7. Reduced glutathione assay

3.7.1. Principle

Glutathione is an important endogenous AO that is composed of glutamate, cysteine and glycine. It exists in either its active reduced state (GSH) or oxidised state (GSSG). Reduced GSH acts as an e⁻ donor to detoxify ROS, yielding GSSG. Recycling of GSH/GSSG is regulated by the enzymes: GPx, glutathione-s-transferase (GST), glutathione reductase (GR) and glucose-6-phosphate dehydrogenase to neutralize ROS (Figure 3.4) (Rahman, Kode et al. 2007).

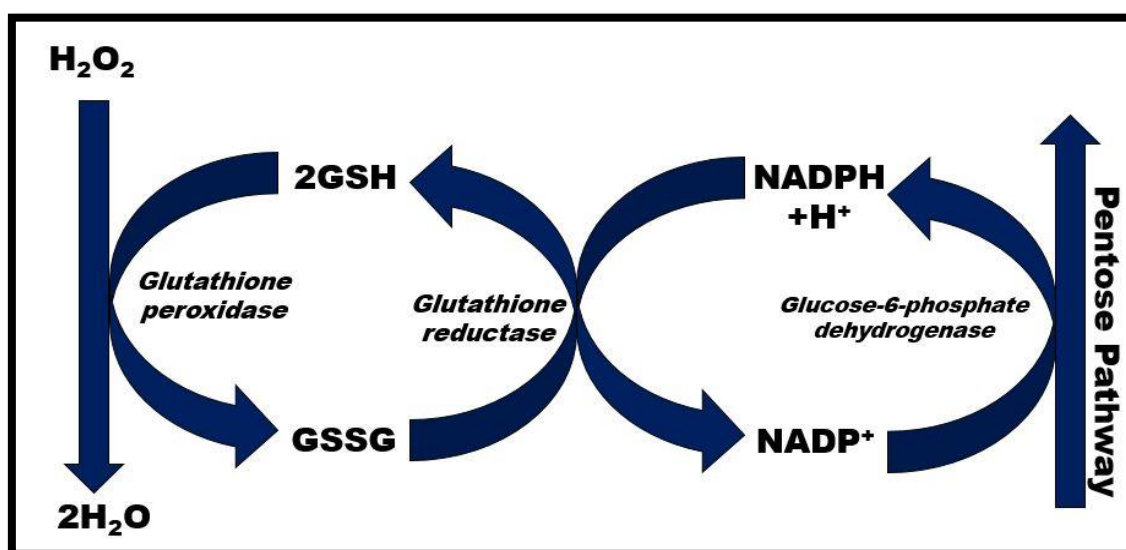


Figure 3.4: The glutathione cycle (prepared by author).

The GSH-Glo® assay is a chemi-luminescent assay that is based on the oxyluciferin-luciferase system. Luciferin-NT is converted to Luciferin, resulting in the consumption of GSH and release of ATP and O₂. Thereafter, luciferase reacts with luciferin to produce a photon of light which can be detected by a luminometer (Figure 3.5). The amount of light produced is directly proportional to the concentration of GSH in the cell (Rahman, Kode et al. 2007).

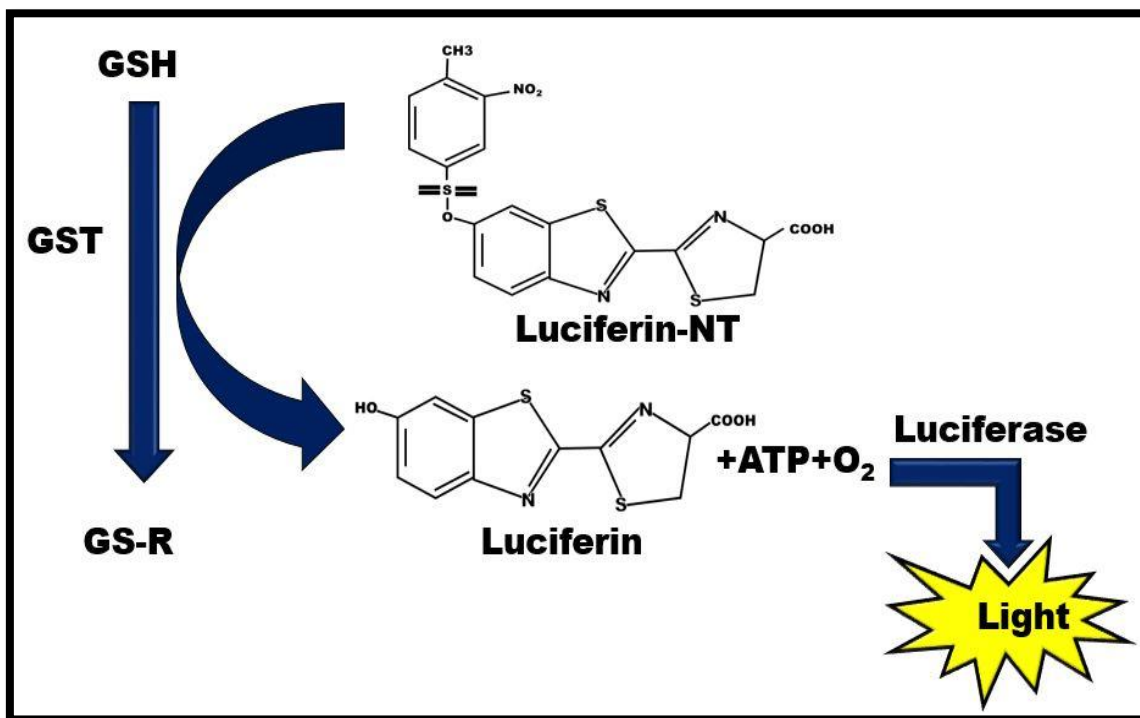


Figure 3.5: The light producing reaction between GSH and luciferin (prepared by author).

3.7.2. Protocol

Control and treated cells were transferred to an opaque microtitre plate (50µl of 20 000 cells/well in 0.1M PBS) in triplicate. Standards (0-50µM) were prepared from a 5mM stock of GSH using deionized water and dispensed in triplicate. GSH-Glo reaction solution (50µl) were added to each well and the plate was left in the dark (RT, 30min). After the 30min incubation, luciferin detection reagent (100µl) was dispensed into each well and the plate was incubated (RT, 15min). The plate was read on a Modulus™ microplate luminometer (Turner Biosystems, Sunnyvale, CA). A standard curve was generated using the standards and the GSH concentration (µM) of the sample were calculated using the standard curve.

3.8. Catalase activity assay

3.8.1. Principle

Anti-oxidants (AO) are essential in inhibiting or delaying the effects of excessive ROS. Assessing the AO capacity of cells can be used as an indicator for the occurrence of oxidative stress. Catalase (CAT) is a primary endogenous AO that detoxifies excess H₂O₂ to H₂O and O₂. A simple qualitative procedure using Triton X-100 and H₂O₂ can be used to assess catalase activity of cells. The O₂ bubbles generated from the decomposition of H₂O₂ by CAT (obtained from cells) are trapped by the surfactant Triton X-100. The trapped O₂ bubbles are visualized as foam, the test-tube height of which is measured to quantify the CAT activity (Iwase, Tajima et al. 2013).

3.8.2. Protocol

Cells were washed twice via centrifugation (400xg, 10min, 24°C) and resuspended in 0.1M PBS (400µl). The cell suspension (100µl) was pipetted into test tubes in triplicate. Triton X-100 (1%, 100µl) was added to all samples, followed by H₂O₂ (30%, 100µl). Samples were mixed thoroughly and incubated at RT for 20min. Once samples stopped bubbling, the height of the foam produced was measured. A blank consisting of Triton x-100 and H₂O₂ was prepared along with samples. Catalase activity was calculated using equation 3.3.

$$\text{Catalase activity (\%)} = \frac{\text{Height of bubbles}}{\text{Height of reaction mixture} + \text{Height of bubble}} \times 100$$

Equation 3.3: Equation used to calculate CAT activity. Results were expressed in percentage (%).

3.9. Sodium dodecyl sulphate–polyacrylamide gel electrophoresis and Western Blotting

3.9.1. Principle

Sodium dodecyl sulphate–polyacrylamide gel electrophoresis (SDS-PAGE) and western blotting are powerful techniques used for the identification of proteins. It involves the separation of proteins based on their molecular weight, transfer of these proteins onto a membrane and detection of a specific protein using immunoblotting (Kurien and Scofield 2006).

A) Sample preparation

Before separation by electrophoresis can occur, standardized proteins are prepared in Laemmli buffer and boiled for 5min in a 100°C water bath. Each component of Laemmli buffer serves a specific function that allows for optimum electrophoresis (Table 3.1). The high temperature from

boiling promotes the denaturation of proteins and breakage of disulphide bonds. (Mahmood and Yang 2012).

Table 3.1: Components of Laemmli buffer with their respective functions.

Component	Function
Glycerol	Adds density to the sample, allowing the sample to sink easily into the wells of the gel.
Sodium dodecyl sulphate (SDS)	Denatures proteins and imparts a negative charge onto them.
β-mercaptoethanol	Reduces disulphide bridges allowing for unfolding.
Bromophenol blue	Tracks migration of sample during electrophoresis.
Tris-HCl	Serves as a buffer and maintains pH of proteins during electrophoresis.

B) Sodium Dodecyl Sulphate – Polyacrylamide Gel Electrophoresis

Proteins were separated based on their molecular weight using SDS-PAGE. Charged molecules usually migrate in an electric field towards the electrode of the opposite charge. Denaturing samples in Laemmli buffer containing of SDS ensures that all proteins are uniformly charged (negative charge) and consequently migrate towards the positive electrode. Laemmli buffer also ensures proteins are in their primary form, allowing for separation to occur based on the molecular weight of the proteins and not their shape or charge (Mahmood and Yang 2012).

Proteins migrate through polyacrylamide gels, which are polymers formed by the crosslinking of acrylamide with N, N'-methylene bis-acrylamide. These crosslinks impede the migration of molecules based on their size. High percentage gels, have more crosslinks and allow for smaller molecules to pass through. Conversely, low percentage gel have larger pores and allow for larger molecules to pass through. Two types of gels are used in SDS-PAGE: resolving gel and stacking gel. The resolving gel is cast first and has a high polyacrylamide content therefore it has smaller pores, allowing better separation of proteins based on their size (Figure 3.6). In contrast to the resolving gel, the stacking gel has a low polyacrylamide content and therefore larger pores. These large pores separate proteins poorly however it serves as a start line that ensures separation begins at the same point (Mahmood and Yang 2012).

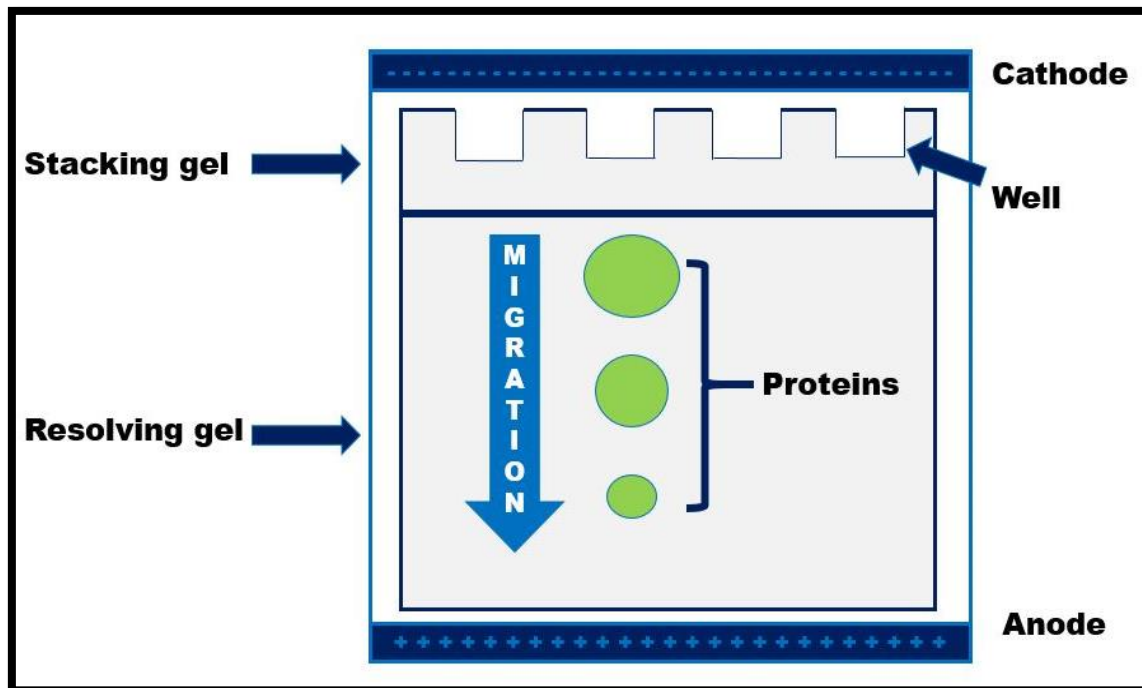


Figure 3.6: Migration of proteins through gel layers based on size (prepared by author).

C) Western blotting

Once proteins are separated; western blotting allows for the transfer of proteins from the polyacrylamide gel to a solid support such as a nitrocellulose membrane. The electrophoresed gel and membrane are sandwiched between two fibre pads and plate electrodes, which allows for uniform transfer to occur. An electric current is applied perpendicular to the surface of the gel prompting negatively charged proteins to migrate out of the gel and onto the nitrocellulose membrane (Kurien and Scofield 2006).

After transfer, proteins of interest are detected using specific antibodies. A species specific primary antibody binds to the protein of interest on the membrane, while the secondary antibody probes for the bound primary antibody. This secondary antibody is conjugated with horse radish peroxidase (HRP), which emits a signal when the secondary antibody binds to the primary antibody (Figure 3.7). The intensity of the emitted light is directly proportional to the expression

of the protein of interest. Chemiluminescent detection reagent is used to amplify the signal (Kurien and Scofield 2006).

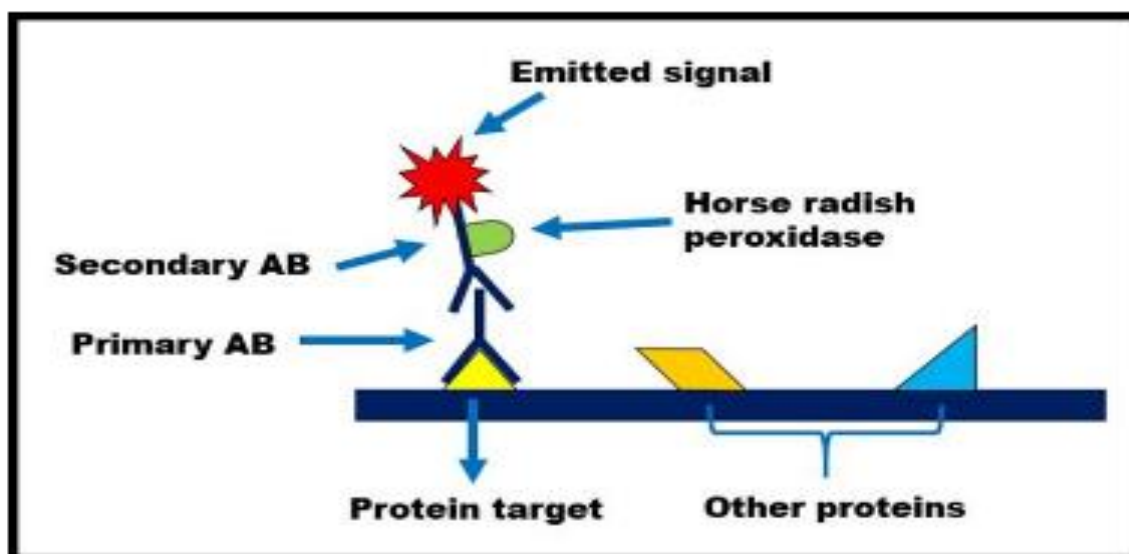


Figure 3.7: Signal emission after immunoblotting (prepared by author).

3.9.2. Protocol

A) Sample preparation

Laemmli buffer [dH₂O, 0.5M Tris-HCl (pH6.8), glycerol, 10% SDS, β-mercaptoethanol, and 1% bromophenol blue] was added to standardized proteins and boiled for 5min in a 100°C water bath.

B) Sodium Dodecyl Sulphate – Polyacrylamide Gel Electrophoresis

Gels for SDS-PAGE were prepared using the Mini-PROTEAN Tetra Cell casting frame (Bio-Rad). A 10% resolving gel [dH₂O, Tris (1.5M, pH 8.8), SDS, Bis-acrylamide, Ammonium persulphate (APS), Tetramethylethylenediamine (TEMED)] was prepared and allowed to polymerize for 1h. Thereafter, a 4% stacking gel [dH₂O, Tris (0.5M, pH 6.8), SDS, Bis-acrylamide, APS, and TEMED] was cast on top of the resolving gel. A 1cm plastic comb was placed between the glass plates to enable the formation of wells and the gel was allowed to set (40min).

Once the stacking gel was set, the gel cassettes were transferred into the electrode assembly stand and placed in the electrode tank (Mini-PROTEAN Tetra Cell System, Bio-Rad). Running buffer (25mM Tris, 192mM glycine and 0.1% SDS) was poured into the tank, the combs were removed and protein samples (25μl) along with a molecular weight marker (5μl) (Precision Plus Protein

All Blue Standards, catalogue no. #161-0373, Bio-Rad) were loaded into the wells. The tank was topped with running buffer and the samples were electrophoresed [150 volts (V), 1h] using Bio-Rad compact power supply; whilst kept on ice.

C) Western blotting

Electrophoresed gels, fibre pads and nitrocellulose membranes were placed in transfer buffer (25mM Tris, 191.8mM glycine and 20% methanol) for 10min to equilibrate. Thereafter a gel sandwich consisting of a fibre pad, nitrocellulose membrane, gel and fibre pad was prepared and placed between the two electrodes of the transfer apparatus and the separated proteins were electro-transferred onto the nitrocellulose membrane using the Bio-Rad Trans-Blot Turbo Transfer System (30 min, 20V).

After transfer, membranes were blocked in 5ml of blocking solution consisting of either 5% BSA or 5% non-fat dry milk (NFDm) in Tween 20-Tris buffered saline [TTBS: 150mM NaCl, 3mM KCl, 25mM Tris, 0.05% Tween 20, dH₂O, pH 7.5] for 1h at RT with gentle shaking to prevent non-specific binding of proteins. Immunoblotting of the membranes with primary antibodies (Table 3.2) occurred overnight (4°C). Following overnight incubation, membranes were equilibrated to RT, primary antibodies were discarded and membranes were washed using TTBS (5 times, 10 minutes). Membranes were subsequently probed with a HRP-conjugated secondary antibody (Table 3.2) for 2h at RT with gentle shaking. TTBS was used to wash membranes (5 times, 10 minutes) and protein bands were visualized using Clarity Western ECL Substrate detection reagent (BioRad, Hercules, USA). Images were captured using the Bio-Rad Chemidoc gel documentation system.

After detection, membranes were quenched with 5% H₂O₂ for 30min, incubated in blocking solution (5% BSA for 1h at RT), rinsed thrice in TTBS and probed with HRP-conjugated anti- β -actin (housekeeping protein). Protein expression was analysed using the Image Lab Software version 5.0 (Bio-Rad) and the results were expressed as relative band density (RBD). The expression of proteins of interest were normalised against β -Actin by dividing the RBD of the protein of interest by the RBD of β -actin.

The expected size of proteins probed for is as follows: pNrf2 – 68kDa; Nrf2 – 68kDa; SOD2 – 28kDa; CAT – 60kDa; Sirt 3 – 50kDa; Lon-P1 – 106kDa; c-Myc -57kDa; p-ser20-p53 – 53kDa; p53 – 53kDa and β -actin – 42kDa.

Table 3.2: Antibodies and antibody dilutions used in western blotting.

	Antibody	Dilution	Catalogue number
Primary Antibodies	Rabbit Anti-pNrf2 (phosphorylated-serine 40)	1:1 000 in 5% BSA	ab76026 (Abcam)
	Rabbit Anti-Nrf2	1:1 000 in 5% BSA	ab31163 (Abcam)
	Anti-SOD2	1:1 000 in 5% NFDM	HPA001814 (Sigma-Aldrich)
	Mouse Anti-CAT	1:1 000 in 5% NFDM	C0979 (Sigma-Aldrich)
	Rabbit Anti-Sirt 3	1:1 000 in 5% BSA	C73E3 (Cell signalling technologies)
	Rabbit Anti-Lon-P1	1:1 000 in 5% BSA	HPA002034 (Sigma-Aldrich)
	Rabbit Anti-cMyc	1:1 000 in 5% BSA	9402S (Cell signalling technologies)
	Rabbit Anti-p53 (phosphorylated-serine 20)	1:1 000 in 5% BSA	9287S (Cell signalling technologies)
	Rabbit Anti-p53	1:1 000 in 5% BSA	Sc-6243 (Santa Cruz)
Secondary Antibodies	Goat Anti-mouse IgG HRP	1: 10 000	Sc-2005 (Santa Cruz)
	Goat Anti-rabbit IgG HRP	1:10 000	sc-2004 (Santa Cruz)
Housekeeping antibody	Anti- β -actin	1:5 000 in 5% BSA	A3854 (Sigma-Aldrich)

3.10. Real time quantitative polymerase chain reaction

3.10.1. Principle

Conventional polymerase chain reaction (PCR) is used for the rapid amplification of specific gene sequences. The thermostable *Taq* polymerase drives the synthesis of complementary DNA (cDNA) strands by adding deoxynucleoside triphosphates (dNTPs) to oligonucleoside primers that are complementary to the DNA sequence flanking the target gene (Pestana, Belak et al. 2010). For PCR to occur, the following components are necessary:

- DNA template – Contains the target sequence
- Forward and Reverse primers – Binds to the 3' ends of the forward and reverse strands of the target sequence
- *Taq* polymerase – Catalyses the synthesis of new strands of DNA complementary to the target sequence
- Deoxynucleoside triphosphates (dNTPs) –Building blocks required for the synthesis of new DNA strands
- $MgCl_2$ – Stabilizes DNA and ensures the optimal functioning of *Taq* polymerase
- Buffer system – Maintains optimum pH for PCR reaction to occur

The PCR reaction is performed in a thermocycler where it undergoes repetitive cycling of three steps at different temperatures. The three steps include: denaturation, annealing and extension (Figure 3.8). Denaturation is initiated at 95°C and ensures that the H bonds between double stranded DNA are broken, producing single stranded DNA. The temperature is then lowered to 55°C to allow for the annealing step. During annealing, primers hybridize to complementary sequences flanking the 3' end of the target sequence. The temperature is then raised to 72°C, which allows for optimal *Taq* polymerase activity during the extension step. *Taq* polymerase attaches dNTPs to the annealed primers, forming a copy of the DNA target gene. These three steps make up one cycle of a PCR reaction (Figure 3.8). This cycle is repeated 30 to 40 times to achieve acceptable amplification (Arya, Shergill et al. 2005).

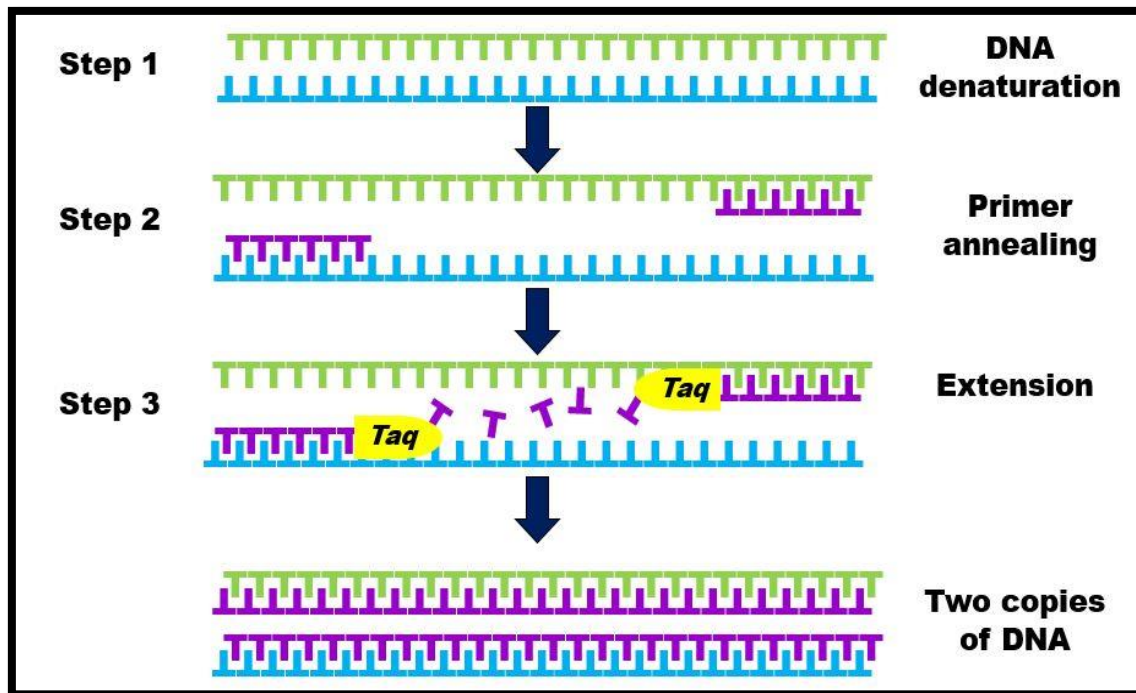


Figure 3.8: The steps of one PCR cycle leading up to DNA amplification (prepared by author).

Conventional PCR allows for the exponential amplification of the DNA target sequence but it does not have the ability to quantify PCR amplicons. Quantitative PCR (qPCR) overcomes this problem, as it is able to measure the PCR amplicons generated during each cycle of the PCR process (Pestana, Belak et al. 2010). Amplicons are detected using the DNA-intercalating dye, SYBR[®] Green 1, which fluoresces intensely when it binds to the minor grooves of double stranded DNA. The intensity of the fluorescence emitted is therefore directly proportional to the double stranded DNA present (Arya, Shergill et al. 2005).

Along with the gene of interest, samples are analysed for expression of a house keeping gene, and the amount of target DNA is reported relative to the amount of the house keeping gene for each sample. Housekeeping genes are usually expressed at constant levels among different tissues at all stages of development and their expression levels should remain relatively constant amongst samples (Arya, Shergill et al. 2005). This provides a control by which the quantity of the amplified target gene can be measured. Gene expression is analysed by comparing the target gene with the house-keeping gene using the Livak and Schmittgen method of quantitation reported as fold change ($2^{-\Delta\Delta Ct}$) (Livak and Schmittgen 2001).

3.10.2. Protocol

A) Ribonucleic acid isolation

Once treatment was removed, cells were incubated with 500µl of Qiazol (Qiagen, Hilden, Germany) and 500µl of 0.1M PBS (5min, RT). Cells were mechanically lysed transferred into eppendorfs and stored overnight in Qiazol (-80°C). Chloroform (100µl) was added to thawed samples and centrifuged (2 000xg, 15min, 4°C). Isopropanol (250µl) was added to the collected supernatant and samples were left overnight (-80°C). Thawed samples were centrifuged (12 000xg, 20min, 4°C), the supernatant was removed and the pellet was washed with 500µl of ethanol (75%). Thereafter, samples were centrifuged (7 400xg, 15min, 4°C) and the pellet was allowed to air dry (10min). The RNA pellet was resuspended in nuclease free water (15µl) and placed on ice. The RNA was quantified using the Nanodrop2000 spectrophotometer and the A260/A280 ratio was used to assess the RNA integrity. The concentration of RNA was standardised to 1 000ng/µl and used to prepare cDNA.

B) Complementary deoxyribonucleic acid synthesis

Standardised RNA was used to synthesize cDNA using the iScript cDNA synthesis Kit (Bio-Rad) as per manufacturer's instructions. A reaction mix containing: 5x iScript reaction (2µl), iScript reverse transcriptase (0.5µl), nuclease free water (1µl) and standardized RNA template (1µl), was prepared for each sample. The samples were then incubated in a thermocycler (GeneAmp® PCR System 9700, Applied Biosciences) for 40min (5min at 25°C, 30min at 42°C and 5min at 85°C).

C) Quantitative Polymerase Chain Reaction

Gene expression was analysed using the ssoAdvanced™ Universal SYBR® Green Supermix kit (Bio-Rad), according to the manufacturer's instructions. The mRNA expressions of *OGG1*, *CAT*, *SOD2*, *GPx*, *c-myc* and *Tfam* were investigated using specific forward and reverse primers (Table 3.3). *GAPDH* was used as a house-keeping gene. Reaction volumes consisting of the following were prepared: SYBR green (5µl), forward primer (1µl), reverse primer (1µl) and nuclease free water (2µl) and cDNA template (1µl). All reactions were carried out in triplicate.

The samples were amplified using a CFX96 Touch™ Real-Time PCR Detection System (Bio-Rad). The initial denaturation occurred at 95°C (4min), followed by 37 cycles of denaturation [95°C, 15 second (sec)]; annealing (40sec; Temperatures – Table 3.3) and extension (72°C, 30 sec) followed by a plate read. The method described by Livak and Schmittgen was employed to determine the changes in relative mRNA expression, where $2^{-\Delta\Delta C_t}$ represents the fold change observed in mRNA expression (Livak and Schmittgen 2001). The expression of the gene of

interest was normalised against the house-keeping gene, *GAPDH*, which was amplified simultaneously under the same conditions.

Table 3.3: The annealing temperatures and primer sequences for the genes of interest.

Gene	Annealing temperature	Primer	Sequence
<i>OGGI</i>	60°C	Forward	5'-GCATCGTACTCTAGCCTCCAC-3'
		Reverse	5'-AGGACTTTGCTCCCTCCAC-3'
<i>CAT</i>	58°C	Forward	5'-TAAGACTGACCAGGGCATC-3'
		Reverse	5'-CAACCTTGGTGAGATCGAA-3'
<i>GPx</i>	58°C	Forward	5'-GACTACACCCAGATGAACGAGC-3'
		Reverse	5'-CCCACCAGGAACTTCTCAAAG-3'
<i>SOD</i>	57°C	Forward	5'-GAGATGTTACACGCCAGATAGC-3'
		Reverse	5'-AATCCCCAGCAGTGGGAATAAGG-3'
<i>c-Myc</i>	55°C	Forward	5'-AAACACAACTTGAACAGCTAC-3'
		Reverse	5'-ATTTGAGGCAGTTTACATTATGG-3'
<i>Tfam</i>	50°C	Forward	5'-TATCAAGTGCTTATAGGC-3'
		Reverse	5'-CACTCCTCAGCACCATATTTTCG-3'
<i>GAPDH</i>		Forward	5'-TCCACCACCCTGTTGCTGTA-3'
		Reverse	5'-ACCACAGTCCATGCCATCAC-3'

3.11. JC-1 - Mitochondrial Membrane Potential Assay

3.11.1 Principle

Mitochondrial membrane potential ($\Delta\psi_m$) is an indicator of cellular health. The ETC maintains the membrane potential of the mitochondria therefore any changes to the ETC alters $\Delta\psi_m$. Cationic fluorescent dyes such as the JC-1, Rhodamine and Tetramethylrhodamine methyl ester; are able to penetrate the mitochondria and can be used to measure $\Delta\psi_m$. These cations have an affinity for the negative potential across the inner mitochondrial membrane and are able to accumulate within the mitochondria. Therefore, the more negative the $\Delta\psi_m$, the more cationic dye will accumulate within the mitochondria, emitting fluorescence which can be quantified. In

this study the JC-1 dye was used as it has been reported to be the most reliable indicator of $\Delta\psi_m$ (Perry, Norman et al. 2011).

3.11.2. Protocol

Control and treated cells (50 000 cells per treatment) were incubated in 200 μ l of 5 μ g/ml JC-1 stain (BD Biosciences, San Jose, NJ, USA) (20min, 37°C). The stain was removed via centrifugation (400xg, 10min, 24°C) and the cells were washed twice using JC-1 staining buffer. Cells were resuspended in 400 μ l of JC-1 staining buffer and seeded in an opaque 96 well plate in triplicate (100 μ l/well). A blank containing only JC-1 staining buffer was plated in triplicate as well (100 μ l/well). Fluorescence was quantified on a Modulus™ microplate reader (Turner Biosystems, Sunnyvale, CA). JC-1 monomers was measured using a blue filter with an excitation wavelength of 488nm and emission wavelength of 529nm, while JC-1 aggregates were measured using a green filter with an excitation wavelength of 524nm and emission wavelength of 594nm. Mitochondrial membrane potential was calculated using equation 3.3.

$$\begin{aligned} \text{Blue Filter: } & \text{Fluorescence}_{\text{Sample}} - \text{Average Fluorescence}_{\text{Blank}} = \text{Fluorescence}_{\text{Monomers}} \\ \text{Green Filter: } & \text{Fluorescence}_{\text{Sample}} - \text{Average Fluorescence}_{\text{Blank}} = \text{Fluorescence}_{\text{Aggregates}} \\ & \frac{\text{Fluorescence}_{\text{Aggregates}}}{\text{Fluorescence}_{\text{Monomers}}} = \text{Fluorescence}_{\text{final}} \end{aligned}$$

Equation 3.3: Calculation used to determine mitochondrial membrane potential

3.12. Statistical analysis

Microsoft Excel 2013 and GraphPad Prism version 5.0 (GraphPad Software Inc., California) were used to perform all statistical analyses. The unpaired t-test was used for all assays. All results were represented as the mean \pm standard deviation unless otherwise stated. A value of $p < 0.05$ was considered statistically significant.

CHAPTER 4 – RESULTS

4.1. Assessment of oxidative stress

Oxidative stress was evaluated by measuring changes in intracellular ROS, lipid peroxidation, protein carbonylation and *OGG1* transcript expression levels.

4.1.1. Analysis of intracellular reactive oxygen species

Intracellular ROS levels following FB₁ exposure was assessed using the H₂DCF-DA assay. There was a significant increase in intracellular ROS generated by FB₁ (116200±9020 RFU) exposure when compared to control cells (34740±5739 RFU) (Figure 4.1).

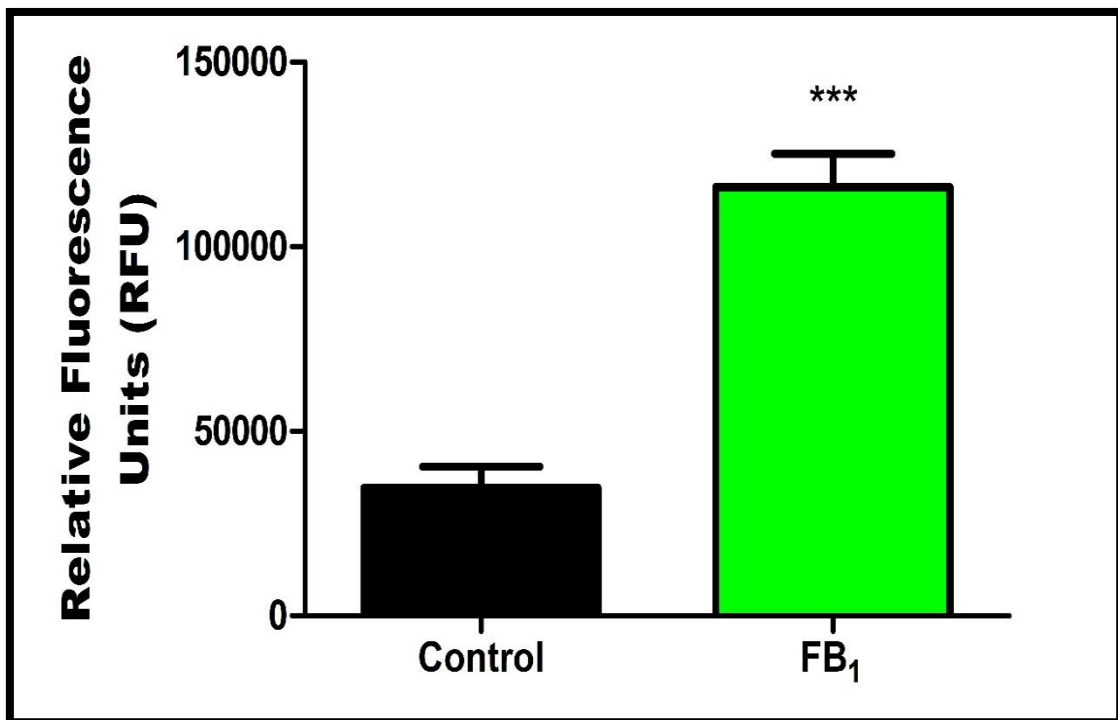


Figure 4.1: FB₁ exposure heightened the production of intracellular ROS (**p=0.0002).

4.1.2. Lipid peroxidation

Lipid peroxidation was measured by quantifying its by-product – MDA. Higher levels of MDA were observed in FB₁ treated cells in relation to control cells (Control: 0.1517±0.01443µM vs FB₁: 0.1857±0.006506µM) (Figure 4.2).

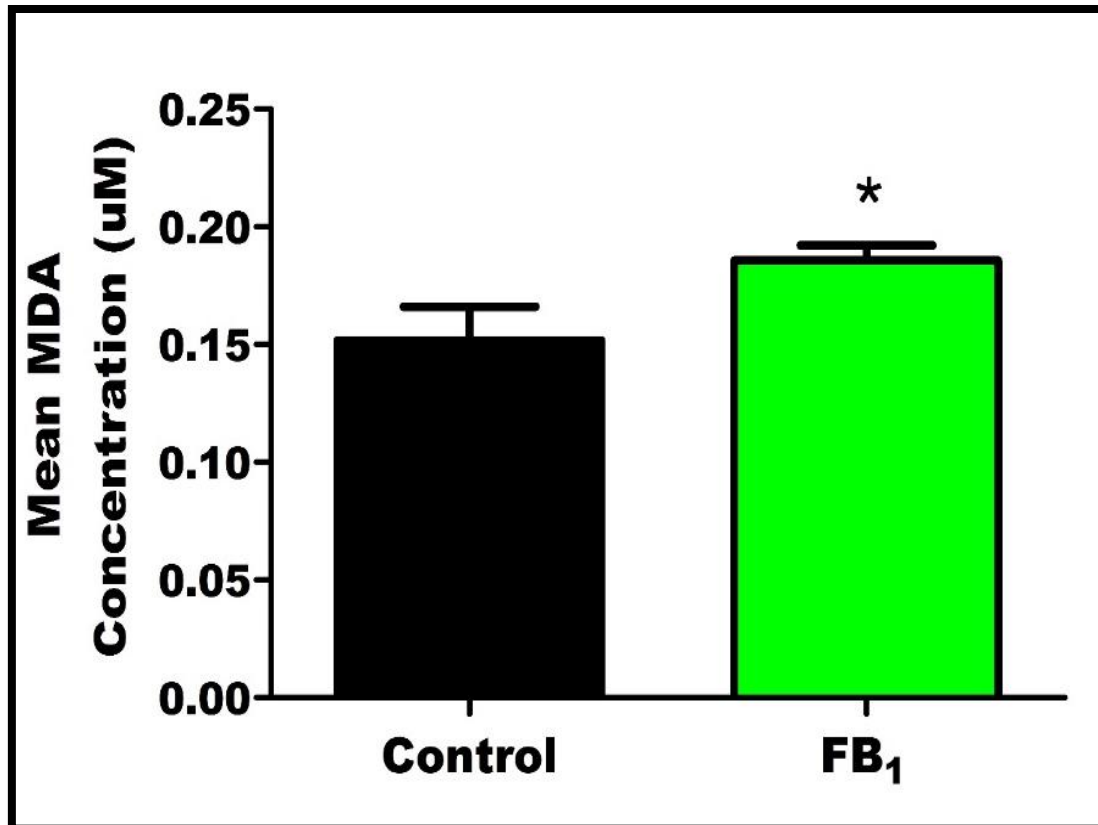


Figure 4.2: Extracellular MDA concentration was significantly higher in FB₁ treated cells (*p=0.0205).

4.1.3. Protein carbonylation

The protein carbonyl assay assessed ROS-induced damage to proteins by quantifying the concentration of protein carbonyls. Cellular protein carbonyls formed after FB₁ exposure were 11.9 fold higher than control cells (Control: 3.877±0.1202 nmol/mg vs 44.10±1.104 nmol/mg) (Figure 4.3).

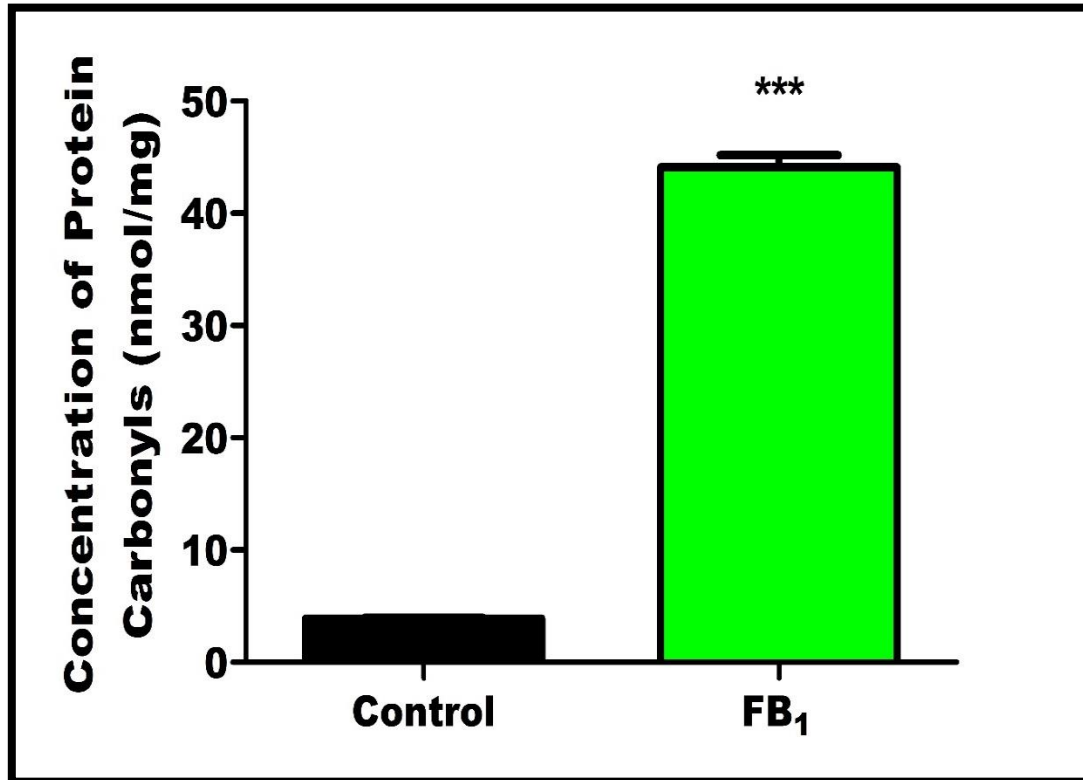


Figure 4.3: FB₁ induced oxidative stress in HepG2 cells as evidenced by the significant increase in the concentration of protein carbonyls (**p<0.0001).

4.1.4. DNA oxidation

The mRNA expression of the oxidative DNA base excision enzyme, *OGG1* was used as an indirect measurement of DNA oxidation. The expression of *OGG1* was negatively regulated in FB₁-treated cells (0.2976±0.1115 fold) in contrast to control cells (1.000±5.528×10⁻⁷ fold) (Figure 4.4).

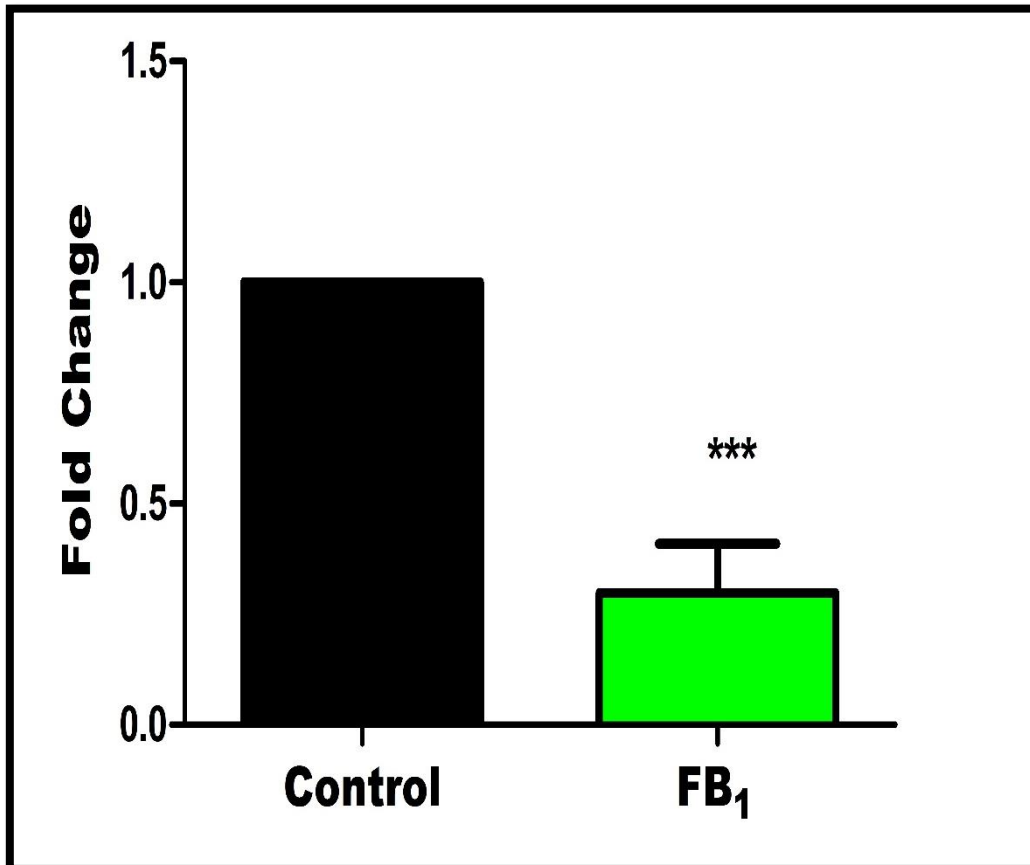


Figure 4.4: The expression of *OGG1* was negatively regulated by FB₁ (**p=0.0004).

4.2. The anti-oxidant response

4.2.1. Anti-oxidant regulation

Elevated ROS generated by FB₁ altered the AO status in HepG2 cells. The master regulator of endogenous AO is the transcription factor, Nrf2. As seen in figure 4.5, the protein expression of total Nrf2 was reduced in FB₁ treated cells (Control: 0.3711±0.1001 RBD vs FB₁: 0.2455±0.03701 RBD; Figure 4.5A).

High concentrations of ROS result in phosphorylation of Nrf2, which marks Nrf2 for nuclear translocation. Phosphorylated Nrf2 (pNrf2) protein expression was significantly elevated by FB₁ (Control: 7.241±0.8566 RBD vs FB: 13.71±3.331 RBD; Figure 4.5B).

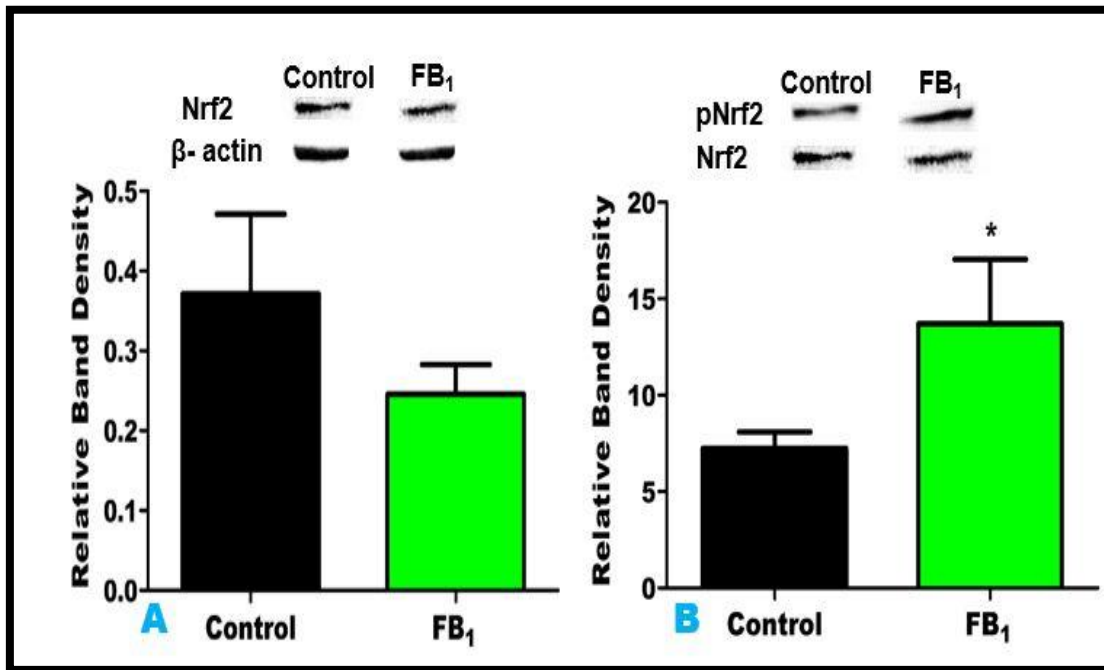


Figure 4.5: There was a decrease in total Nrf2 expression (A: p=0.1111) after FB₁ exposure, however pNrf2 expression was significantly increased (B: *p=0.0311).

The protein and mRNA expression of AO genes and proteins regulated by Nrf2 were subsequently assessed via western blotting and qPCR.

4.2.2. Superoxide detoxification

Figure 4.6 shows that a 4.485 fold increase in the protein expression of mitochondrial AO, SOD2 (Control: 0.9237 ± 0.08307 RBD vs FB_1 : 4.479 ± 0.8482 RBD). To validate the increased expression of SOD2 at the protein level, *SOD2* mRNA expression was investigated with qPCR. These results revealed that there was a 1.759 fold increase in *SOD2* mRNA expression (Control: $1.000 \pm 6.075 \times 10^{-6}$ fold vs FB_1 : 1.759 ± 0.3353 fold).

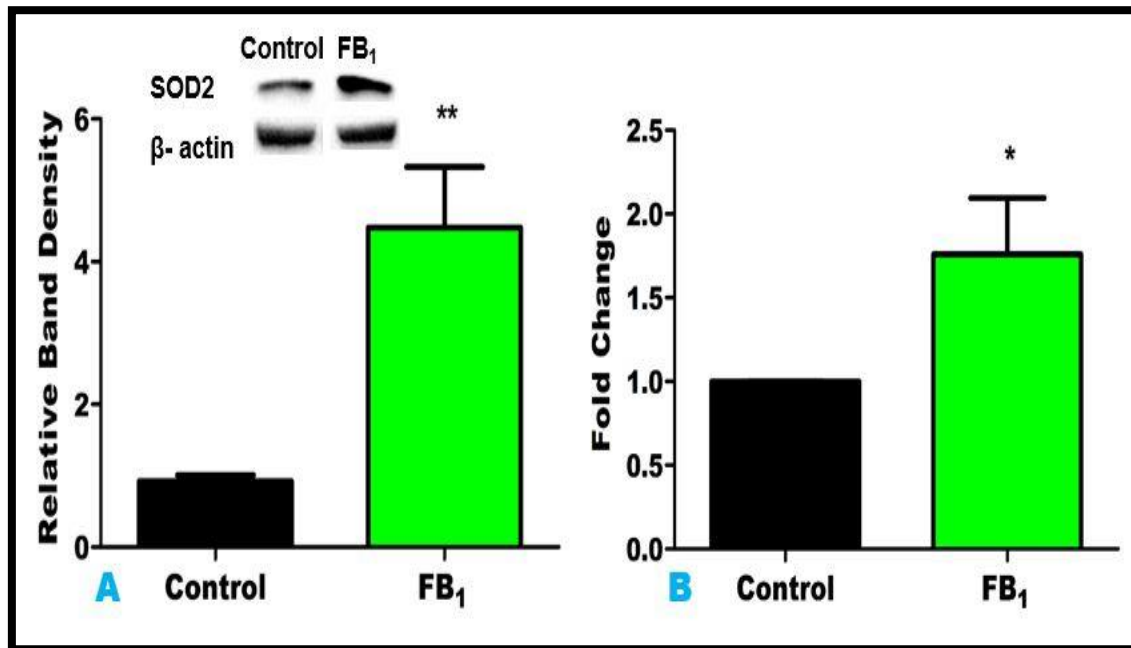


Figure 4.6: *SOD2* protein expression was positively regulated (A: ** $p= 0.0043$) with an accompanying increase in *SOD2* mRNA levels (B: * $p= 0.0172$) after FB_1 exposure.

4.2.3. Detoxification of peroxides

A) Catalase

In comparison to control cells (0.2717 ± 0.09224 RBD), CAT protein expression was significantly higher in FB₁ treated cells (0.4918 ± 0.1275 RBD). This was further confirmed by a significant increase in CAT mRNA expression after FB₁ exposure (Control: $1.000 \pm 6.095 \times 10^{-7}$ fold vs FB₁: 1.522 ± 0.1651 fold). In spite of the elevated expression of CAT (Figure 4.7A and B), the activity of CAT (Figure 4.7C) was significantly lower in cells incubated with FB₁ ($58.83 \pm 3.175\%$) in comparison to controls cells ($71.81 \pm 1.570\%$).

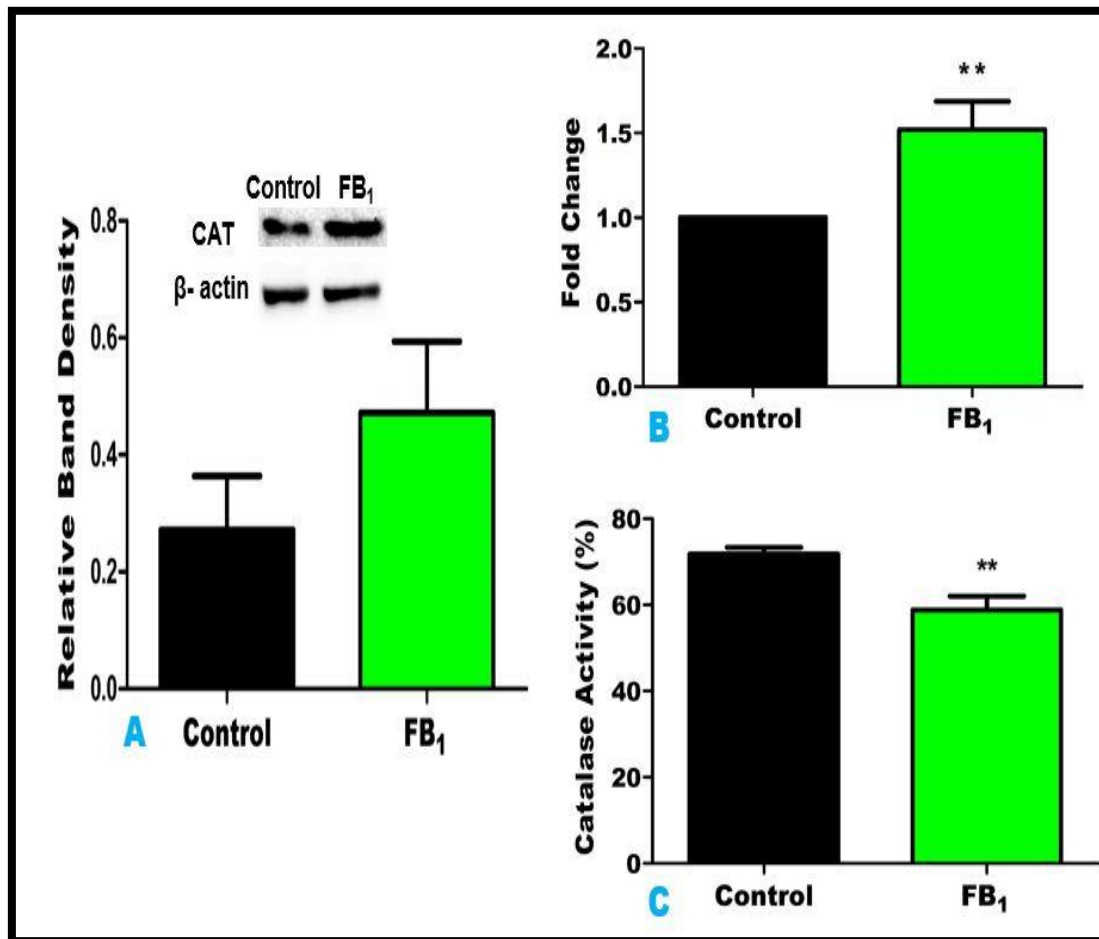


Figure 4.7: FB₁ enhanced the CAT protein (A: $p=0.0725$) and CAT mRNA levels (B: $**p=0.0093$), however CAT activity was significantly reduced (C: $**p=0.0032$).

B) Glutathione peroxidase and glutathione

The qPCR results for GPx (Figure 4.8 A) showed a significant up-regulation in FB₁ treated cells (1.895±0.06500 fold) in contrast to control cells (1.000±6.095×10⁻⁶ fold). The concentration of GSH (Figure 4.8 B), a co-factor for GPx, was 2.27 folds greater in FB₁ treated cells (Control: 7.712±1.136 μM vs FB₁: 17.51±3.753 μM).

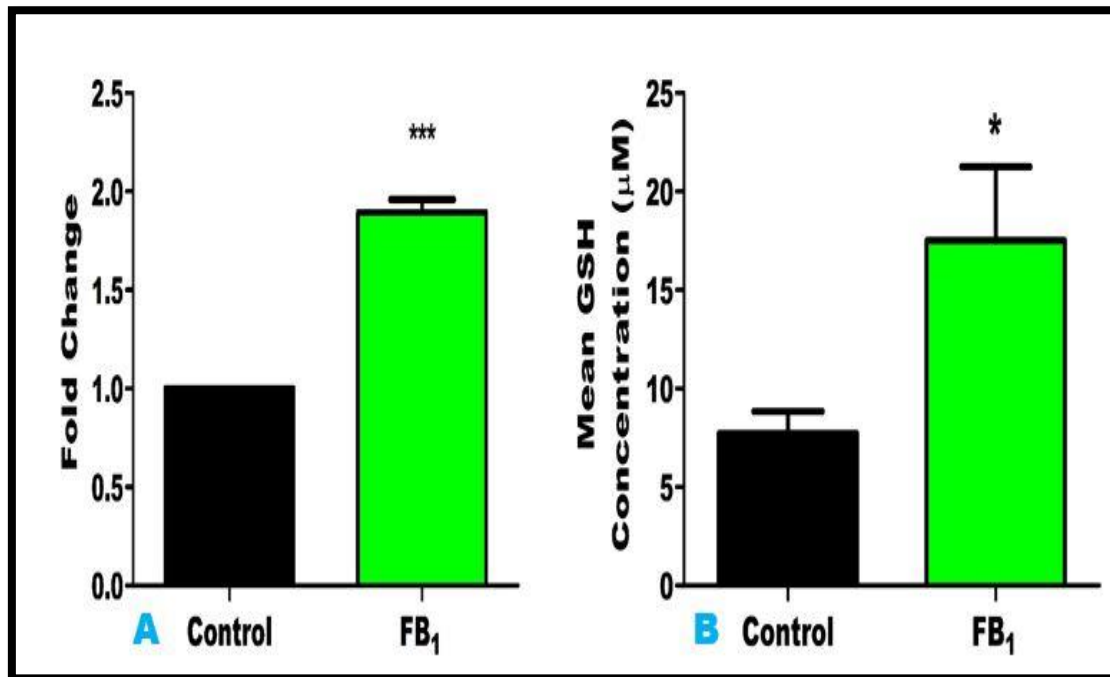


Figure 4.8: The transcript levels of the enzyme GPx (A: ***p= 0.0001) and the associated AO, GSH (B:*p= 0.0124) was significantly higher after FB₁ exposure.

4.3. Mitochondrial stress response

Mitochondrial membrane potential ($\Delta\psi$) is an indicator of mitochondrial health. The JC-1 assay was used to determine $m\psi$ and found that it was slightly reduced in FB₁ treated cells (Control: 0.03377 ± 0.02004 JC-1 fluorescence ratio vs FB₁: 0.02714 ± 0.009389 JC-1 fluorescence ratio) (Figure 4.9).

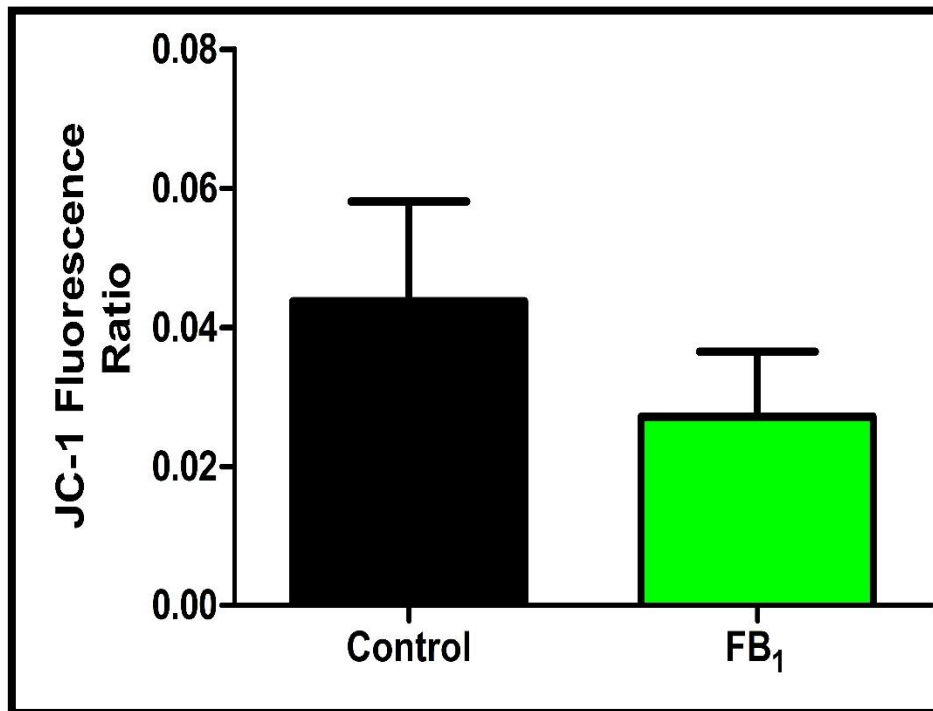


Figure 4.9: After a 24h exposure to FB₁, there was a minor reduction in the $\Delta\psi$ of HepG2 cells ($p= 0.2049$).

Mitochondrial DNA (mtDNA) is extremely susceptible to oxidative damage due to the close proximity to the ETC. Mitochondrial DNA is stabilized by the transcription factor, *Tfam*. Transcript levels of *Tfam* were significantly increased by FB₁ stimulation (Control: $1.000 \pm 6.095 \times 10^{-6}$ fold vs FB₁: 4.124 ± 1.230 fold) (Figure 4.10).

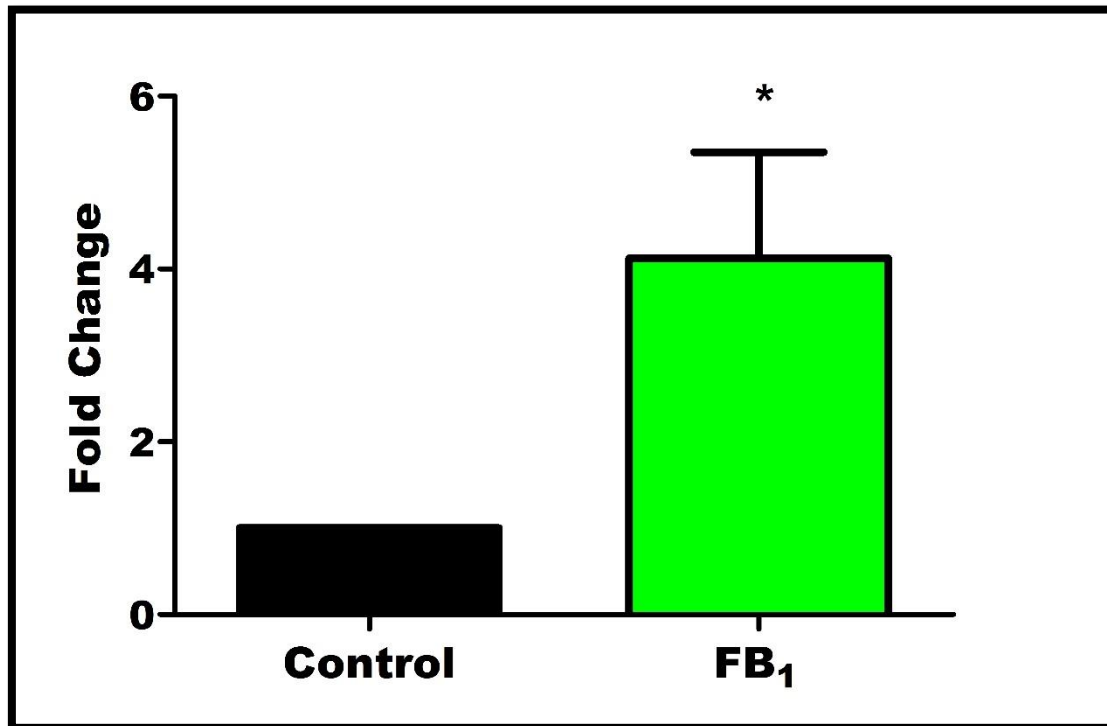


Figure 4.10: FB₁ stimulated cells exhibited a significant increase in *Tfam* gene expression (*p= 0.0117).

Mitochondrial stress response proteins, Sirt 3 and Lon-P1 are highly expressed during oxidative and mitochondrial stress. Western blot analysis of Sirt 3 revealed a 2.03 fold increase in FB₁ treated cells (**Control:** 3.756±0.5772 RBD vs **FB₁:** 7.630±0.003007 RBD; Figure 4.11A). The protein expression of the protease, Lon-P1 (Figure 4.11 B) was also significantly higher in cells exposed to FB₁ (0.3243±0.01713 RBD) when compared to control cells (0.1885±0.01222 RBD).

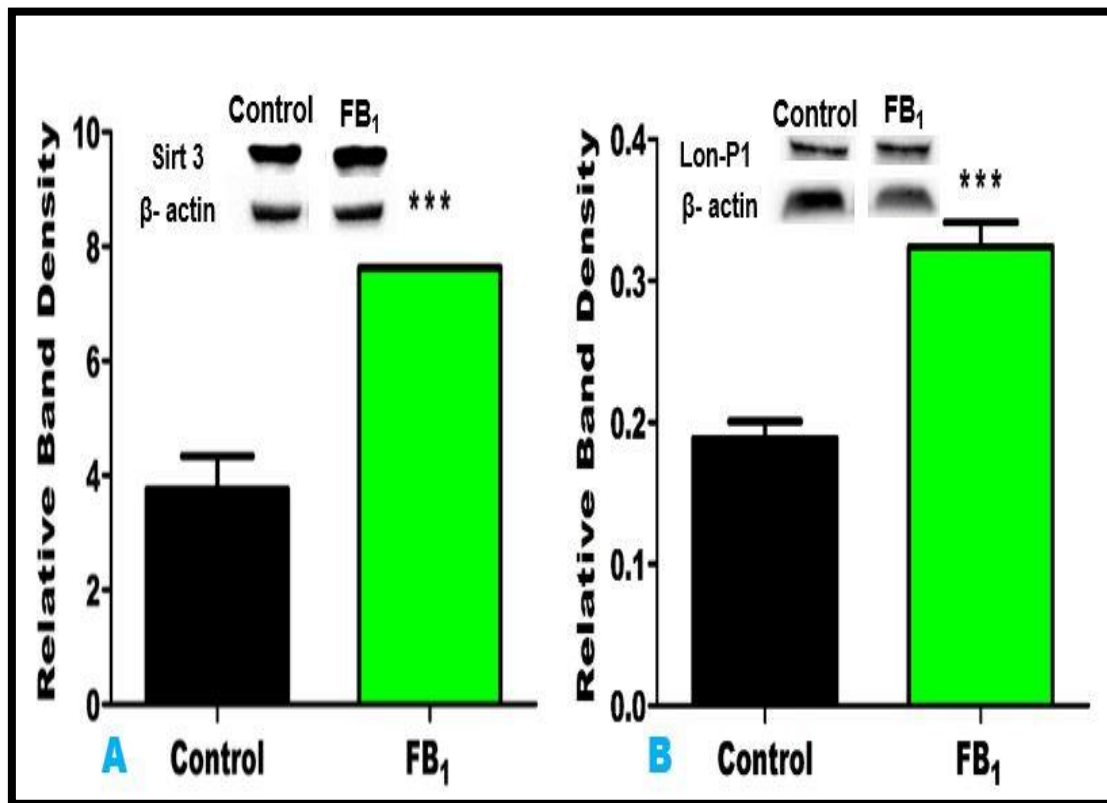


Figure 4.11: Mitochondrial stress response was heightened after FB₁ exposure; Sirt 3 (A: ***p= 0.0003) and Lon-P1 (B:***p= 0.0004) were both significantly upregulated.

4.4. Expression of cancer-related genes

The expression of specific oncogenes and tumour suppressor genes are regulated by excessive intracellular ROS that may trigger the onset of cancer. Western blotting and qPCR was used to determine the expression of these proteins/genes in HepG2 cells.

4.4.1. *c-Myc* expression

The oncogenic *c-Myc* is an early response gene that is responsible for many of the changes that occur in normal cells that induces malignancy. Fumonisin B₁ (1.564 ± 0.08688 fold) upregulated *c-Myc* gene expression relative to the untreated control ($1.000 \pm 6.095 \times 10^{-6}$ fold) (Figure 4.12B). However, the protein expression of *c-Myc* was reduced (Control: 1.560 ± 0.5135 RBD vs FB₁: 1.193 ± 0.2505 RBD) (Figure 4.12A).

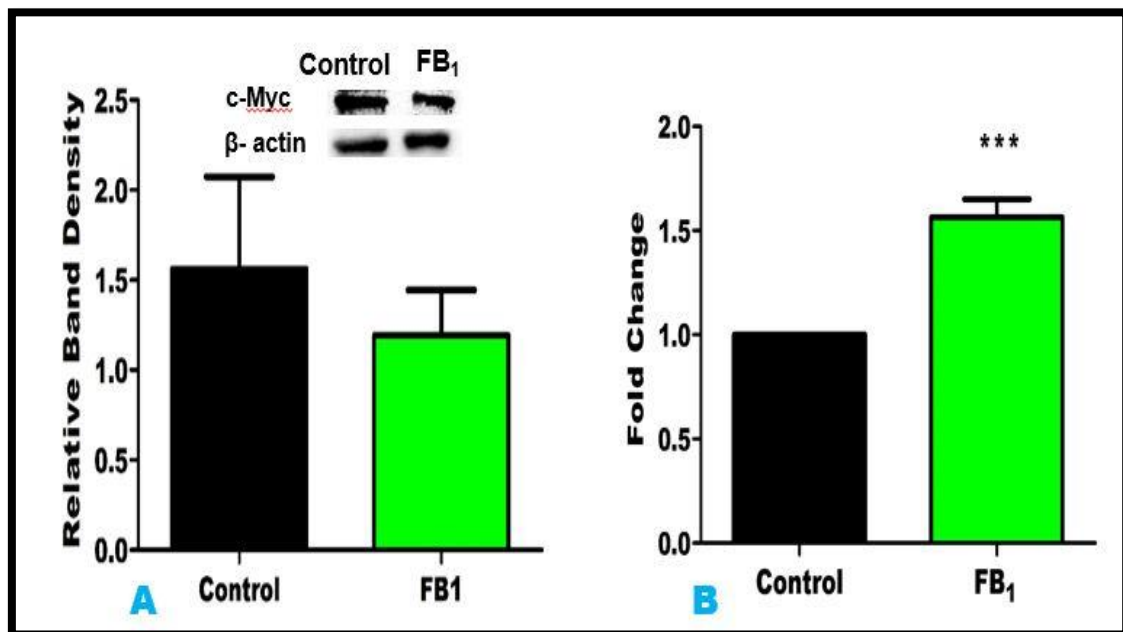


Figure 4.12: Analysis of *c-Myc* protein expression revealed that there was a decrease (A:p= 0.4594) however *c-Myc* transcript levels were significantly increased (B:***p= 0.0004) after exposure to FB₁.

4.4.2. p53 expression

The tumour suppressor p53 is one of the most frequently altered genes in human cancers. Elevated levels of ROS generated after FB₁ exposure induced significant phosphorylation of serine 20 of p53 (Figure 4.13A; Control: 1.765 ± 0.3261 RBD vs FB₁: 7.346 ± 0.2069 RBD) yet the expression of total p53 was reduced after incubation with FB₁ (Figure 4.13B; Control: 0.4381 ± 0.07887 RBD vs FB₁: 0.2306 ± 0.1091 RBD).

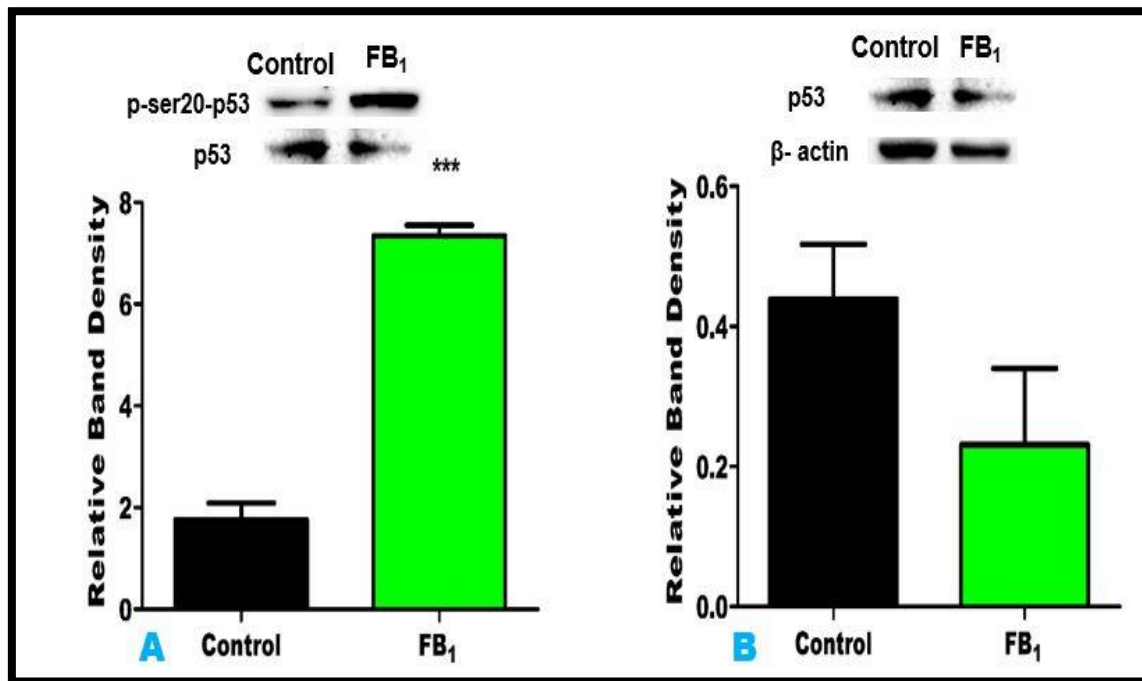


Figure 4.13: The protein expression of phosphorylated p-ser20-p53 was significantly increased post FB₁ exposure (A: *** $p < 0.0001$), however total p53 expression was lower (B: $p = 0.0558$).

Chapter 5 – Discussion

The mycotoxin, FB₁, is a world-wide contaminant of maize and maize-based products. It is nephrotoxic, cytotoxic and hepatotoxic to both animals and humans (WHO 2001). Although FB₁ is poorly absorbed in humans, a major portion of absorbed FB₁ is distributed to the liver (Voss, Howard et al. 2002). The liver is the oxidative hub for many metabolic and detoxification reactions. Hepatocytes have a high density of mitochondria, putting it at great risk to oxidative insult (Degli Esposti, Hamelin et al. 2012).

The primary function of the mitochondria is to generate ATP via the ETC. Normal mitochondrial metabolism contributes to the generation of ROS, by leaking unpaired e⁻s into the mitochondrial matrix. These e⁻s react with molecular O₂ forming O₂^{-•}; which is converted to H₂O₂ and eventually to the most damaging form of ROS – OH^{-•}. Unwarranted production of ROS from the ETC can be stimulated by a number of factors; one being the inhibition of complex I of the ETC (Bratic, Larsson et al.). Domijan and Abramov have reported that FB₁ inhibits complex I of the ETC, resulting in the enhanced generation of ROS and mitochondrial depolarisation; which further contributes to the oxidative environment (Domijan and Abramov 2011). Hence, inhibition of complex I of the ETC may explain the mitochondrial depolarization and increased levels of intracellular ROS observed after FB₁ exposure in HepG2 cells. Previous studies have also reported that FB₁ triggered the generation of intracellular ROS in mouse GT1-7 hypothalamic cells, rat C6 glioblastoma cells and human U-118MG glioblastoma cells (Stockmann-Juvala, Mikkola et al. 2004a, Stockmann-Juvala, Mikkola et al. 2004b). Interestingly, FB₁ did not alter ROS production in neuroblastoma SH-SY5Y cells as reported by Stockmann-Juvala, et al., however Domijan and Abramov observed significantly higher levels of ROS in SH-SY5Y cells after incubation with FB₁ (Stockmann-Juvala, Mikkola et al. 2004a, Domijan and Abramov 2011).

This study supports previous studies that showed oxidative stress was induced by FB₁ exposure. One consequence of uncontrolled production of ROS is the peroxidation of lipids (Ayala, Mu et al. 2014). The TBARS assay – which quantifies ROS mediated damage to lipids – showed that FB₁ significantly increased lipid peroxidation in cells. This is supported by findings in a number of different studies involving human cell lines and animal *in vivo* and *in vitro* models (Kouadio, Mobio et al. 2005, Bernabucci, Colavecchia et al. 2011, Wang, Wu et al. 2016)

Additional downstream repercussions of elevated ROS include nucleic acid and protein oxidation. FB₁ has been implicated in both these outcomes as evidenced by Mary, Theumer et al., who showed a significant increase in the formation of protein carbonyls and mis-incorporation of 8-oxoG in the DNA of smooth muscle cells after a 48h incubation with FB₁ (Mary, Theumer et al.

2012). A 24h exposure to FB₁ resulted in significant increase in protein oxidation as measured using the protein carbonyl assay. Although DNA oxidation was not measured, the mRNA expression levels of the DNA base excision repair enzyme – *OGG1* was measured. 8-Oxoguanine glycosylase is responsible for removing the major oxidative lesion, 8-oxoG from DNA (Ba, Aguilera Aguirre et al. 2015). Acute exposure to FB₁ downregulated *OGG1* transcript levels, and by implication would not be able to reduce or inhibit accelerated DNA damage under oxidative conditions. A similar result was observed after a 48h incubation with FB₁ in oesophageal cells (Khan, Phulukdaree et al. 2017). Moreover, developing cancer cells maintain low levels of *OGG1*, as 8-oxoG lesions promote genome instability and aids the development of carcinogenesis (Nyaga, Lohani et al. 2006, Nakabeppu 2014).

The induction of the AO defence system is responsible for detoxifying and negating the effects of excess ROS within cells. Redox homeostasis relies on the disassociation of the AO transcription factor, Nrf2, from Keap-1. Surplus ROS targets Keap-1, altering its conformation; which allows Nrf2 to translocate to the nucleus where it binds to the ARE and promotes AO transcription (Nguyen, Nioi et al. 2009). The expression of total Nrf2 was only slightly reduced post-FB₁ exposure, however pNrf2 was significantly elevated. Most transcription factors – including Nrf2 – are regulated by phosphorylation. Excess ROS activates phosphorylation pathways such as mitogen-activated protein kinase (MAPK) and protein kinase c (PKC), which in turn participate in the phosphorylation and activation of the Nrf2-ARE (Chen, Lu et al. 2015). Phosphorylation of Nrf2 triggers its disassociation from Keap-1 ubiquitination, allowing it to translocate to the nucleus and promote the transcription of AO (Huang, Nguyen et al. 2002). Studies have shown that FB₁ activates both the MAPK and PKC pathways contributing further to Nrf2 phosphorylation (Yeung, Wang et al. 1996, Pinelli, Poux et al. 1999)

Major AO enzymes regulated by Nrf2 include: SOD2, CAT and GPx. These AO enzymes are the first to respond to excessive ROS and therefor serve as redox biomarkers (Wang, Wu et al. 2016). Surplus O₂^{•-}, produced by dysregulated ETC, are detoxified to H₂O₂ by SOD2. Hydrogen peroxide is further detoxified by CAT and GPx to H₂O and O₂ (Weir, Lane et al. 2013). The expression of SOD2, CAT and GPx were all upregulated in HepG2 cells after exposure to FB₁. The expression of these AO, however, were reduced in Balb/c mice and peripheral blood mononuclear cells (PBMC) exposed to FB₁ (Bernabucci, Colavecchia et al. 2011, Abbas, Ben Salah-Abbes et al. 2016). Although the protein and mRNA expression of CAT was higher after incubation with FB₁; its activity was reduced. These results were supported by Domijan and Peraica et al (Domijan, Peraica et al. 2007). Reduced activity of CAT results in the poor detoxification of H₂O₂. If left in its native form, H₂O₂ is converted to OH[•], resulting in further oxidative damage.

An alternative mechanism for H₂O₂ detoxification is modulated by GPx and its co-factor GSH. Glutathione is a major intra-cellular AO in hepatocytes that protects against oxidative damage and is involved in detoxification of xenobiotics. After a 24h incubation with FB₁, GPx mRNA and GSH concentration was significantly elevated in HepG2 cells. This is in agreement with results obtained by Domijan and Abramov, who showed a significant increase of GSH in SH-SY5Y cells after a 24h incubation with FB₁ (Domijan and Abramov 2011). Long term exposure to FB₁ however, reduces GSH concentration (Stockmann-Juvala, Mikkola et al. 2004b). Elevation of GSH could be a result of the increased availability of GSH's cofactor, NADPH and components required for GSH synthesis. Inhibition of sphingolipid synthesis by FB₁ distorts the structure of membrane receptors such as the folate receptor (Stevens and Tang 1997). Inhibition of folate uptake promotes the conversion of homocysteine to cysteine, a key amino acid required for the synthesis of GSH (Stevens and Tang 1997, Lu 2009). Inhibition of sphingolipid synthesis also increases the concentration of available NADPH as sphingolipid synthesis requires the oxidation of NADPH (Gault, Obeid et al. 2010).

As discussed previously, ROS produced by ETC results in the depolarization of the mitochondria, which may lead to mitochondrial dysfunction. After observing a mild reduction in $\Delta\psi_m$, mitochondrial stress responses to FB₁ were assessed.

Considering mtDNA is in close proximity to the ETC, it is highly vulnerable to oxidative damage as they lack protective histone packaging (Gao, Laude et al. 2008). In order to deal with oxidative insult, mtDNA is organized within a nucleoid. The core components of the nucleoid are regulated by the transcription factor Tfam (Gilkerson, Bravo et al. 2013). This transcription factor belongs to a family of high mobility group (HMG) proteins that regulate the transcription of genes encoded by mtDNA and controls mtDNA copy number. Due to the abundance of Tfam and its ability to bind non-specifically to DNA, Tfam protects mtDNA further by binding directly to the whole genome (Kanki, Ohgaki et al. 2004). The increased transcript levels of Tfam after exposure to FB₁ maybe a mechanism that mitochondria employ to protect mtDNA from oxidative damage. However, high levels of ROS trigger the phosphorylation of Tfam, preventing it from binding to mtDNA. This leaves mtDNA vulnerable to ROS-induced mutations that could alter the bio-energetic and bio-synthetic state of the mitochondria that favour cancer cell survival. Phosphorylation of Tfam is also mediated via cAMP-dependent protein kinase (PKA) and extracellular signal-regulated kinases (ERK) cascades (Lu, Lee et al. 2013, Wang, Zhu et al. 2014). Although phosphorylation of Tfam was not measured in this study, FB₁ is a known activator of the ERK pathway and is thus involved in Tfam phosphorylation. (Rumora, Domijan et al. 2007). This further enhances Tfam phosphorylation, leaving mtDNA vulnerable to ROS and

may promoting mutagenesis and genome instability. Phosphorylation of Tfam leads to its rapid degradation by the primary mitochondrial protease – Lon-P1. By controlling Tfam degradation, Lon-P1 also regulates mtDNA copy number and transcription (Bota and Davies 2016).

Furthermore, Lon-P1 is responsible for degrading oxidised proteins such as protein carbonyls within the mitochondrial matrix (Gibellini, Pinti et al. 2014). Several reports indicate that Lon-P1 expression and activity increases in the presence of high levels of carbonylated proteins (Pinti, Gibellini et al. 2015). The 11.9 fold increase in protein carbonyls by FB₁ may have induced the upregulation in Lon-P1 expression in HepG2 cells. The clearance of oxidised proteins within the mitochondria is essential as oxidised proteins tend to aggregate and crosslink, resulting in mitochondrial toxicity (Ugarte, Petropoulos et al. 2010). Thus, the upregulation of Lon-P1, reduces mitochondrial stress and maintains mitochondrial integrity (Ngo, Pomatto et al. 2013).

Lon-protease 1 is post-transcriptionally activated by the mitochondrial deacetylase enzyme, Sirt 3 (Bota and Davies 2016). Sirtuin 3 upregulation by FB₁ counteracts the highly oxidative environment of the mitochondria. Sirtuin 3 does not have any direct AO capabilities but is able to upregulate the mitochondrial AO capacity via two methods. The first method involves activating the mitochondrial AO, SOD2, via deacetylation. The second method involves the enhancing IDH2 activity through Sirt3-mediated deacetylation. The activity of IDH2 produces increased levels of NADPH, which in turn can increase the activity of GR to further facilitate regeneration of GSH from GSSG. Together increased SOD2 and IDH activity increases the detoxification capacity of the mitochondria (Bause and Haigis 2013). Oxidative damage to mtDNA can also be repaired by Sirt 3 through the deacetylation and stabilisation of mitochondrial OGG1, and hence reduce mitochondrial stress (Kincaid and Bossy-Wetzel 2013).

Functional mitochondria are essential for the survival of cancer cells. While high levels of ROS within the mitochondrial matrix cause mutations to mtDNA, these mutation do not usually disrupt the functioning of mitochondria but rather alter the bio-energetic and bio-synthetic states to ensure that the energy and growth requirements of cancer cells are met (Wallace 2012). While high ROS levels are beneficial to cancer cells they must be maintained at certain levels to ensure that cell death pathways are not initiated (Liou and Storz 2010) Therefore, Tfam, Sirt 3 and Lon-P1 work together to maintain mitochondrial integrity.

A close relationship exists between Nrf2, ROS and the tumour suppressor gene – p53. High levels of ROS activates p53 resulting in cell cycle arrest, AO induction and DNA repair. When oxidative damage exceeds cellular AO capacity, p53 provokes a pro-oxidant response, which subsequently elicits p53-dependant apoptosis (Liu, Chen et al. 2008). High levels of ROS also lead to the phosphorylation of serine 20 of p53. Serine 20 lies within the Mouse double minute 2 (MDM-2)

binding site of p53. Phosphorylation of p53's serine 20 disrupts p53 degradation by MDM-2 thereby activating its growth arrest and apoptotic function (Jabbur, Huang et al. 2000). Although intracellular ROS levels and phosphorylated-p53 expression was upregulated, the expression of total-p53 was reduced. Sirtuin 3 suppresses p53 expression and activity thus rescuing cells from cell cycle arrest and promoting tumour cell survival (Alhazzazi, Kamarajan et al. 2011).

At low levels, p53 upregulates the expression of Nrf2 and its downstream targets through p21. p21 binds directly to Nrf2 preventing Keap1-mediated degradation of Nrf2 (Chen, Jiang et al. 2012). This prolonged activation of Nrf2 favours the proliferation of cancer cells by promoting the transcription of genes that support glucose flux and generate the building blocks of macromolecules; as observed in lung, breast, ovarian and endometrial cancer cells (Jaramillo and Zhang 2013). Moreover, Nrf2 establishes resistances to chemotherapeutic drugs by promoting the expression drug metabolising enzymes and drug efflux transporters (Bai, Chen et al. 2016).

Recently the transcriptional activation of oncogenes, such as *KRAS*, *BRAF* and *c-Myc*, have been found to increase the transcription and activity of Nrf2, resulting in an increase in cytoprotective activity in the cell (Sporn and Liby 2012). Although cancer cells require a high concentration of ROS, it must be kept under certain levels that would otherwise initiate cell death (Liou and Storz 2010). The detoxification capacity of Nrf2 maintains ROS concentration under these levels, protecting cancer cells from cell death pathways. Thus, oncogenes may promote tumorigenesis in part through Nrf2 (Sporn and Liby 2012). The expression of c-Myc was assessed in this study. c-Myc regulates the transcription of genes involved in growth control, cell survival, cell adhesion and protein synthesis (Dang, Resar et al. 1999). It is also involved in oxidative damage to DNA and is able to mitigate the effects of p53 (Vafa, Wade et al. 2002). Although FB₁ significantly increased *c-Myc* transcript levels, c-Myc protein expression levels were reduced. c-Myc is abundantly expressed at the transcript level in a number of cancers including hepatocellular carcinoma (Dang, Resar et al. 1999, Koutb, Abdel-Rahman et al. 2017). Overexpression of the c-Myc protein triggers apoptotic events, therefore inhibition of c-Myc translation may be a mechanism to prevent cell death (Hoffman and Liebermann 2008).

Exposure to FB₁ generated oxidative stress within HepG2 cells, inducing mitochondrial and AO responses to mitigate the effects of elevated ROS. These responses were compromised to promote the development and survival of cancer cells by creating a more favourable intracellular environment that promotes the development of carcinogenesis and aids cancer cell survival. Further research must still be done on the role ROS and Nrf2 play in regulating other oncogenes and tumour suppressor genes.

A summary of the effect of FB₁ on oxidative stress related responses and its involvement in tumorigenesis in HepG2 cells is represented in Figure 5.1.

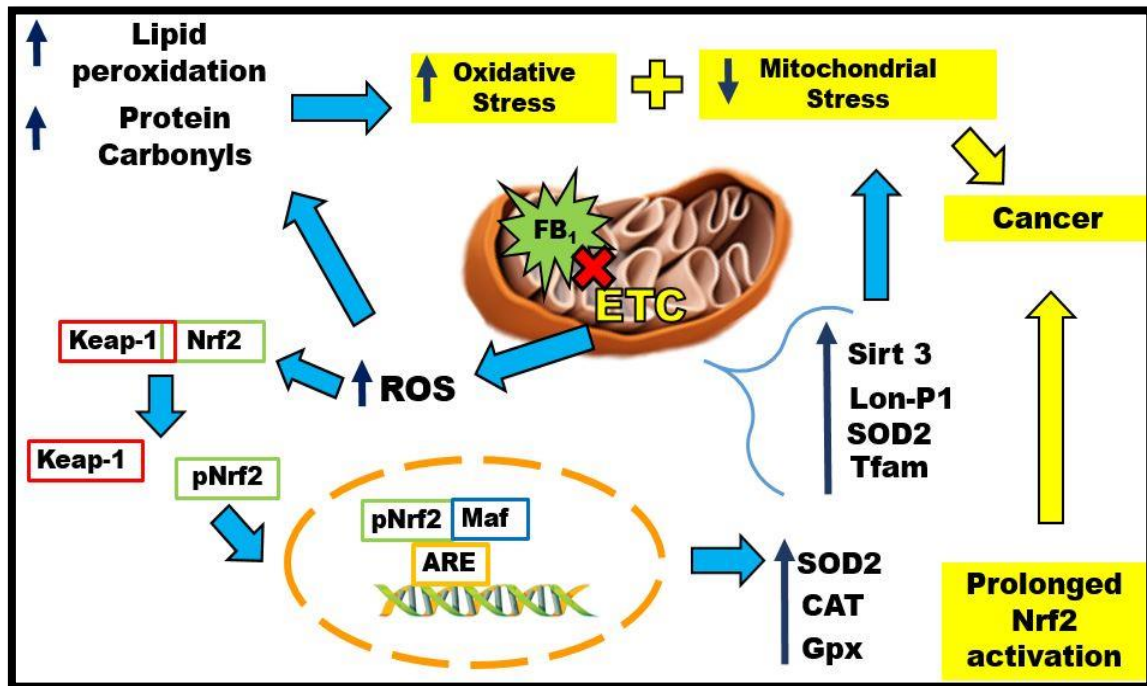


Figure 5.1: Summarised account of events. FB₁ inhibits the ETC, accelerating ROS production. Excessive ROS results in the formation of lipid peroxides and protein carbonyls. ROS also results in the phosphorylation and translocation of Nrf2 and hence the increased expression of SOD2, CAT and GPx. Tfam, Sirt 3 and Lon-P1 expression were also increased. Along with SOD2, these proteins reduce mitochondrial stress. With excessive ROS, improved functioning of the mitochondria and prolonged activation of Nrf2, FB₁ is able to mediate cancer progression (prepared by author).

5.1. Limitations and future studies

In this study an *in vitro* liver model was used to assess oxidative stress related responses after FB₁ exposure. *In vitro* studies allow for more detailed analysis than can be done in *in vivo* studies, however a shortcoming of this model is that cells are removed from their natural environment, thereby eliminating interactions and mechanisms that may otherwise be seen in an intact organism. In order to improve this study the use of an *in vivo* mouse model in addition to the primary hepatocyte cell model may give a better understanding of how cells respond to FB₁ and oxidative stress.

Cells were only exposed to FB₁ for 24h in this study. Cells may respond differently to toxins under acute, sub-chronic and chronic conditions, therefore it would be interesting to determine

the effects of FB₁ in the HepG2 cell line after 6h, 48h and 72h exposure periods to simulate acute, sub-chronic and chronic exposures respectively.

The effect of FB₁ and ROS were only assessed on the onco-gene, *c-Myc*, and tumour suppressor protein, p53. The effect FB₁ has on other oncogenes regulated by ROS such as *KRAS* and *ERK* should be further investigated. Additionally, Nrf2's role in FB₁-mediated tumorigenesis should be investigated further.

CHAPTER 6 – CONCLUSION

This study demonstrated that exposure to FB₁ triggers increased ROS production. Although AO responses were initiated (upregulated pNrf2, CAT, SOD, GPx and GSH), the anti-oxidant capacity was not enough to deal with the excessive ROS generated by the cell as evidenced by formation of lipid peroxides and protein carbonyls. Furthermore mitochondrial survival responses (upregulated SOD2, Tfam Sirt 3 and Lon-P1) initiated by the cell unintentionally contributed to its own downfall by reducing mitochondrial stress and inhibiting the tumour suppressor p53, thereby promoting tumorigenesis. Hence the excessive ROS induced by FB₁, and compromised survival responses may be implicated in FB₁ cancer progression.

REFERENCES

- Abbes, S., J. Ben Salah-Abbes, R. Jebali, R. B. Younes and R. Oueslati (2016). "Interaction of aflatoxin B1 and fumonisin B1 in mice causes immunotoxicity and oxidative stress: Possible protective role using lactic acid bacteria." *J Immunotoxicol* 13(1): 46-54.
- Aguiar, P. H., C. Furtado, B. M. Repoles, G. A. Ribeiro, I. C. Mendes, E. F. Peloso, F. R. Gadelha, A. M. Macedo, G. R. Franco, S. D. Pena, S. M. Teixeira, L. Q. Vieira, A. A. Guarneri, L. O. Andrade and C. R. Machado (2013). "Oxidative stress and DNA lesions: the role of 8-oxoguanine lesions in *Trypanosoma cruzi* cell viability." *PLoS Negl Trop Dis* 7(6): e2279.
- Alberts B, Johnson A and Lewis J (2002). "Structure and Function of DNA." *Molecular Biology of the cell* 4.
- Alhazzazi, T. Y., P. Kamarajan, E. Verdin and Y. L. Kapila (2011). "SIRT3 and cancer: Tumor promoter or suppressor?" *Biochimica et Biophysica Acta (BBA) - Reviews on Cancer* 1816(1): 80-88.
- Alizadeh, A. M., G. Rohandel, S. Roudbarmohammadi, M. Roudbary, H. Sohanaki, S. A. Ghiasian, A. Taherkhani, S. Semnani and M. Aghasi (2012). "Fumonisin B1 contamination of cereals and risk of esophageal cancer in a high risk area in northeastern Iran." *Asian Pac J Cancer Prev* 13(6): 2625-2628.
- Ansari, A., M. S. Rahman, S. K. Saha, F. K. Saikot, A. Deep and K. H. Kim (2017). "Function of the SIRT3 mitochondrial deacetylase in cellular physiology, cancer, and neurodegenerative disease." *Aging Cell* 16(1): 4-16.
- Apel, K. and H. Hirt (2004). "Reactive oxygen species: metabolism, oxidative stress, and signal transduction." *Annu Rev Plant Biol* 55: 373-399.
- Arya, M., I. S. Shergill, M. Williamson, L. Gommersall, N. Arya and H. R. H. Patel (2005). "Basic principles of real-time quantitative PCR." *Expert Review of Molecular Diagnostics* 5(2): 209-219.
- Ayala, A., Mu, #xf1, M. F. oz, Arg, #xfc and S. elles (2014). "Lipid Peroxidation: Production, Metabolism, and Signaling Mechanisms of Malondialdehyde and 4-Hydroxy-2-Nonenal." *Oxidative Medicine and Cellular Longevity* 2014: 31.
- Ba, X., L. Aguilera Aguirre, S. Sur and I. Boldogh (2015). "8-oxoguanine DNA glycosylase-1 driven DNA base excision repair: role in asthma pathogenesis." *Current opinion in allergy and clinical immunology* 15(1): 89-97.

- Bai, X., Y. Chen, X. Hou, M. Huang and J. Jin (2016). "Emerging role of NRF2 in chemoresistance by regulating drug-metabolizing enzymes and efflux transporters." *Drug Metabolism Reviews* 48(4): 541-567.
- Barzilai, A. and K. Yamamoto (2004). "DNA damage responses to oxidative stress." *DNA Repair (Amst)* 3(8-9): 1109-1115.
- Bause, A. S. and M. C. Haigis (2013). "SIRT3 regulation of mitochondrial oxidative stress." *Exp Gerontol* 48(7): 634-639.
- Bayir, H. (2005). "Reactive oxygen species." *Crit Care Med* 33(12 Suppl): S498-501.
- Bennett, J. W. and M. Klich (2003). "Mycotoxins." *Clinical Microbiology Reviews* 16(3): 497-516.
- Berlett, B. S. and E. R. Stadtman (1997). "Protein oxidation in aging, disease, and oxidative stress." *J Biol Chem* 272(33): 20313-20316.
- Bernabucci, U., L. Colavecchia, P. P. Danieli, L. Basiricò, N. Lacetera, A. Nardone and B. Ronchi (2011). "Aflatoxin B1 and fumonisin B1 affect the oxidative status of bovine peripheral blood mononuclear cells." *Toxicology in Vitro* 25(3): 684-691.
- Bezawork-Geleta, A., E. J. Brodie, D. A. Dougan and K. N. Truscott (2015). "LON is the master protease that protects against protein aggregation in human mitochondria through direct degradation of misfolded proteins." *Scientific Reports* 5: 17397.
- Birben, E., U. M. Sahiner, C. Sackesen, S. Erzurum and O. Kalayci (2012). "Oxidative Stress and Antioxidant Defense." *The World Allergy Organization journal* 5(1): 9-19.
- Bota, D. A. and K. J. A. Davies (2016). "Mitochondrial Lon protease in human disease and aging: Including an etiologic classification of Lon-related diseases and disorders." *Free radical biology & medicine* 100: 188-198.
- Bratic, A., N.-G. Larsson, xF and ran "The role of mitochondria in aging." *The Journal of Clinical Investigation* 123(3): 951-957.
- Chen, B., Y. Lu, Y. Chen and J. Cheng (2015). "The role of Nrf2 in oxidative stress-induced endothelial injuries." *Journal of Endocrinology* 225(3): R83-R99.
- Chen, Q., E. J. Vazquez, S. Moghaddas, C. L. Hoppel and E. J. Lesnefsky (2003). "Production of Reactive Oxygen Species by Mitochondria: CENTRAL ROLE OF COMPLEX III." *Journal of Biological Chemistry* 278(38): 36027-36031.
- Chen, W., T. Jiang, H. Wang, S. Tao, A. Lau, D. Fang and D. D. Zhang (2012). "Does Nrf2 Contribute to p53-Mediated Control of Cell Survival and Death?" *Antioxidants & Redox Signaling* 17(12): 1670-1675.

- Chuturgoon, A., A. Phulukdaree and D. Moodley (2014). "Fumonisin B1 induces global DNA hypomethylation in HepG2 cells - An alternative mechanism of action." *Toxicology* 315: 65-69.
- Claudia Borza, Danina Muntean, Cristina Dehelean, Germaine Săvoiu, Corina Șerban, Georgeta Simu, Mihaiela Andoni, M. Butur and S. Drăgan (2013). "Oxidative Stress and Lipid Peroxidation – A Lipid Metabolism Dysfunction, Lipid Metabolism." [https://www.intechopen.com/books/lipid-metabolism/oxidative-stress-and-lipid-peroxidation-a-lipid-metabolism-dysfunction\(2013\)](https://www.intechopen.com/books/lipid-metabolism/oxidative-stress-and-lipid-peroxidation-a-lipid-metabolism-dysfunction(2013)).
- Costa, V., A. Quintanilha and P. Moradas-Ferreira (2007). "Protein oxidation, repair mechanisms and proteolysis in *Saccharomyces cerevisiae*." *IUBMB Life* 59(4-5): 293-298.
- Dang, C. V., L. M. Resar, E. Emison, S. Kim, Q. Li, J. E. Prescott, D. Wonsey and K. Zeller (1999). "Function of the c-Myc oncogenic transcription factor." *Exp Cell Res* 253(1): 63-77.
- Degli Esposti, D., J. Hamelin, N. Bosselut, R. Saffroy, M. Sebah, A. Pommier, C. Martel, C. Cile and A. Lemoine (2012). "Mitochondrial Roles and Cytoprotection in Chronic Liver Injury." *Biochemistry Research International* 2012: 16.
- Desai, K., M. C. Sullards, J. Allegood, E. Wang, E. M. Schmelz, M. Hartl, H. U. Humpf, D. C. Liotta, Q. Peng and A. H. Merrill, Jr. (2002). "Fumonisin analogs as inhibitors of ceramide synthase and inducers of apoptosis." *Biochim Biophys Acta* 1585(2-3): 188-192.
- Devasagayam, T. P., K. K. Bloor and T. Ramasarma (2003). "Methods for estimating lipid peroxidation: an analysis of merits and demerits." *Indian J Biochem Biophys* 40(5): 300-308.
- Domijan, A. M. and A. Y. Abramov (2011). "Fumonisin B1 inhibits mitochondrial respiration and deregulates calcium homeostasis--implication to mechanism of cell toxicity." *Int J Biochem Cell Biol* 43(6): 897-904.
- Domijan, A. M., M. Peraica, A. L. Vrdoljak, B. Radić, V. Žlender and R. Fuchs (2007). "The involvement of oxidative stress in ochratoxin A and fumonisin B1 toxicity in rats." *Molecular nutrition & food research* 51(9): 1147-1151.
- EC (2002). "Opinion of the scientific committee on food on the Fusarium toxin Fumonisin B1." European Commission (Health and consumer protection directorate).
- Fandohan, P., K. Hell, W. F. O. Marasas and M. J. Wingfield (2003). "Infection of maize by *Fusarium* species and contamination with fumonisin in Africa." *African Journal of Biotechnology* 2(12): 570.

- Filomeni, G., G. Rotilio and M. R. Ciriolo (2002). "Cell signalling and the glutathione redox system." *Biochemical pharmacology* 64(5): 1057-1064.
- Futerman, A. H. and H. Riezman (2005). "The ins and outs of sphingolipid synthesis." *Trends Cell Biol* 15(6): 312-318.
- Gao, L., K. Laude and H. Cai (2008). "Mitochondrial Pathophysiology, Reactive Oxygen Species, and Cardiovascular Diseases." *The Veterinary clinics of North America. Small animal practice* 38(1): 137-vi.
- Gault, C. R., L. M. Obeid and Y. A. Hannun (2010). "An overview of sphingolipid metabolism: from synthesis to breakdown." *Advances in experimental medicine and biology* 688: 1-23.
- Gibellini, L., M. Pinti, F. Beretti, C. L. Pierri, A. Onofrio, M. Riccio, G. Carnevale, S. De Biasi, M. Nasi, F. Torelli, F. Boraldi, A. De Pol and A. Cossarizza (2014). "Sirtuin 3 interacts with Lon protease and regulates its acetylation status." *Mitochondrion* 18: 76-81.
- Gilkerson, R., L. Bravo, I. Garcia, N. Gaytan, A. Herrera, A. Maldonado and B. Quintanilla (2013). "The Mitochondrial Nucleoid: Integrating Mitochondrial DNA into Cellular Homeostasis." *Cold Spring Harbor Perspectives in Biology* 5(5): a011080.
- Gorrini, C., I. S. Harris and T. W. Mak (2013). "Modulation of oxidative stress as an anticancer strategy." *Nat Rev Drug Discov* 12(12): 931-947.
- Grotto, D., L. S. Maria, J. Valentini, C. Paniz, G. Schmitt, S. C. Garcia, V. J. Pomblum, J. B. T. Rocha and M. Farina (2009). "Importance of the lipid peroxidation biomarkers and methodological aspects FOR malondialdehyde quantification." *Química Nova* 32: 169-174.
- Haschek, W. M., L. A. Gumprecht, G. Smith, M. E. Tumbleson and P. D. Constable (2001). "Fumonisin toxicosis in swine: an overview of porcine pulmonary edema and current perspectives." *Environmental Health Perspectives* 109(Suppl 2): 251-257.
- Heidtmann-Bemvenuti, R., G. L. Mendes, P. T. Scaglioni, E. Badiale-Furlong and L. A. Souza-Soares (2011). "Biochemistry and metabolism of mycotoxins: A review." *African Journal of Food Science* 5(16): 8.
- Hoffman, B. and D. A. Liebermann (2008). "Apoptotic signaling by c-MYC." *Oncogene* 27: 6462.
- Huang, H.-C., T. Nguyen and C. B. Pickett (2002). "Phosphorylation of Nrf2 at Ser-40 by Protein Kinase C Regulates Antioxidant Response Element-mediated Transcription." *Journal of Biological Chemistry* 277(45): 42769-42774.

- Huang, T., M. Long and B. Huo (2010). "Competitive Binding to Cuprous Ions of Protein and BCA in the Bicinchoninic Acid Protein Assay." *The Open Biomedical Engineering Journal* 4: 271-278.
- Istiaq Alam, T., T. Kanki, T. Muta, K. Ukaji, Y. Abe, H. Nakayama, K. Takio, N. Hamasaki and D. Kang (2003). "Human mitochondrial DNA is packaged with TFAM." *Nucleic Acids Research* 31(6): 1640-1645.
- Itoh, K., K. I. Tong and M. Yamamoto (2004). "Molecular mechanism activating Nrf2-Keap1 pathway in regulation of adaptive response to electrophiles." *Free Radic Biol Med* 36(10): 1208-1213.
- Iwase, T., A. Tajima, S. Sugimoto, K.-i. Okuda, I. Hironaka, Y. Kamata, K. Takada and Y. Mizunoe (2013). "A Simple Assay for Measuring Catalase Activity: A Visual Approach." *Scientific Reports* 3: 3081.
- Jabbur, J. R., P. Huang and W. Zhang (2000). "DNA damage-induced phosphorylation of p53 at serine 20 correlates with p21 and Mdm-2 induction in vivo." *Oncogene* 19: 6203.
- Jaramillo, M. C. and D. D. Zhang (2013). "The emerging role of the Nrf2–Keap1 signaling pathway in cancer." *Genes & Development* 27(20): 2179-2191.
- Jimenez-Del-Rio, M. and C. Velez-Pardo (2012). "The Bad, the Good, and the Ugly about Oxidative Stress." *Oxidative Medicine and Cellular Longevity* 2012: 13.
- Kabel, A. M. (2014). "Free Radicals and Antioxidants: Role of Enzymes and Nutrition." *World Journal of Nutrition and Health* 2(3): 35-38.
- Kalyanaraman, B., V. Darley-USmar, K. J. A. Davies, P. A. Dennery, H. J. Forman, M. B. Grisham, G. E. Mann, K. Moore, L. J. Roberts and H. Ischiropoulos (2012). "Measuring reactive oxygen and nitrogen species with fluorescent probes: challenges and limitations." *Free radical biology & medicine* 52(1): 1-6.
- Kanki, T., K. Ohgaki, M. Gaspari, C. M. Gustafsson, A. Fukuoh, N. Sasaki, N. Hamasaki and D. Kang (2004). "Architectural Role of Mitochondrial Transcription Factor A in Maintenance of Human Mitochondrial DNA." *Molecular and Cellular Biology* 24(22): 9823-9834.
- Khan, R., B., A. Phulukdaree and A. Chuturgoon (2017). Concentration-dependent effect of fumonisin B 1 on apoptosis in oesophageal cancer cells.
- Kincaid, B. and E. Bossy-Wetzel (2013). "Forever young: SIRT3 a shield against mitochondrial meltdown, aging, and neurodegeneration." *Frontiers in Aging Neuroscience* 5(48).

- Kouadio, J. H., T. A. Mobio, I. Baudrimont, S. Moukha, S. D. Dano and E. E. Creppy (2005). "Comparative study of cytotoxicity and oxidative stress induced by deoxynivalenol, zearalenone or fumonisin B1 in human intestinal cell line Caco-2." *Toxicology* 213(1–2): 56-65.
- Koutb, F., S. Abdel-Rahman, E. Hassona and A. Haggag (2017). "Association of C-myc and p53 Gene Expression and Polymorphisms with Hepatitis C (HCV) Chronic Infection, Cirrhosis and Hepatocellular Carcinoma (HCC) Stages in Egypt." *Asian Pacific Journal of Cancer Prevention* 18(8): 2049-2057.
- Krinsky, N. I. (1992). "Mechanism of action of biological antioxidants." *Proc Soc Exp Biol Med* 200(2): 248-254.
- Kurien, B. T. and R. H. Scofield (2006). "Western blotting." *Methods* 38(4): 283-293.
- Liou, G.-Y. and P. Storz (2010). "Reactive oxygen species in cancer." *Free radical research* 44(5): 10.3109/10715761003667554.
- Liu, B., Y. Chen and D. K. St. Clair (2008). "ROS and p53: versatile partnership." *Free radical biology & medicine* 44(8): 1529-1535.
- Livak, K. J. and T. D. Schmittgen (2001). "Analysis of relative gene expression data using real-time quantitative PCR and the 2(-Delta Delta C(T)) Method." *Methods* 25(4): 402-408.
- Lu, B., J. Lee, X. Nie, M. Li, Yaroslav I. Morozov, S. Venkatesh, Daniel F. Bogenhagen, D. Temiakov and Carolyn K. Suzuki (2013). "Phosphorylation of Human TFAM in Mitochondria Impairs DNA Binding and Promotes Degradation by the AAA+ Lon Protease." *Molecular Cell* 49(1): 121-132.
- Lü, J.-M., P. H. Lin, Q. Yao and C. Chen (2010). "Chemical and molecular mechanisms of antioxidants: experimental approaches and model systems." *Journal of Cellular and Molecular Medicine* 14(4): 840-860.
- Lu, S. C. (2009). "REGULATION OF GLUTATHIONE SYNTHESIS." *Molecular aspects of medicine* 30(1-2): 42-59.
- Lushchak, V. I. (2012). "Glutathione Homeostasis and Functions: Potential Targets for Medical Interventions." *Journal of Amino Acids* 2012: 26.
- Mahmood, T. and P.-C. Yang (2012). "Western blot: Technique, theory, and trouble shooting." *North American Journal of Medical Sciences* 4(9): 429-434.
- Marasas, W. (2001). "Discovery and occurrence of the fumonisins: a historical perspective." *Environmental Health Perspectives* 109(Suppl 2): 239.

- Mary, V. S., M. G. Theumer, S. L. Arias and H. R. Rubinstein (2012). "Reactive oxygen species sources and biomolecular oxidative damage induced by aflatoxin B1 and fumonisin B1 in rat spleen mononuclear cells." *Toxicology* 302(2-3): 299-307.
- Mercier, Y., P. Gatellier and M. Renner (2004). "Lipid and protein oxidation in vitro, and antioxidant potential in meat from Charolais cows finished on pasture or mixed diet." *Meat Sci* 66(2): 467-473.
- Merrill, A. H., Jr., E. M. Schmelz, D. L. Dillehay, S. Spiegel, J. A. Shayman, J. J. Schroeder, R. T. Riley, K. A. Voss and E. Wang (1997). "Sphingolipids--the enigmatic lipid class: biochemistry, physiology, and pathophysiology." *Toxicol Appl Pharmacol* 142(1): 208-225.
- Merrill, A. H., M. C. Sullards, E. Wang, K. A. Voss and R. T. Riley (2001). "Sphingolipid metabolism: roles in signal transduction and disruption by fumonisins." *Environmental Health Perspectives* 109(Suppl 2): 283-289.
- Nakabeppu, Y. (2014). "Cellular Levels of 8-Oxoguanine in either DNA or the Nucleotide Pool Play Pivotal Roles in Carcinogenesis and Survival of Cancer Cells." *International Journal of Molecular Sciences* 15(7): 12543-12557.
- Ncube, E., Bradley C. Flett, Cees Waalwijk and A. Viljoen. (2011). "Fusarium spp. and levels of fumonisins in maize produced by subsistence farmers in South Africa." *South African Journal of Science* 107(1-2): 7.
- Ngo, J. K., L. C. Pomatto and K. J. Davies (2013). "Upregulation of the mitochondrial Lon Protease allows adaptation to acute oxidative stress but dysregulation is associated with chronic stress, disease, and aging." *Redox Biol* 1: 258-264.
- Nguyen, T., P. Nioi and C. B. Pickett (2009). "The Nrf2-antioxidant response element signaling pathway and its activation by oxidative stress." *J Biol Chem* 284(20): 13291-13295.
- Noori, S. (2012). An Overview of Oxidative Stress and Antioxidant Defensive System.
- Nyaga, S. G., A. Lohani, P. Jaruga, A. R. Trzeciak, M. Dizdaroglu and M. K. Evans (2006). "Reduced repair of 8-hydroxyguanine in the human breast cancer cell line, HCC1937." *BMC Cancer* 6: 297-297.
- Oka, S., J. Leon, K. Sakumi, T. Ide, D. Kang, F. M. LaFerla and Y. Nakabeppu (2016). "Human mitochondrial transcriptional factor A breaks the mitochondria-mediated vicious cycle in Alzheimer's disease." *Scientific reports* 6.
- Pamplona, R. (2008). "Membrane phospholipids, lipoxidative damage and molecular integrity: a causal role in aging and longevity." *Biochim Biophys Acta* 1777(10): 1249-1262.

- Patekar, D., S. Kheur, N. Bagul, M. Kulkarni, A. Mahalle, Y. Ingle and V. Dhas (2013). "ANTIOXIDANT DEFENCE SYSTEM." *Oral & Maxillofacial Pathology Journal* 4(1).
- Perry, S. W., J. P. Norman, J. Barbieri, E. B. Brown and H. A. Gelbard (2011). "Mitochondrial membrane potential probes and the proton gradient: a practical usage guide." *BioTechniques* 50(2): 98-115.
- Persson, E. C., V. Sewram, A. A. Evans, W. T. London, Y. Volkwyn, Y.-J. Shen, J. A. Van Zyl, G. Chen, W. Lin, G. S. Shephard, P. R. Taylor, J.-H. Fan, S. M. Dawsey, Y.-L. Qiao, K. A. McGlynn and C. C. Abnet (2012). "Fumonisin B(1) and Risk of Hepatocellular Carcinoma in Two Chinese Cohorts." *Food and Chemical Toxicology* 50(3-4): 679-683.
- Pestana, E. A., S. Belak, A. Diallo, J. R. Crowther and G. J. Viljoen (2010). *Real-Time PCR – The Basic Principles. Early, rapid and sensitive veterinary molecular diagnostics - real time PCR applications.* Dordrecht, Springer Netherlands: 27-46.
- Phaniendra, A., D. B. Jestadi and L. Periyasamy (2015). "Free radicals: properties, sources, targets, and their implication in various diseases." *Indian J Clin Biochem* 30(1): 11-26.
- Pinelli, E., N. Poux, L. Garren, B. Pipy, M. Castegnaro, D. J. Miller and A. Pfohl-Leskowicz (1999). "Activation of mitogen-activated protein kinase by fumonisin B1 stimulates cPLA2 phosphorylation, the arachidonic acid cascade and cAMP production." *Carcinogenesis* 20(9): 1683-1688.
- Pinti, M., L. Gibellini, Y. Liu, S. Xu, B. Lu and A. Cossarizza (2015). "Mitochondrial Lon protease at the crossroads of oxidative stress, ageing and cancer." *Cell Mol Life Sci* 72(24): 4807-4824.
- Purdel, N. C., D. Margina and M. Ilie (2014). "Current methods used in the protein carbonyl assay." *Annual Research & Review in Biology* 4(12): 2015-2026.
- Rahal, A., A. Kumar, V. Singh, B. Yadav, R. Tiwari, S. Chakraborty and K. Dhama (2014). "Oxidative Stress, Prooxidants, and Antioxidants: The Interplay." *BioMed Research International* 2014: 19.
- Rahman, I., A. Kode and S. K. Biswas (2007). "Assay for quantitative determination of glutathione and glutathione disulfide levels using enzymatic recycling method." *Nat. Protocols* 1(6): 3159-3165.
- Ranum, P., J. P. Peña-Rosas and M. N. Garcia-Casal (2014). "Global maize production, utilization, and consumption." *Annals of the New York Academy of Sciences* 1312(1): 105-112.

- Reuter, S., S. C. Gupta, M. M. Chaturvedi and B. B. Aggarwal (2010). "Oxidative stress, inflammation, and cancer: How are they linked?" *Free radical biology & medicine* 49(11): 1603-1616.
- Rheeder, J. P., W. F. Marasas and H. F. Vismer (2002). "Production of fumonisin analogs by *Fusarium* species." *Appl Environ Microbiol* 68(5): 2101-2105.
- Rice-Evans, C. (1994). "Formation of free radicals and mechanisms of action in normal biochemical processes and pathological states." *Free Radical Damage and Its Control*: 129-151.
- Rojo de la Vega, M., M. Dodson, E. Chapman and D. D. Zhang (2016). "NRF2-targeted therapeutics: New targets and modes of NRF2 regulation." *Current Opinion in Toxicology* 1: 62-70.
- Rumora, L., A. M. Domijan, T. Z. Grubisic and M. Peraica (2007). "Mycotoxin fumonisin B1 alters cellular redox balance and signalling pathways in rat liver and kidney." *Toxicology* 242(1-3): 31-38.
- Sadler, T. W., A. H. Merrill, V. L. Stevens, M. C. Sullards, E. Wang and P. Wang (2002). "Prevention of fumonisin B1-induced neural tube defects by folic acid." *Teratology* 66(4): 169-176.
- Šegvić, M. and S. Pepeljnjak (2001). "Fumonisin and their effects on animal health—a brief review." *Vet arhiv* 5(71).
- Shah, D., N. Mahajan, S. Sah, S. Nath and B. Paudyal (2014). Oxidative stress and its biomarkers in systemic lupus erythematosus.
- Sharma, P., A. B. Jha, R. S. Dubey and M. Pessarakli (2012). "Reactive Oxygen Species, Oxidative Damage, and Antioxidative Defense Mechanism in Plants under Stressful Conditions." *Journal of Botany* 2012: 26.
- Sichak, S. P. and A. L. Dounce (1986). "Analysis of the peroxidatic mode of action of catalase." *Arch Biochem Biophys* 249(2): 286-295.
- Sosa, V., T. Moliné, R. Somoza, R. Paciucci, H. Kondoh and M. E. Lleonart (2013). "Oxidative stress and cancer: An overview." *Ageing Research Reviews* 12(1): 376-390.
- Sporn, M. B. and K. T. Liby (2012). "NRF2 and cancer: the good, the bad and the importance of context." *Nat Rev Cancer* 12(8): 564-571.
- Stevens, V. L. and J. Tang (1997). "Fumonisin B1-induced sphingolipid depletion inhibits vitamin uptake via the glycosylphosphatidylinositol-anchored folate receptor." *J Biol Chem* 272(29): 18020-18025.

- Stockmann-Juvala, H., J. Mikkola, J. Naarala, J. Loikkanen, E. Elovaara and K. Savolainen (2004a). "Oxidative stress induced by fumonisin B1 in continuous human and rodent neural cell cultures." *Free radical research* 38(9): 933-942.
- Stockmann-Juvala, H., J. Mikkola, J. Naarala, J. Loikkanen, E. Elovaara and K. Savolainen (2004b). "Fumonisin B1-induced toxicity and oxidative damage in U-118MG glioblastoma cells." *Toxicology* 202(3): 173-183.
- Stockmann-Juvala, H. and K. Savolainen (2008). "A review of the toxic effects and mechanisms of action of fumonisin B1." *Hum Exp Toxicol* 27(11): 10.
- Strober, W. (2001). "Trypan blue exclusion test of cell viability." *Curr Protoc Immunol Appendix 3: Appendix 3B*.
- Sun, G., S. Wang, X. Hu, J. Su, T. Huang, J. Yu, L. Tang, W. Gao and J. S. Wang (2007). "Fumonisin B1 contamination of home-grown corn in high-risk areas for esophageal and liver cancer in China." *Food Addit Contam* 24(2): 181-185.
- Ugarte, N., I. Petropoulos and B. Friguet (2010). "Oxidized mitochondrial protein degradation and repair in aging and oxidative stress." *Antioxid Redox Signal* 13(4): 539-549.
- Vafa, O., M. Wade, S. Kern, M. Beeche, T. K. Pandita, G. M. Hampton and G. M. Wahl (2002). "c-Myc Can Induce DNA Damage, Increase Reactive Oxygen Species, and Mitigate p53 Function: A Mechanism for Oncogene-Induced Genetic Instability." *Molecular Cell* 9(5): 1031-1044.
- Voss, K. A., P. C. Howard, R. T. Riley, R. P. Sharma, T. J. Bucci and R. J. Lorentzen (2002). "Carcinogenicity and mechanism of action of fumonisin B1: a mycotoxin produced by *Fusarium moniliforme* (= *F. verticillioides*)." *Cancer Detect Prev* 26(1): 1-9.
- Wallace, D. C. (2012). "Mitochondria and cancer." *Nature reviews. Cancer* 12(10): 685-698.
- Wan, X. S., Z. Zhou, J. H. Ware and A. R. Kennedy (2005). "Standardization of a Fluorometric Assay for Measuring Oxidative Stress in Irradiated Cells." *Radiation Research* 163(2): 232-240.
- Wang, E., W. P. Norred, C. W. Bacon, R. T. Riley and A. H. Merrill, Jr. (1991). "Inhibition of sphingolipid biosynthesis by fumonisins. Implications for diseases associated with *Fusarium moniliforme*." *J Biol Chem* 266(22): 14486-14490.
- Wang, K. Z. Q., J. Zhu, R. K. Dagda, G. Uechi, S. J. Cherra, A. M. Gusdon, M. Balasubramani and C. T. Chu (2014). "ERK-mediated phosphorylation of TFAM

- downregulates mitochondrial transcription: Implications for Parkinson's disease." *Mitochondrion* 17(Supplement C): 132-140.
- Wang, X., Q. Wu, D. Wan, Q. Liu, D. Chen, Z. Liu, M. R. Martinez-Larranaga, M. A. Martinez, A. Anadon and Z. Yuan (2016). "Fumonisin: oxidative stress-mediated toxicity and metabolism in vivo and in vitro." *Arch Toxicol* 90(1): 81-101.
 - WHO (2001). "WHO. Safety evaluation of certain mycotoxins in food (WHO food additives series 47)." International programme on chemical safety. Geneva: World Health Organization: 103–279.
 - WHO (2012). "World Health Statistics 2012. ." WHO Press, Geneva, Switzerland.
 - Yazar, S. and G. Z. Omurtag (2008). "Fumonisin, Trichothecenes and Zearalenone in Cereals." *International Journal of Molecular Sciences* 9(11): 2062-2090.
 - Yeung, J. M., H. Y. Wang and D. B. Prelusky (1996). "Fumonisin B1 induces protein kinase C translocation via direct interaction with diacylglycerol binding site." *Toxicol Appl Pharmacol* 141(1): 178-184.
 - Yin, H., L. Xu and N. A. Porter (2011). "Free radical lipid peroxidation: mechanisms and analysis." *Chem Rev* 111(10): 5944-5972.
 - Zhang, D. D. (2006). "Mechanistic studies of the Nrf2-Keap1 signaling pathway." *Drug Metab Rev* 38(4): 769-789.

APPENDIX A

Cytochrome P450 3A4 assay

Cytochrome P450 3A4 (CYP450 3A4) is expressed abundantly in the liver and detoxifies a wide variety of xenobiotics. Cytochrome P450 3A4 activity (Figure 6) was significantly increased ($p=0.0383$) from 206.1 ± 9.860 (Relative light units (RLU)) in the control cells to 264.4 ± 13.17 RLU in cells treated with FB_1 and 296.0 ± 16.83 RLU in cells treated with Dexamethasone (DEX-positive control).

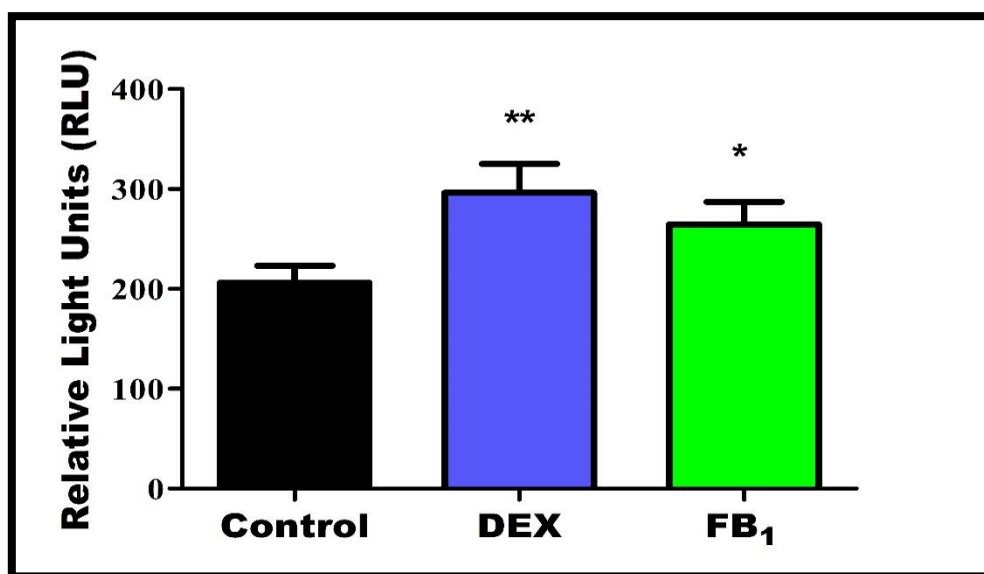


Figure 6: There was a 1.3 fold increase in the activity of CYP 3A4 in FB_1 treated cells ($*p<0.05$).

CYP450 3A4 activity could be an additional mechanism for oxidative stress in FB_1 treated cells. CYP450 3A4 is expressed in high levels in the liver, where it catalyses oxidation and detoxification of a wide variety of xenobiotics. The metabolism of xenobiotics by CYP450 3A4 leads to the formation of ES and ROS. The increase in CYP450 3A4 activity in cells treated with FB_1 , indicates that CYP450 3A4 could play a role in FB_1 metabolism. ROS generated by CYP450 3A4 activity could hence contribute to the observed FB_1 -induced oxidative stress.

APPENDIX B

Expression of phosphorylated Sirtuin 1

Sirtuin 1 (Sirt 1) is a cystolic protein that belongs to the same SIR2 family as Sirt 3. Figure 7 shows that the expression of phosphorylated Sirt 1 was reduced in cells treated with FB₁ (Control: 0.5492±0.03891 RBD vs FB₁: 0.1558±0.01843 RBD).

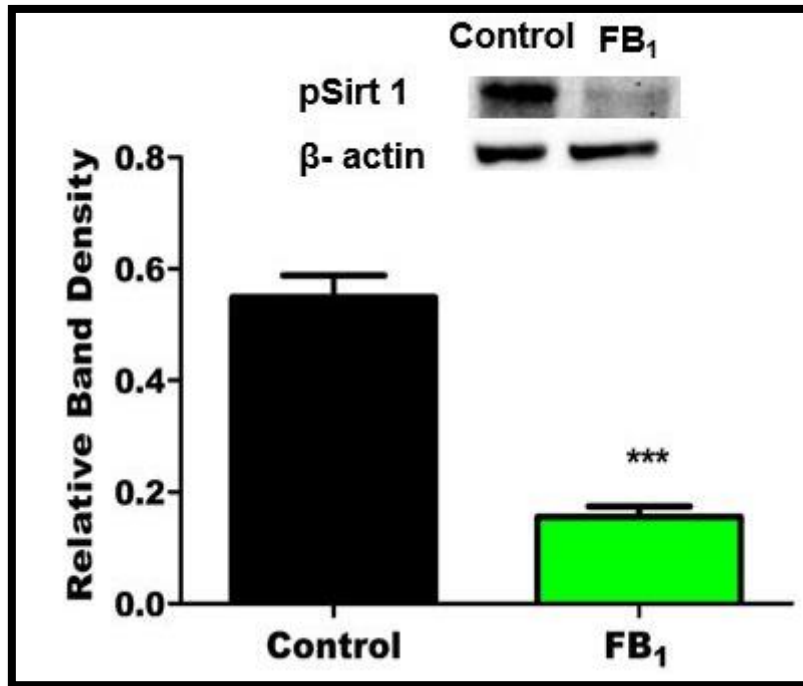


Figure 7: FB₁ significantly downregulated the expression of pSirt 1 (***) ($p < 0.0001$).

Phosphorylated Sirt 1 has tumour suppressor properties and protects against oxidative stress by inducing the expression of CAT. Therefore the significant decrease in Sirt 1 expression may contribute to carcinogenesis and reduced detoxification by cystolic CAT.

APPENDIX C

Lactate dehydrogenase assay

Fumonisin B₁ induced significant ($p=0.0177$) cell membrane damage indicating necrosis evidenced by increased lactate dehydrogenase (LDH) leakage compared to control (control: 1.035 ± 0.03602 Optical density vs. FB₁: 1.146 ± 0.03424 Optical density) (Figure 8).

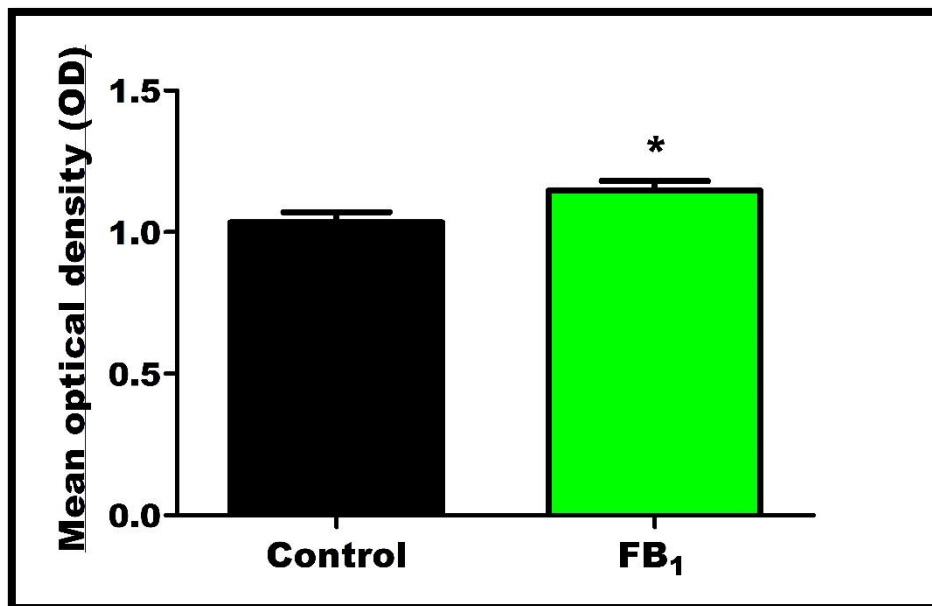


Figure 8: FB₁ disrupted membrane integrity evidenced by significant LDH leakage (* $p=0.0177$).

There was a 1.1 fold increase in LDH leakage in FB₁ treatments.

Elevated LDH in the extracellular matrix is an indicator of necrosis. Although p53-dependant apoptosis was inhibited by FB₁; cell death via necrosis may still occur.

APPENDIX D

Calculation of GSH concentration using a standard curve.

Mean relative light units (RLU) obtained from GSH standards.

Concentration GHS (μM)	RLU 1	RLU 2	Mean RLU
0	106865	119095	112980
3.125	210051	241158	225604.5
6.25	889358	10001540	945449
12.5	1105770	1747520	1426645
25	2301910	1493460	1897685
50	2194630	3522770	2858700

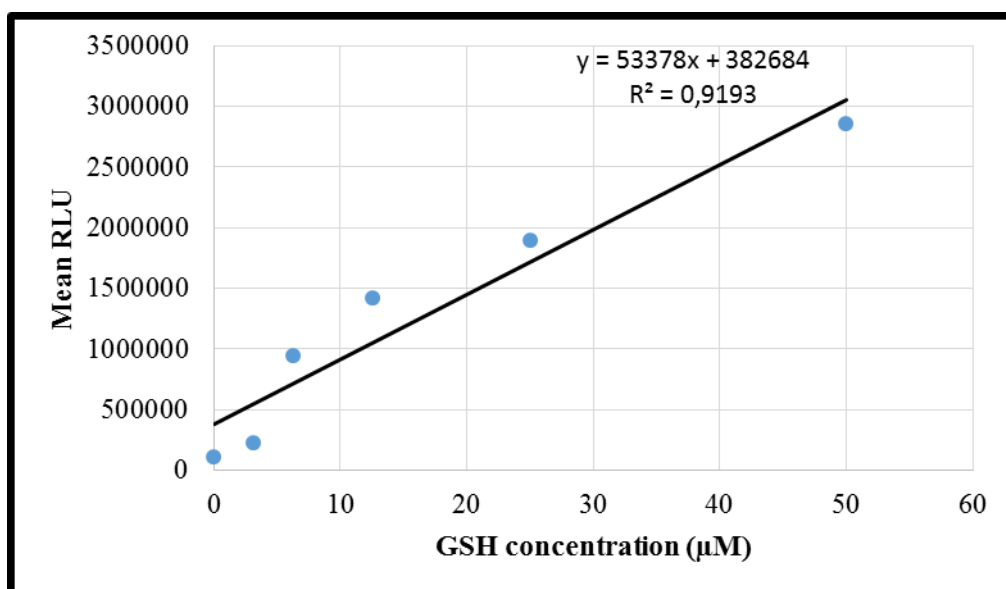


Figure 9: Standard curve obtained from GSH standards and the equation obtained from it.

The equation obtained from the GSH standard curve is $y = 53378x + 382684$; where y = RLU of the sample and x = the concentration of GSH of sample. Therefore the equation can be re-

arranged to: $x = \frac{y - 382684}{53378}$. The GSH concentration in μM (x) can be calculated by substituting

RLU obtained from each sample into y .

APPENDIX E

The concentration of RNA extracted from cells was determined using the Nanodrop 2000 spectrophotometer. Concentration of RNA that was extracted is as follows:

- Control cells: 13 200.9 ng/ μ l
- FB₁ exposed cells: 13 877.9 ng/ μ l.

The extracted RNA was standardised to 1 000 ng/ μ l.

APPENDIX F

Supplementary qPCR data; which includes the amplification curves and melt peaks for each qPCR undertaken are shown below.

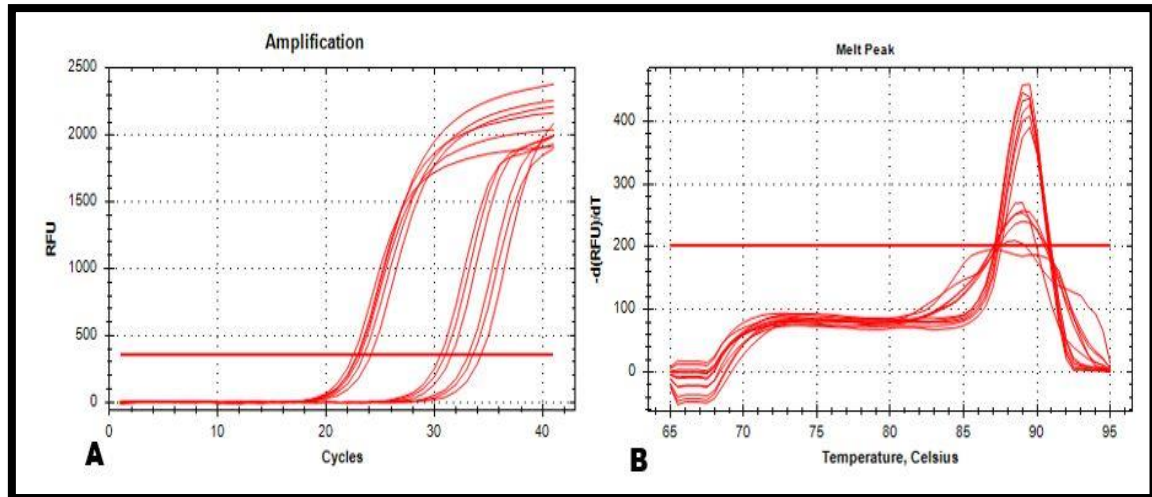


Figure 10: Amplification curve (A) and melt peak (B) analysis for *OGG1*.

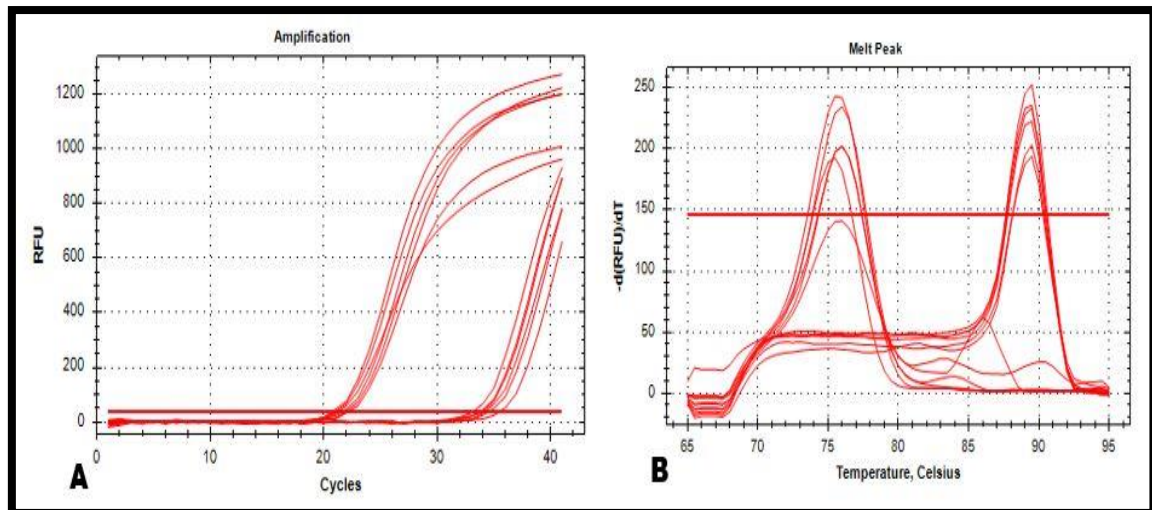


Figure 11: Amplification curve (A) and melt peak analysis for *SOD2*.

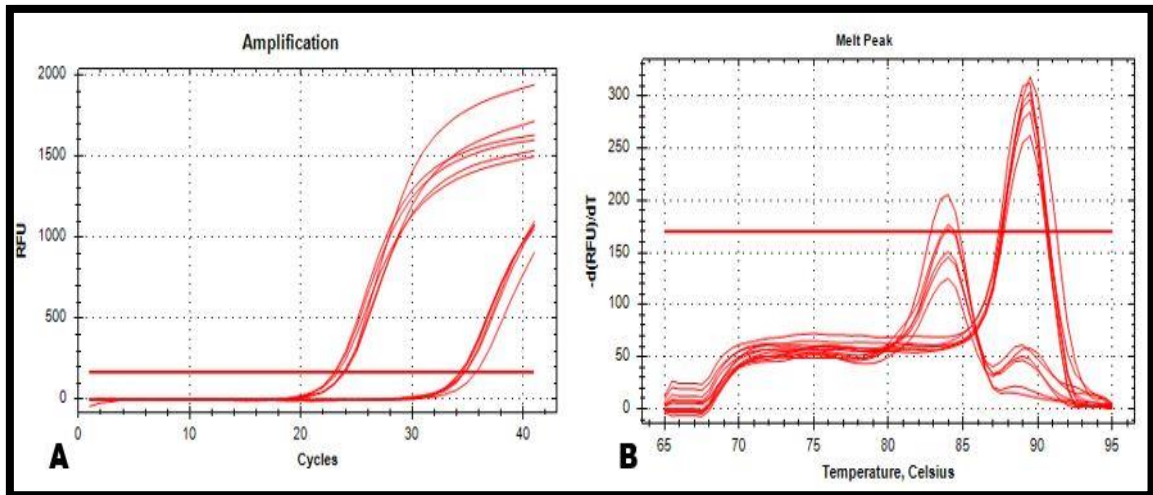


Figure 12: Amplification curve (A) and melt peak (B) analysis of CAT.

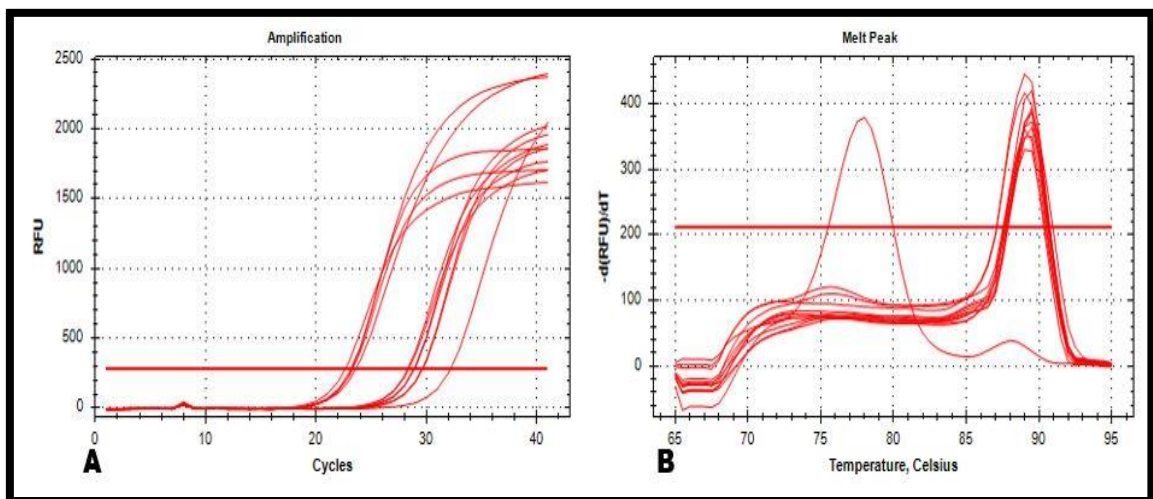


Figure 13: Amplification curve (A) and melt peak (B) analysis of GPx.

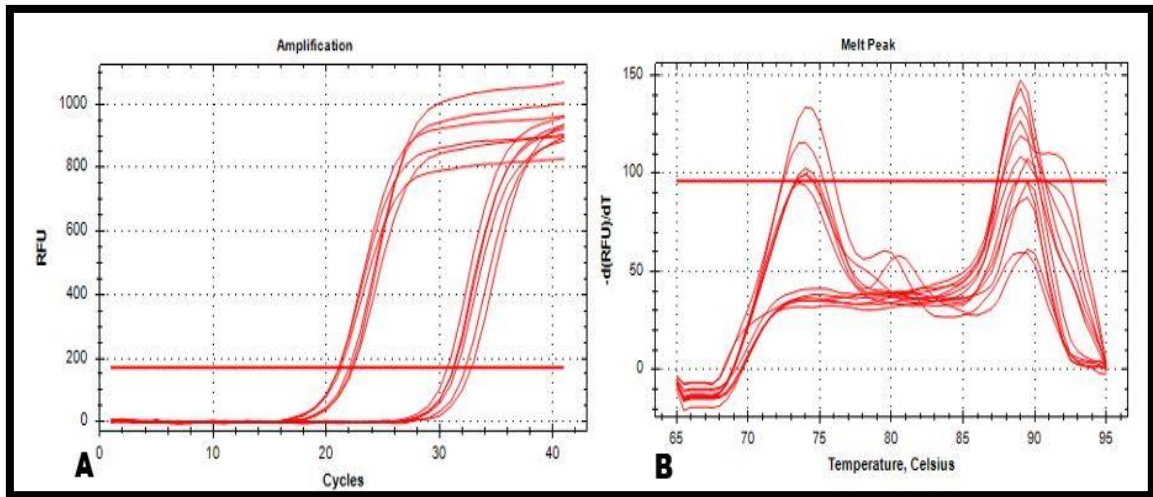


Figure 14: Amplification curve (A) and melt peak (B) analysis of *Tfam*.

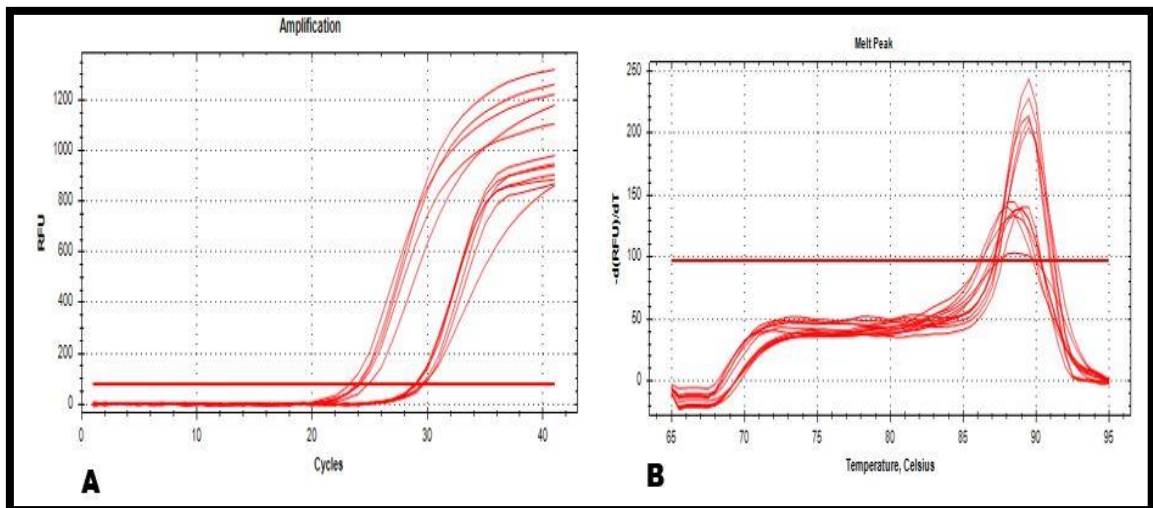


Figure 15: Amplification curve (A) and melt peak (B) analysis of *c-myc*.